

**Modelling seasonal rainfall characteristics over
South Africa**

by

Steven Phakula

Submitted in partial fulfilment of the requirements

for the degree of

MASTER OF SCIENCE

in the

Faculty of Natural and Agricultural Sciences

University of Pretoria

September 2016

Modelling seasonal rainfall characteristics over South Africa

Steven Phakula

Supervisor: Prof. Willem A. Landman
Co-supervisor: Dr. Asmerom F. Beraki
Department: Department of Geography, Geoinformatics and Meteorology
Faculty: Faculty of Natural and Agricultural Sciences
University: University of Pretoria
Degree: Master of Science

Abstract

Aspects of seasonal forecast skill using global climate models (GCMs) are assessed over South Africa. The GCMs output is configured to predict low and high number of rainfall days exceeding predefined threshold values for the summer rainy seasons and to predict the rainfall totals of the onset of the rainy seasons for eight homogeneous rainfall regions of South Africa. Using canonical correlation analysis (CCA) as statistical downscaling tool the forecast skill levels of both coupled ocean-atmosphere and uncoupled atmospheric models are determined through retro-actively generated hindcasts. Both approaches have skill in predicting the low and high number of rainfall days exceeding predefined threshold values for the summer rainy seasons as well as rainfall totals of onset of the rainy seasons for the homogeneous rainfall regions. In addition to the forecast verification results, CCA pattern analysis is also performed to determine the dominating atmospheric circulation systems predicted to be controlling rainfall variations for the seasons of interest. CCA pattern analysis for both the GCMs indicate that when there are anomalously negative (positive) predicted 850hPa geopotential heights over South Africa, there are anomalously wet (dry) rainfall conditions over the most part of South Africa for the different seasons of interest. This work has paved the way for the operational production of seasonal rainfall characteristics over South Africa.

I declare that the dissertation that I hereby submit for the degree Master of Science at the University of Pretoria is my own work and has not previously been submitted by me for degree purposes at any other university or institution.

SIGNATURE

DATE

Preface

The southern Africa region is prone to droughts and flooding due to its significant rainfall variability on a range of temporal and spatial scales. For example in late 2015 almost the whole of South Africa experienced one of the most severe drought since 1982. Such extreme rainfall variability is a challenge since most countries in southern Africa depend significantly in rain-fed agriculture. In fact, agriculture is the backbone of most economies in African countries, including South Africa. Therefore, accurate predictions of rainfall at different time scales including seasonal and intra-seasonal predictions are very important for decision-makers in sectors such as agriculture, energy, and health, among others. The character of the rainfall within the season often exerts a greater influence than does the seasonal total, as a result the seasonal forecasts are only marginally useful. Studies in predicting seasonal rainfall totals in South Africa have been conducted in the past and they show that climate models have skill in predicting summer rainfall totals. Moreover, most of the climate models show that the highest skill is found in the northeastern parts of South Africa. In contrast to seasonal rainfall totals predictions, very few studies have been conducted so far to test for the feasibility in predicting intra-seasonal rainfall characteristics in an operational environment in South Africa. However, intra-seasonal predictions are regarded as most important because they provide detailed information needed by users of climate information.

The chaotic nature of the atmosphere makes prediction of about two weeks to two months not easy. Furthermore, the intra-seasonal range is influenced by initial conditions of the atmosphere and land, as well as the ocean. Hence, intra-seasonal forecasts tend to be less skillful than seasonal climate forecasts. For that reason most researchers do not take interest in studying the intra-seasonal time-scale. It is well documented that seasonal rainfall totals during summer in South Africa is predictable due to the predictability of the Pacific El Niño-Southern Oscillation (ENSO), which is known to be the main climate driver of seasonal predictions. Recently it was found that there is a possible interconnection between ENSO and winter rainfall season of South Africa. At this stage it is not clear if there is an ENSO-rainfall relationship for the intra-seasonal climate predictions over South Africa.

The main aim of this research is to investigate forecast skill levels of both coupled ocean-atmosphere and uncoupled atmospheric GCMs in predicting seasonal rainfall characteristics over South Africa. The aim will be achieved through the following objectives:

- To evaluate the forecast skill levels of coupled and uncoupled GCM's in predicting 3-months seasonal rainfall totals for October to December (OND), November to January (NDJ), December to February (DJF) and January to March (JFM) seasons.
- To evaluate the forecast skill levels of coupled and uncoupled GCM's in predicting number of rainfall days exceeding 1mm, 5mm, 10mm, 15mm, 20mm, 30mm, 40mm and 50mm threshold values for OND, NDJ, DJF and JFM seasons.
- To evaluate the forecast skill levels of coupled and uncoupled GCM's in predicting the onset months of the rainy seasons.
- To determine the dominating atmospheric circulation systems predicted to be controlling rainfall variations for the seasons as well as onset months.

This dissertation comprises of six chapters as follows. Chapter 1 is the introduction discussing the climate of South Africa, rainfall characteristics and circulation patterns as well as the status of seasonal rainfall predictions in South Africa. The aim and approach of this research as well as the summary of the chapter is included. Data used and methods for forecasts verification are described in Chapter 2. Verification results for the predictability of 3-months seasonal rainfall totals is presented in Chapter 3. Chapter 4 and Chapter 5 present the verification results for the predictability of seasonal rainfall characteristics, the number of rainfall days exceeding predefined threshold values and the onset months of the rainy seasons, respectively. Finally the results are summarized and conclusions are made in Chapter 6.

Acknowledgements

My sincere thanks and appreciations to the following wonderful individuals and institutions for their valued contribution that made this study a success:

- Prof. Willem A. Landman (UP) for his support, mentorship and guidance throughout this research study.
- Dr. Asmerom Beraki (SAWS) for his support, ideas and guidance during the course of this study. Above all, I thank you for making available the models data to conduct this research.
- Mr. Cobus Olivier (SAWS) for his assistance with any programming challenges I came across during this study. Thank you for being patient and helpful.
- The South African Weather Service (SAWS) is acknowledged for allowing me time to study and for providing resources needed to conduct this study.
- Ms. Samantha Linnerts (SAWS) is acknowledge for her assistance with GIS issues.
- Many thanks to ACCESS for funding this research study. I cannot thank you enough for your support.
- A very special thanks to my family for their endless support and understanding, especially my wife Venetia Phakula and daughter Khensani Phakula.

TABLE OF CONTENTS

| | |
|-----------------------------------------------------------------------------------------------------------------------------------------|----------|
| Abstract | i |
| Declaration | ii |
| Preface | iii |
| Acknowledgements | v |
| CHAPTER 1: INTRODUCTION | 1 |
| 1.1. Climate of South Africa | 1 |
| 1.2. Rainfall characteristics variables and their effects over South Africa | 5 |
| 1.2.1. <i>Droughts</i> | 5 |
| 1.2.1.1. <i>Meteorological droughts</i> | 5 |
| 1.2.1.2. <i>Agricultural droughts</i> | 5 |
| 1.2.1.3. <i>Hydrological droughts</i> | 6 |
| 1.2.1.4. <i>Socioeconomic droughts</i> | 6 |
| 1.2.2. <i>Wet and dry spells</i> | 6 |
| 1.2.3. <i>Floods</i> | 7 |
| 1.2.4. <i>Onset and cessation of rainy seasons</i> | 7 |
| 1.2.4.1. <i>Agro-meteorological definitions</i> | 8 |
| 1.2.4.2. <i>Meteorological definitions</i> | 8 |
| 1.3. Large scale climate circulation patterns, synoptic systems and climate drivers influencing rainfall variability in southern Africa | 9 |
| 1.3.1. <i>The Pacific El Niño-Southern Oscillation</i> | 9 |
| 1.3.2. <i>The Tropical-Temperate Troughs</i> | 10 |
| 1.3.3. <i>The Inter-Tropical Convergence Zone</i> | 10 |
| 1.3.4. <i>The Madden-Julian Oscillation</i> | 10 |
| 1.3.5. <i>The Sea-Surface Temperatures</i> | 11 |
| 1.4. Climate predictions | 11 |
| 1.4.1. <i>Statistical Downscaling</i> | 12 |
| 1.4.1.1. <i>Weather Classification</i> | 12 |
| 1.4.1.2. <i>Regression Models</i> | 13 |
| 1.4.1.3. <i>Weather Generators</i> | 13 |
| 1.4.2. <i>Dynamical Downscaling</i> | 14 |

| | | |
|----------------------------------------------------------------------------------------------------------------|--------------------------------------------|----|
| 1.5. | Predictability of rainfall in South Africa | 14 |
| 1.5.1. | <i>Seasonal rainfall predictions</i> | 14 |
| 1.5.2. | <i>Intra-seasonal rainfall predictions</i> | 15 |
| 1.6. | Aim and approach of research | 15 |
| 1.7. | Summary | 16 |
| CHAPTER 2: DATA AND METHODOLOGY | | 17 |
| 2.1. | Observed rainfall data | 17 |
| 2.2. | GCM output data | 17 |
| 2.3. | Model Output Statistics | 23 |
| 2.4. | Verification of forecasts | 25 |
| 2.4.1. | <i>ROC</i> | 25 |
| 2.4.2. | <i>Reliability diagrams</i> | 26 |
| 2.4.3. | <i>Spearman's rank correlations</i> | 28 |
| 2.5. | CCA pattern analysis | 28 |
| 2.6. | Synopsis | 29 |
| CHAPTER 3: PREDICTABILITY OF SEASONAL RAINFALL DURING SUMMER SEASONS OVER SOUTH AFRICA | | 30 |
| 3.1. | Probabilistic forecast skill | 30 |
| 3.1.1. | <i>ROC scores</i> | 30 |
| 3.1.2. | <i>Reliability diagrams</i> | 34 |
| 3.2. | Deterministic forecast skill | 36 |
| 3.2.1. | <i>Spearman's rank correlations</i> | 36 |
| 3.3. | CCA patterns analysis | 42 |
| 3.4. | Synopsis | 46 |
| CHAPTER 4: PREDICTABILITY OF RAINFALL DAYS EXCEEDING PRE-DEFINED THRESHOLD VALUES WITHIN SUMMER SEASONS | | 47 |
| 4.1. | ROC scores | 47 |
| 4.2. | Reliability diagrams | 52 |
| 4.3. | Spearman' rank correlations | 56 |
| 4.4. | CCA pattern analysis | 63 |
| 4.5. | Synopsis | 71 |

| | |
|--------------------------------------------------------------------------------------|----|
| CHAPTER 5: PREDICTABILITY OF THE ONSET OF THE RAINY SEASONS OVER SOUTH AFRICA | 72 |
| 5.1. Definition of onset | 72 |
| 5.2. ROC scores | 73 |
| 5.3. Reliability diagrams | 76 |
| 5.4. Spearman's rank correlations | 80 |
| 5.5. CCA patterns analysis | 81 |
| 5.5.1. <i>OAGCM</i> | 81 |
| 5.5.2. <i>AGCM</i> | 85 |
| 5.6. Synopsis | 89 |
| CHAPTER 6: SUMMARY AND CONCLUSIONS | 90 |
| REFERENCES | 93 |

LIST OF FIGURES

| | |
|---------------------------------------------------------------------------------------------------------------------------------------------------------------------------------------------------|----|
| Figure 1.1. Topography of South Africa in metres above sea level | 2 |
| Figure 1.2. The Climate Research Unit mean observed annual rainfall over South Africa from 1970 to 2006 | 3 |
| Figure 1.3. The Climate Research Unit observed rainfall totals for DJF seasons over South Africa from 1970 to 2006 | 4 |
| Figure 1.4. As in Figure 1.3, but for JJA seasons | 4 |
| Figure 2.1. Climatological stations seasonal rainfall totals for JJA, SON, DJF and MAM seasons over South Africa from 1982 to 2009 | 18 |
| Figure 2.2. Number of rainfall days exceeding 1mm, 5mm, 10mm, 15mm, 20mm and 30mm threshold values for OND seasons over South Africa from 1982 to 2009 | 19 |
| Figure 2.3. As in Figure 2.2, but for NDJ seasons | 20 |
| Figure 2.4. As in Figure 2.3, but for DJF seasons | 21 |
| Figure 2.5. As in Figure 2.4, but for JFM seasons | 22 |
| Figure 2.6. ROC curve diagram showing the hit rate and false alarm rate (adapted from www.cawcr.gov.au/projects/verification) | 27 |
| Figure 2.7. Reliability diagram (adapted from www.cawcr.gov.au/projects/verification) | 27 |
| Figure 3.1. ROC score maps of the OAGCM (left panel) and the AGCM (right panel) in predicting seasonal rainfall totals for the summer rainy seasons | 33 |

| | |
|--------------------------------------------------------------------------------------------------------------------------------------------------------------------------------------------------------|----|
| Figure 3.2. Reliability diagrams and frequency histograms for the OAGCM (top panel) and the AGCM (bottom panel) in predicting above-normal and below-normal rainfall totals for NDJ seasons | 35 |
| Figure 3.3. As in Figure 3.2, but for DJF seasons | 35 |
| Figure 3.4. Spearman's rank correlations of the OAGCM and their level of significance at 0- to 3-months lead-times in predicting rainfall totals for NDJ seasons | 37 |
| Figure 3.5. As in Figure 3.4, but for the AGCM | 38 |
| Figure 3.6. Spearman's rank correlations of the OAGCM and their level of significance at 0- to 3-months lead-times in predicting rainfall totals for DJF seasons | 39 |
| Figure 3.7. As in Figure 3.6, but for the AGCM | 41 |
| Figure 3.8. Mode 1 CCA maps of the 850hPa geopotential heights of the OAGCM and the stations observed rainfall totals for (a) OND, (b) NDJ, (c) DJF, and (d) JFM seasons | 44 |
| Figure 3.9. As in Figure 3.8, but for the AGCM | 45 |
| Figure 4.1. ROC score maps of the OAGCM (left panel) and the AGCM (right panel) in predicting high- and low-number of rainfall days exceeding pre-defined threshold values | 51 |
| Figure 4.2. Reliability diagrams of the OAGCM at 1-month lead-time in predicting low (orange) and high (blue) number of rainfall days exceeding pre-defined threshold values within NDJ seasons | 53 |
| Figure 4.3. As in Figure 4.2, but for the AGCM | 53 |

| | |
|-----------------------------------------------------------------------------------------------------------------------------------------------------------------------------------------------------------|----|
| Figure 4.4. Reliability diagrams of the OAGCM at 1-month lead-time in predicting low (orange) and high (blue) number of rainfall days exceeding pre-defined threshold values within DJF seasons | 54 |
| Figure 4.5. As in Figure 4.4, but for the AGCM | 54 |
| Figure 4.6. Reliability diagrams of the OAGCM at 1-month lead-time in predicting low (orange) and high (blue) number of rainfall days exceeding pre-defined threshold values within JFM seasons | 55 |
| Figure 4.7. As in Figure 4.6, but for the AGCM | 55 |
| Figure 4.8. Spearman's rank correlations for the OAGCM and their level of significance in predicting the number of rainfall days exceeding 1mm, 10mm and 20mm threshold values within NDJ seasons | 57 |
| Figure 4.9. As in Figure 4.8, but for the AGCM | 58 |
| Figure 4.10. Spearman's rank correlations for the OAGCM and their level of significance in predicting the number of rainfall days exceeding 1mm, 10mm and 20mm threshold values within DJF seasons | 59 |
| Figure 4.11. As in Figure 4.10, but for the AGCM | 60 |
| Figure 4.12. Spearman's rank correlations for the OAGCM and their level of significance in predicting the number of rainfall days exceeding 1mm, 10mm and 20mm threshold values within JFM seasons | 61 |
| Figure 4.13. As in Figure 4.12, but for the AGCM | 62 |
| Figure 4.14. Mode 1 CCA maps of the OAGCM at 1-month lead-time and the number of rainfall days exceeding (a) 1mm, (b) 10mm, (c) 20mm, and (d) 30mm within NDJ seasons | 65 |
| Figure 4.15. As in Figure 4.14, but for the AGCM | 66 |

| | |
|------------------------------------------------------------------------------------------------------------------------------------------------------------------------------|----|
| Figure 4.16. Mode 1 CCA maps of the OAGCM at 1-month lead-time and the number of rainfall days exceeding (a) 1mm, (b) 10mm, (c) 20mm, and (d) 30mm within DJF seasons | 67 |
| Figure 4.17. As in Figure 4.16, but for the AGCM | 68 |
| Figure 4.18. Mode 1 CCA maps of the OAGCM at 1-month lead-time and the number of rainfall days exceeding (a) 1mm, (b) 10mm, (c) 20mm, and (d) 30mm for JFM seasons | 69 |
| Figure 4.19. As in Figure 4.18, but for the AGCM | 70 |
| Figure 5.1. The eight homogeneous rainfall regions and their annual rainfall cycles | 72 |
| Figure 5.2. ROC scores of the OAGCM 1-month lead-time in predicting onset of the rainy seasons for the eight homogeneous rainfall regions | 75 |
| Figure 5.3. As in Figure 5.2, but for the AGCM | 75 |
| Figure 5.4. Reliability diagrams of both the OAGCM and AGCM 1-month lead-time in predicting onset of the rainy seasons for Region 1 | 77 |
| Figure 5.5. As in Figure 5.4, but for Region 2 | 78 |
| Figure 5.6. As in Figure 5.5, but for Region 3 | 78 |
| Figure 5.7. As in Figure 5.6, but for Region 4 | 78 |
| Figure 5.8. As in Figure 5.7, but for Region 5 | 79 |
| Figure 5.9. As in Figure 5.8, but for Region 6 | 79 |
| Figure 5.10. As in Figure 5.9, but for Region 7 | 79 |
| Figure 5.11. As in Figure 5.10, but for Region 8 | 80 |

| | |
|--------------------------------------------------------------------------------------------------------------------------------------------------------------------------------------------------------|----|
| Figure 5.12. Spearman's correlations between the simulated rainfall from the OAGCM and AGCM at 1-month lead-time and downscaled rainfall totals for the onset for the eight homogeneous regions | 81 |
| Figure 5.13. Mode 1 CCA maps of the OAGCM 1-month lead-time and the onset of the rainy season for Region 1 | 83 |
| Figure 5.14. As in Figure 5.13, but for Region 2 | 83 |
| Figure 5.15. As in Figure 5.14, but for Region 3 | 83 |
| Figure 5.16. As in Figure 5.15, but for Region 4 | 83 |
| Figure 5.17. As in Figure 5.16, but for Region 5 | 84 |
| Figure 5.18. As in Figure 5.17, but for Region 6 | 84 |
| Figure 5.19. As in Figure 5.18, but for Region 7 | 84 |
| Figure 5.20. As in Figure 5.19, but for Region 8 | 84 |
| Figure 5.21. Mode 1 CCA maps of the AGCM 1-month lead-time and the onset of the rainy season for Region 1 | 87 |
| Figure 5.22. As in Figure 5.21, but for Region 2 | 87 |
| Figure 5.23. As in Figure 5.22, but for Region 3 | 87 |
| Figure 5.24. As in Figure 5.23, but for Region 4 | 88 |
| Figure 5.25. As in Figure 5.24, but for Region 5 | 88 |
| Figure 5.26. As in Figure 5.25, but for Region 6 | 88 |

Figure 5.27. As in Figure 5.26, but for Region 7 88

Figure 5.28. As in Figure 5.27, but for Region 8 89

LIST OF TABLES

| | |
|----------------------------------------------------------------------------------------------------------------------------------------------------------------------------------------------------------|----|
| Table 3.1. ROC scores of the OAGCM at 0- to 4-months lead-time in predicting seasonal rainfall totals for OND, NDJ, DJF and JFM | 31 |
| Table 3.2. As in Table 3.1, but for the AGCM | 32 |
| Table 4.1. ROC scores of the OAGCM at 1-month lead-time in predicting number of days with rainfall exceeding 1mm, 5mm, 10mm, 15mm, 20mm, 30mm, 40mm and 50mm within OND, NDJ, DJF and JFM seasons | 49 |
| Table 4.2. As in Table 4.1, but for the AGCM | 50 |
| Table 5.1. ROC scores of the OAGCM at 1-month lead-time in predicting onset of the rainy seasons for the eight homogeneous rainfall regions of South Africa | 74 |
| Table 5.2. As in Table 5.1, but for the AGCM | 74 |

CHAPTER 1

INTRODUCTION

The southern Africa is a region characterized by significant climate variability on a range of temporal and spatial scales which have an impact on agriculture, water resources and economy at large. In fact, the variations of rainfall is a major concern for agricultural production in the region. The variability of rainfall makes southern Africa vulnerable to extreme climate events (Shongwe *et al.* 2009). The most severe impacts of climate on human society and natural environment over southern Africa are as a result of the extreme climate events such as droughts and floods, among others. The devastating floods in Mozambique during February/March 2000 and severe droughts of 1991/92, 2002/03 and 2003/04 over northern South Africa are the example of such extreme events (Cook *et al.*, 2004). Therefore, better understanding of the climatology and variability of the climate characteristics variables could be invaluable to the users of weather and climate information. Different institutions in South Africa such as the South African Weather Service (SAWS) and the Council for Scientific and Industrial Research (CSIR) are currently producing rainfall and temperature forecasts at different time scale, including seasonal forecasts. However, seasonal forecasts does not give detailed information of specific needs of the users. In addition, there has been an increasing demand for intra-seasonal forecasts from agricultural and other user communities in decision making (Hudson *et al.*, 2011; Tadross *et al.*, 2005), The intra-seasonal forecasts are needed mainly because seasonal forecasts have limited benefits without medium-term information (Landman and Tennant, 2000). Moreover, intra-seasonal forecasts bridge the gap between weather and seasonal forecasting, covering the time scale of about 10 to 60 days (Hudson *et al.*, 2011). Intra-seasonal forecasts are regarded as the most difficult to predict but are of great importance for the economic and agricultural sectors. The chaotic nature of the atmosphere makes prediction of about two weeks to two months difficult (Luo and Wood, 2006). Furthermore, the intra-seasonal range is influenced by initial conditions of the atmosphere and land, as well as the ocean (Hudson *et al.*, 2011), hence intra-seasonal forecasts tend to be less skillful than seasonal climate forecasts. The objective of this study is to test the skill of both the coupled and uncoupled general circulation models (GCMs) in predicting the intra-seasonal rainfall variables, viz. the number of rainfall days exceeding different rainfall thresholds for the austral summer seasons as well as the onset months of the rainy seasons over South Africa.

1.1. Climate of South Africa

South Africa is located in the subtropics and is affected by atmospheric circulation in the tropics, subtropics and temperate latitudes (Taljaard 1996). Rainfall in South Africa is variable spatially and temporally (Schulze, 2005). The variation is due to the topography as well as the sea-surface temperatures (SSTs) adjacent the country with the warm Agulhas current pushing warm water to the east coast while the west coast is cold due to the cold Benguela current (van Heerden and Taljaard, 1998). The topography of South Africa varies from the altitudes of less than 300 metres along the coastal areas and above 3000 metres over the eastern escarpment (Figure 1.1). The high resolution topography data was obtained from <http://eros.usgs.gov>. The annual average rainfall calculated on high-resolution (0.5 x 0.5 degree) grids from Climate Research Unit (CRU) data (http://browse.ceda.ac.uk/badc/cru/data/cru_ts/cru_ts_3.23/data) from the University of East Anglia increases from west to east with the maximum rainfall occurring over the eastern escarpment and the minimum rainfall occurring north-western parts of the country (Figure 1.2).

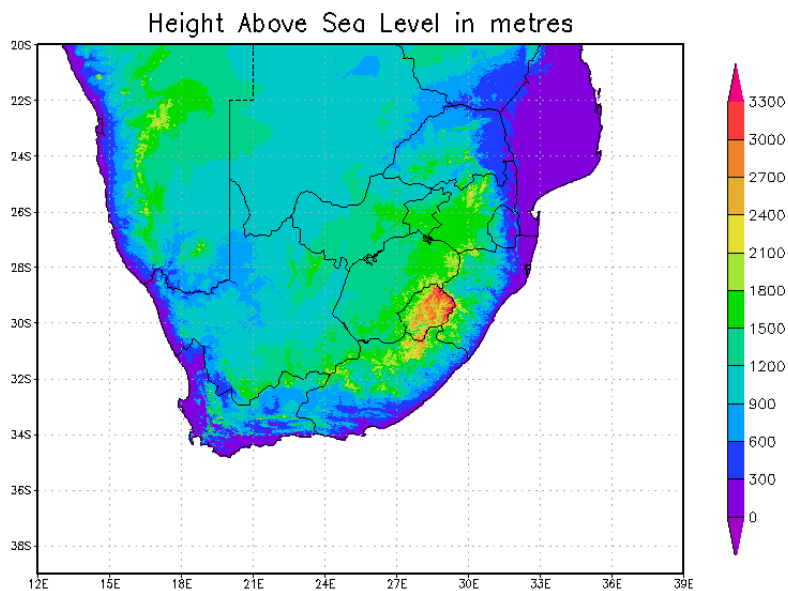


Figure 1.1. The topography of South Africa in metres above sea level.

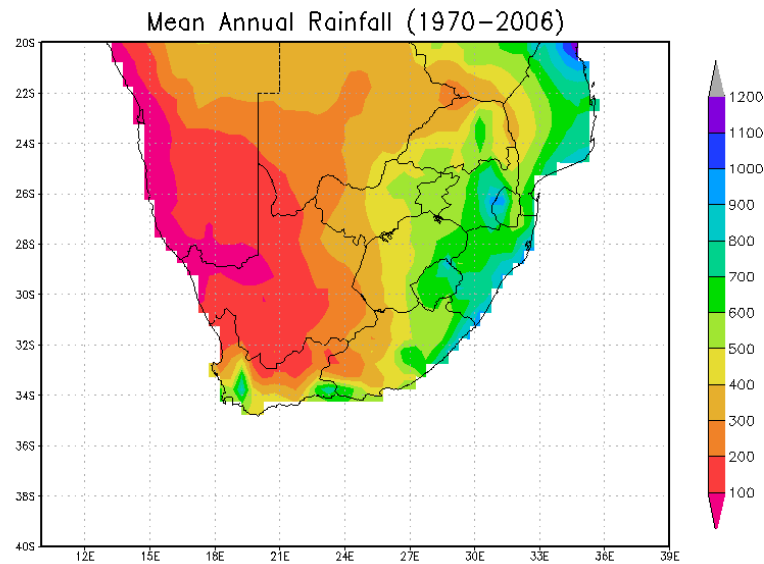


Figure 1.2. CRU observed mean annual rainfall over South Africa.

The majority of the rainfall in South Africa is received during austral summer seasons (November to March), except for the south western and south coast which receives its rainfall during austral winter and throughout the year, respectively (e.g. Phillipon *et al.*, 2011; Fauchereau *et al.*, 2009; Cretat *et al.*, 2010). Summer rainfall is mostly of convective nature, whereas the winter rains which is maximum from May to August when the track of the temperate weather systems such as extratropical cyclones, cold fronts and cut-off lows shift northward (Phillipon *et al.*, 2011). Average seasonal rainfall totals for summer December-January-February (DJF) and winter June-July-August (JJA) seasons calculated from CRU dataset are shown in Figure 1.3 and Figure 1.4, respectively. The maximum rainfall occurs over the eastern escarpment during summer seasons and southern escarpment during winter.

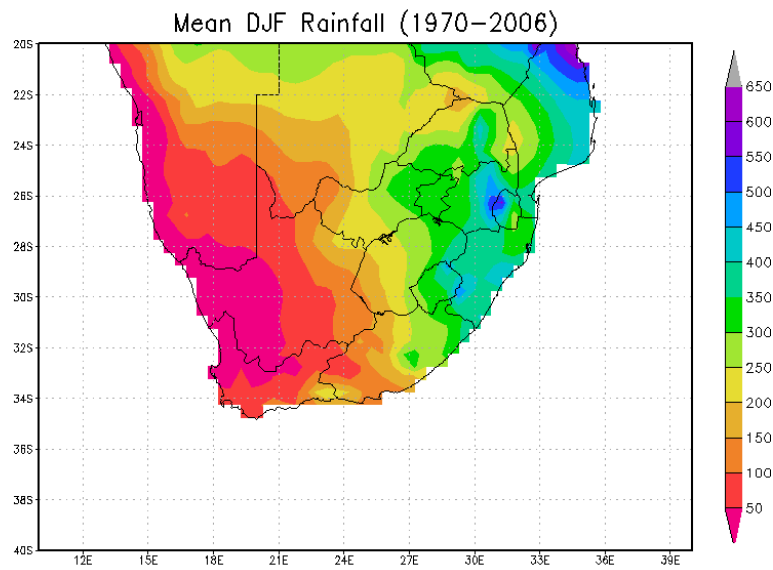


Figure 1.3. CRU observed mean DJF rainfall seasons.

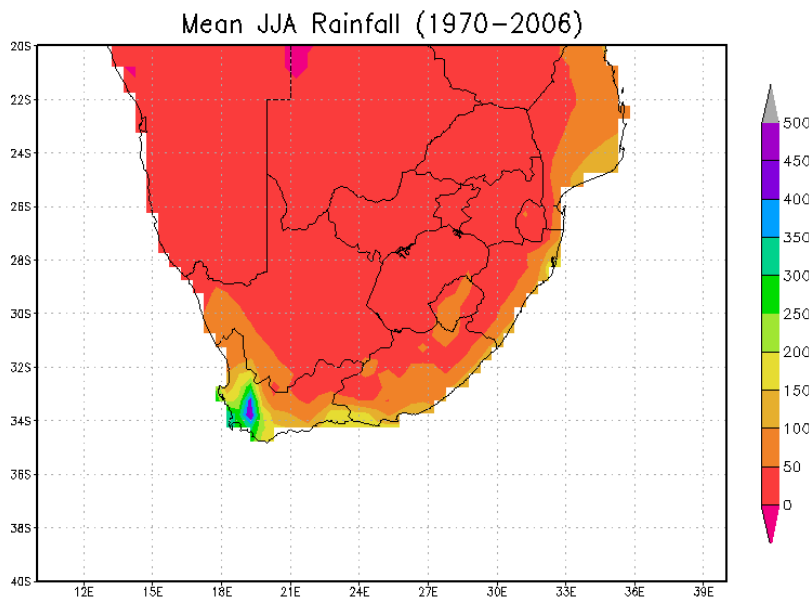


Figure 1.4. As in Figure 1.3, but for JJA seasons.

1.2. Rainfall characteristics variables and their effects over South Africa

1.2.1. Droughts

Southern Africa is prone to drought events (Ambrosino *et al.*, 2011; Usman and Reason, 2004). For example, severe droughts of 1991/92, 2002/03 and 2003/04 over northern South Africa and surrounding areas (Cook *et al.*, 2004). During the 1991/1992 summer drought approximately 3 million tons of grain productions were lost in southern Africa (Lyon, 2009). In South Africa alone during the drought of 1992 it was estimated that 50 000 jobs in the agriculture sector were lost and a further 20 000 in related sectors, affecting 250 000 people. During the same event the gross domestic product (GDP) loss was US\$ 500 Million. In the 2007/2008 drought event, South Africa spent R 285 Million on drought relief, with R 20 Million and R 25 Million of that amount allocated to the Eastern Cape and Free State provinces, respectively (Ngaka, 2012). Most severe droughts over the subtropical southern Africa are influenced either by strong El Niño events or regional anomalies over the southeast Atlantic Ocean (Reason *et al.*, 2006). There are four main definitions of drought in the literature: meteorological, agricultural, hydrological and socio-economic. They were described by Usman *et al.* (2005) as follows

1.2.1.1. Meteorological droughts

Meteorological drought is defined on the basis of the degree of dryness, in comparison to a normal or average amount, and the duration of the dry period. Definitions of meteorological drought must be region-specific, since the atmospheric conditions that result in deficiencies of precipitation are highly region-specific.

1.2.1.2. Agricultural droughts

Agricultural drought links various characteristics of meteorological drought to agricultural impacts, focusing on precipitation shortages, differences between actual and potential evapotranspiration, soil-water deficit, reduced groundwater or reservoir levels. A good definition of agricultural drought should account for the susceptibility of crops during different stages of crop development. Deficient topsoil moisture at planting may hinder germination, leading to low plant populations per hectare and a reduction of yield.

1.2.1.3. Hydrological droughts

Hydrological drought refers to a persistently low discharge and/or volume of water in streams and reservoir, lasting for months to years. Hydrological drought is a natural phenomenon, but it may be exacerbated by human activities. They are related to meteorological droughts and their recurrence interval varies according. Changes in land use and land degradation can affect the magnitude and frequency of hydrological drought.

1.2.1.4. Socio-economic droughts

Socioeconomic definitions of drought associate the supply and demand of some economic good with elements of meteorological, hydrological and agricultural drought. It differs from the other type of drought in that its occurrence depend on the processes of supply and demand. Due to the natural variability of climate, water supply is ample in some years, but insufficient to meet human and environmental needs in other year.

1.2.2. Wet and dry spells

The frequency and intensity distribution of rainfall have an effect on dry and wet spells (Cook *et al.*, 2004). The temporal distribution and nature of wet and dry spells have an impact to agriculture in South Africa. The amount and timing of rainfall determines the rainy season and in turn affect the agricultural activities (Kijazi and Reason, 2011). The occurrence of extreme dry conditions over southern Africa during the austral summer (DJF) are associated with high dry spell frequency, while the extreme wet conditions are associated with high wet spell frequency (Usman and Reason 2004). According to Usman and Reason (2004) wet (dry) spells are occurring when at least 3 consecutive days having area-average rainfall above (below) 1 mm per day. Dry spell frequency parameter can be used to provide another measure of a season's rainfall characteristics besides the totals and its deviation from the mean (Usman and Reason, 2004). As an example, Usman and Reason (2004) used the 1997/98 where good rains were received over large parts of the region but the dry spell frequency was above average, the results was due to the above-average rainfall in March received during a few heavy rainfall events.

1.2.3. Floods

Floods are defined as the overflowing of the normal confines of a stream or other body of water or the accumulation of water over area that are not normally submerged (Kundzewicz *et al.*, 2014). Floods includes river floods, flash floods, urban floods and coastal floods among others. Floods are as a result of various characteristics of the climate system, most notable precipitation (intensity, duration, amount and timing), drainage conditions (such as pre-existing water levels in rivers), soil character and status (permeability, soil moisture content and its vertical distribution), the rate of urbanization, and the dams and reservoirs (Kundzewicz *et al.*, 2014). Southern Africa is equally vulnerable to flood events as it is to droughts. Examples include floods in Mozambique and northeastern parts of South Africa during 2000/2001 which left hundreds of people dead and affected about 200 000 people, with the total cost of the damage to approximately US\$ 500 million (Washington and Preston, 2006). As a result of these recurring flood events a warning system for flash flood-prone regions, called the South African Flash Flood Guidance (SAFFG) is developed and used operationally at the SAWS to monitor floods (de Coning, 2013).

1.2.4. Onset and cessation of the rainy seasons

The onset and cessation of rainy seasons are regarded as the most critical rainfall characteristics for agricultural activities (Camberlin and Mbeye, 2003; Marengo *et al.*, 2001; Ati *et al.*, 2002; Kniveton *et al.*, 2008; Majisola, 2010). Typically the onset of the rainy season occurs towards the end of October and beginning of November over the summer rainfall region of South Africa, however there is considerable variation of these dates between different parts of the region. A delay in the onset of rains may result in poor seasonal distribution, even when the total amount of rainfall received within the same season is normal (Otun and Adewuni, 2009). The late onset and early cessation of rainy seasons may lead to drought, sometimes even loss of animals and human lives, as occurred during the El Niño episodes of 1982/1983 and 1991/1992 (Cheruiyot and Osunmakinde, 2010). On the other hand early onset and late cessation can lead to flooding, damage of property and loss of lives. Various definitions of the onset and the cessation of the rainy season for different regions exist in literature (e.g. Liebmann *et al.*, 2007; Mhita and Nassib, 1987; Ndomba, 2010; Nicholls, 1984; Omotosho *et al.*, 2000; Kijazi and Reason, 2011; Reason *et al.*, 2005; Sivakumar, 1988).

1.2.4.1. Agro-climatological definitions

In agro-climatology, the rainy season onset and cessation dates are often defined from rainfall thresholds. These thresholds are parameterized empirically in order to fit the requirements of a given crop and to account for local-scale climatic conditions. For Tanzania for instance, Kijazi and Reason (2011) defined the onset of the rainy season as the first pentad of rainfall exceeding 10 mm followed by three consecutive pentads having rainfall amount of not less than 10 mm per pentad. They defined cessation occurring when three consecutive pentads have a mean rainfall of less or equal to 2mm per day, the preceding pentad is considered to be the cessation of the rainy season. Reason *et al.* (2005) defined onset of the rainy season over Limpopo province of South Africa as the first date of the two pentads with at least 25mm of rainfall, given the following five pentads within which at least 20mm of rainfall occurs. They considered the cessation as when six consecutive pentads each with less than 10mm of rainfall occurs. Marengo *et al.* (2001) defined the onset (cessation) date of the rainy season in Amazon Basin as that pentad with daily average precipitation greater (less) than 4mm per day, provided that six of eight subsequent (subsequent) pentads had precipitation of greater (less) than 4.5mm per day.

1.2.4.2. Meteorological definitions

Climatologists use objective methodologies to determine onset and cessation of the rainy season. The advantage of using the objective methodology is that they are not using any threshold values. Objective methods determine the climatological onset and cessation rather than for specific crops of interest. In order to determine the onset and cessation of the rainy season in South America, Liebmann and Marengo (2001) and Liebmann *et al.* (2007) firstly summed the climatological daily rainfall average minus the climatological annual-mean daily rainfall average at each grid point. Then defined the onset (cessation) of rains as the first day after the anomalous accumulation reaches the minimum (maximum) values, computed as departure from the long term average. In North Australia, Lo *et al.* (2007) defined onset of wet season as the date at which an accumulation of 15% of station's climatological mean wet season (September to April) rainfall is reached. For this study meteorological definition is used to define the onset since the study is interested in climatological definition rather than that of specific crops.

1.3. Large-scale circulation patterns, synoptic systems and climate drivers influencing rainfall in southern Africa

There are a number of different large-scale climate phenomena and synoptic systems that influence the characteristics of rainfall in southern Africa.

1.3.1. Pacific El Niño-Southern Oscillation

The Pacific El Niño-Southern Oscillation (ENSO) is the disturbance of the ocean-atmosphere system in the equatorial eastern Pacific Ocean and has large influence on global weather systems (e.g. Horel and Wallace, 1981; Ropelewski and Halpert, 1987; Matthews, 2000; Rautenbach and Smith, 2001; Ashok *et al.*, 2007; Izumo *et al.*, 2010). At the larger scale, ENSO is known to be an important control of rainfall variability on seasonal scale in southern Africa (Cook *et al.*, 2004; Cretat *et al.*, 2010). The Southern Oscillation refers to variations in the temperature of the surface of the tropical eastern Pacific Ocean, with the warming known as El Niño and the cooling known as La Niña, and in air surface pressure in the tropical western Pacific (Trenberth, 1997). The two variations are coupled, with the warm phase (El Niño) accompanies high air surface pressure in the western Pacific, while the cold phase (La Niña) accompanies low air surface pressure in the western Pacific. ENSO events are usually studied in order to understand the seasonal climate variability over a lead time of a few months to a year (Oldenborgh, 2004). ENSO influence generally results in anomalously wet (dry) conditions during La Niña (El Niño) events during austral summer over southern Africa (Barnston and He, 1996; Landman *et al.*, 2001; Washington and Preston, 2006; Cretat *et al.*, 2010). However, it must be noted that not all El Niño events result in dry conditions over southern Africa. For instant, the strong 1997/98 event did not result in the anticipated drought over a larger part of South Africa (Lyon and Mason, 2007; Richard *et al.*, 2001). Pohl *et al.* (2007) established that the intra-seasonal variability is higher during El Niño events. According to Padon and Dorado (2008) there is an ENSO effect in monthly precipitation in different regions. El Niño (La Niña) events are associated with higher (lower) dry spell frequencies over most parts of southern Africa (Tadross *et al.*, 2009) and their occurrence is associated with shifts in the location of the tropical-temperate trough systems (Thomas *et al.*, 2007).

1.3.2. Tropical-Temperate Troughs

The high frequency variability of South African rainfall is mainly related to tropical-temperate troughs (TTTs) (Cretat *et al.*, 2010). The TTTs are synoptic-scale cloud bands that link tropical disturbance over the sub-continent with an upper-tropospheric frontal system embedded in the mid-latitude westerly circulation (Cretat *et al.*, 2010; Pohl *et al.*, 2007, 2009). The TTT systems are associated with the northwest to southeast cloud bands extending from tropical southern Africa to the southwest Indian Ocean and which have been linked to the occurrence of intense rainfall (about 30-60% of summer rainfall totals) in December through February (Cretat *et al.*, 2012). However, most of southern Africa tends to receive significantly less rainfall when the TTTs are located further east (Usman and Reason, 2004). Tropical areas of southern and central Africa rainfall regimes are largely dependent on deep convection processes and water vapour convergence at different tropospheric levels (Vigaud *et al.*, 2006; Cretat *et al.*, 2012).

1.3.3. Inter-Tropical Convergence Zone

The tropical circulation consists of a pair of large convective cells known as Hadley cells (HC). HC is defined as a zonally symmetric meridional circulation with an ascending motion over the Inter-tropical Convergence Zone (ITCZ) associated with the zone of maximum global heating and a descending motion over the subtropical high-pressure belt (Tanaka *et al.*, 2004). The ITCZ is a zone of convergence of north-eastern and south-eastern trade winds and is characterized by convective activity. The ITCZ is the major rainfall-bearing system in southern Africa (Cretat *et al.*, 2012). According to Todd *et al.* (2004) the January to February rainfall in southern Africa is associated with the ITCZ, located over central southern Africa at about 10 degree south extending eastward over Indian Ocean. Wet (dry) summers are often associated with a southward (northward) shift and strengthening (weakening) of the ITCZ over tropical southeastern Africa (Cook *et al.*, 2004).

1.3.4. Madden-Julian Oscillation

The Madden-Julian Oscillation (MJO) is regarded as the dominant mode of intra-seasonal variability in the tropical atmosphere (Jones *et al.*, 2004; Liess *et al.*, 2005; Pohl *et al.*, 2007; Padon and Dorado, 2008; Sultan *et al.*, 2009; Tam and Lou, 2005; Wang *et al.*, 2011). The MJO

is characterized by a slow eastward propagation of large-scale tropical deep convection clusters from the Indian Ocean to the western Pacific Ocean (Ambrosino *et al.*, 2011; Pohl *et al.*, 2007). MJO has been found to significantly influence rainfall in the east and south of southern Africa (Ambrosino *et al.*, 2011; Pohl *et al.*, 2007). At longer timescales, the MJO seem to have an influence on wet and dry phases over southern Africa during the summer rainy season (Pohl *et al.*, 2007). The MJO modifies the direction of the lower-layer moisture fluxes, through an influence on the Indian Ocean High (IOH) over the southern African region (Pohl *et al.*, 2007). In their study Pohl *et al.* (2008) established that the IOH anomalies generate easterly flux anomalies in the southern low latitudes, resulting in moisture transport from the Indian basin to the southern Africa and above average rainfall totals.

1.3.5. Sea-Surface Temperatures

The sea-surface temperatures (SSTs) over the adjacent Atlantic and Indian Oceans play an important role in the climate variability of South Africa. At regional scale the inter-annual rainfall fluctuations are influenced by SST variations in the South Atlantic and South Indian Oceans (Cretat *et al.*, 2010). South Atlantic SSTs partially influence moisture fluxes between the South Atlantic and southern Africa, whereas the positive SST anomalies in the South West Indian Ocean (SWIO) are linked with wetter conditions over eastern and central South Africa (Cretat *et al.*, 2010). According to Williams *et al.* (2008) decreasing SST anomalies in the central South Atlantic and increasing SST anomalies off the coast of southwestern Africa are associated with increasing daily rainfall and extreme rainfall over southern Africa. In addition, specific pattern of SSTs in the SWIO, with warm anomalies in the subtropical SWIO and cool anomalies in the northern SWIO plays a crucial role in generating extreme rainfall conditions (Washington and Preston 2006).

1.4. Climate Predictions

Climate predictions can be achieved by using the GCMs (Murphy 1999). GCMs are usually configured at a very coarse resolution of about 100-300km and have demonstrated skill at global or even regional scale. They are, however, unable to represent local sub-grid features and subsequently overestimate rainfall over southern Africa (Landman and Beraki, 2012). In addition, the representation of rainfall at mid-to-high latitudes is complex and often not well estimated. Such systematic biases have created the need to downscale GCM simulations over southern Africa (Landman and Beraki, 2012). Semi-empirical relationship exist between observed large-scale

circulations and rainfall, hence, mathematical equations can be constructed to predict local precipitation from the forecast large-scale circulations. In addition, empirical remapping of GCM fields to regional rainfall has been demonstrated successfully over southern Africa (Landman and Beraki, 2012). In order to address this problem GCM simulations need to be downscaled to generate the required higher resolution data. There are two main downscaling techniques that are widely used, namely statistical downscaling and dynamical downscaling.

1.4.1. Statistical Downscaling

Statistical downscaling (SDS) seek to establish a statistical relationship between the GCM simulated large-scale circulation variables and the required regional or local scale climate variables such as rainfall and temperature (Hewitson and Crane, 1996). This approach is mostly preferred because of its relative ease to use and lower cost compared to dynamical approach. According to Busuioc *et al.* (2001) any successful SDS should satisfy three main conditions: (i) the link between predictors and predictands has to be strong in order to explain satisfactorily the local climate variability; (ii) the predictor variable should be well simulated by the GCM; and (iii) the relationship between predictors and predictands should not change in time, and should remain the same in a changed future climate. SDS is sub-divided into three categories, viz. weather classification, regression models, and weather generators.

1.4.1.1. Weather Classification

Weather classification (WC) downscaling methods involve grouping local meteorological variables in relation to different classes of atmospheric circulation based on a given weather classification scheme (Chen *et al.*, 2012). The synoptic climatology provides a powerful tool for the purpose of studying regional climatic conditions by classifying large scale atmospheric circulation variables into a small number of categories (synoptic patterns) on a physical meaningful basis. Typically synoptic patterns are defined by applying a cluster analysis techniques such as fuzzy classification method (e.g. Yang *et al.*, 2014), self-organizing maps (SOM. e.g. Hewitson and Crane, 2002, 2006) and K-nearest neighbour algorithm (e.g. Oyelade *et al.*, 2010; Zhang *et al.*, 2013) or using subjective circulation classification schemes. In both cases, synoptic patterns are grouped according to their similarity with nearest neighbours or reference set. Within a classification scheme, weather types are grouped and the relationships between large-scale variables and local meteorological variables may be established separately

for each weather type (Chen *et al.*, 2012). The main advantage of weather typing schemes is that local variables are sensitively linked to large-scale atmospheric circulations and its disadvantage is that the reliability depends on the stationary relationship between large-scale circulation and local climate, and that it requires the additional task of weather classification (Chen *et al.*, 2012).

1.4.1.2. Regression Models

Regression models (RM) approach involve establishing statistical linear or non-linear relationships between predictands and the large scale atmospheric predictors (Chen *et al.*, 2012). The most commonly applied RM techniques include multiple linear regression (MLR, e.g. Spak *et al.*, 2007), principal component analysis (PCA, e.g. Jolliffe *et al.*, 2003), canonical correlation analysis (CCA, e.g. Landman and Tennant, 2000; Landman *et al.*, 2012), and artificial neural networks (ANN, e.g. Hewitson and Crane, 1996). The main strength of RM approach to future climate scenario generation is the relative ease of application and its disadvantage is the probable lack of a temporally stable and strong relationship between predictors and predictands (Chen *et al.*, 2012). There is often a problem of under prediction of variance associated with regression approaches. The problem is particularly evident for daily precipitation downscaling because of the relatively low predictability of local amounts by large scale forcing alone.

1.4.1.3. Weather Generators

Weather generator (WG) downscaling approach is achieved by perturbing their parameters according to the changes projected by climate models (Chen *et al.* 2012). There are two main approaches for parametric adjustment of WG. The first involves day-to-day changes to the weather generator parameters based on daily variations in atmospheric circulation; the other one and the most commonly used involves changes in weather generator parameters on changes of monthly statistics projected by climate models (Chen *et al.*, 1012). To represent the longer-term variability and climate change signal, WGs can be used through employing in a perfect prognosis (PP) setting, i.e., their parameters can be conditioned on the large-scale circulation (Wong *et al.*, 2014). The advantage of using WG approach is its ability to rapidly produce sets of climate scenarios for studying the impacts of rare climate events, and its disadvantages are that the precipitation occurrence parameters cannot be easily adjusted for future climate condition as well as that parameter modification for future climate scenarios can lead to unanticipated outcomes (Chen *et al.*, 2012).

1.4.2. Dynamical Downscaling

Dynamical downscaling (DDS) approaches achieve higher resolution by nesting high resolution regional climate models (RCMs) into GCMs (Murphy, 1999; Schmidli *et al.*, 2007). RCMs are formulated in terms of physical principles and therefore have the potential for capturing fine spatial-scale nonlinear effect, which increases confidence in their abilities to downscale future climate (Xu and Yang, 2012). In addition, RCMs can better resolve orographic effects than the course-resolution GCMs. The GCM data are directly used to provide initial conditions, lateral boundary conditions, SSTs, and initial land surface conditions to the nested RCM (Xu and Yang, 2012). DDS simulations is however computationally demanding and expensive. Moreover, there is a challenge to balance the performance of RCMs in adding small-scale features while simultaneously retaining large-scale features (Wang and Katamarthi, 2013). Most RCMs have systematic errors associated with uncertainties in their dynamics, physical parameterization, boundary conditions, initialization, and domain choice, as well as the resolution of the numerical models (Jakob *et al.*, 2011; Wang and Katamarthi, 2013).

1.5. Predictability of rainfall in Southern Africa

1.5.1. Seasonal rainfall predictions

The most common and powerful predictor of seasonal climate is the state of ENSO (e.g. Yuan *et al.*, 2013). Seasonal forecasts provide information on the development of the climate up to 6 to 12 months ahead of time rather than detailed day-by-day variations (Winsemius *et al.* 2014). Previous studies showed that seasonal rainfall totals is predictable over South Africa. Landman *et al.* (2001) found the COLA T30 GCM to have forecast skill in predicting seasonal rainfall over the summer rainfall region of southern Africa. Furthermore, Landman *et al.* (2012) compared coupled and uncoupled prediction systems referred to as One- and Two-Tiered systems, respectively, in predicting seasonal rainfall over South Africa. They found both systems to have forecast skill, however the coupled system generally outperform the uncoupled one. Multi-model forecasts were also compared with single model forecasts and the former outperformed the latter in predicting mid-summer rainfall over southern Africa (Landman and Beraki, 2012). Engelbrecht *et al.* (2011) using conformal-cubic atmospheric model (CCAM) over southern Africa successfully simulated the climate variables across a wide range of spatial and temporal scales.

1.5.2. Intra-seasonal rainfall predictions

Seasonal predictions of rainfall totals and of minimum and maximum temperatures are mostly appreciated by users, but they do not provide detailed information for user specific needs. Users of the climate information are more interested in the characteristics of climate variables within the seasons. Hence intra-seasonal climate predictions are the most important to the users of climate information. In recent study Winsemius *et al.* (2014) demonstrated that climate models are capable of predicting the characteristics of intra-seasonal climate variables. They assessed the skill of the European Centre for Medium-Range Weather Forecasts (ECMWF) seasonal forecasting system in predicting the frequency of dry spells as well as the frequency of heat stress conditions expressed in the temperature heat index over southern Africa. From their investigation they found that the forecasting system have skill in predicting the frequency of the dry spells (5 days) for the DJF seasons for up to 2-months lead-time. According to Bouagila and Sushama (2013) most GCMs overestimate light precipitation (1 to 10mm/day) and underestimate heavy precipitation (>10 mm/day).

1.6. Aim and approach of research

The main aim of this research is to investigate the forecast skill of coupled ocean-atmosphere and uncoupled atmospheric GCMs in predicting intra-seasonal rainfall characteristics over South Africa. The aim will be achieved through the following objectives:

- To evaluate the forecast skill of coupled and uncoupled GCM's in predicting 3-months seasonal rainfall totals for October to December (OND), November to January (NDJ), December to February (DJF) and January to March (JFM) seasons.
- To evaluate the forecast skill of coupled and uncoupled GCM's in predicting number of rainfall days exceeding 1mm, 5mm, 10mm, 15mm, 20mm, 30mm, 40mm and 50mm threshold values for OND, NDJ, DJF and JFM seasons.
- To evaluate the forecast skill of coupled and uncoupled GCM's in predicting the onset months of the rainy seasons.

These objectives are going to be realized:

- By calculating monthly and 3-months seasonal rainfall total over South Africa.
- By calculating indices for number of rainfall days exceeding 1mm, 5mm, 10mm, 15mm, 20mm, 30mm, 40mm and 50mm for OND, NDJ, DJF and JFM seasons over South Africa.
- By downscaling the output of both coupled and uncoupled GCM's to seasonal rainfall totals and number of rainfall days exceeding 1mm, 5mm, 10mm, 15mm, 20mm, 30mm, 40mm and 50mm for OND, NDJ, DJF and JFM, as well as the onset months of the rainy seasons over South Africa.
- By verifying the forecasting systems (coupled and uncoupled) in predicting seasonal rainfall totals and the number of rainfall days exceeding 1mm, 5mm, 10mm, 15mm, 20mm, 30mm, 40mm and 50mm for OND, NDJ, DJF and JFM seasons, as well as the onset of the rainy seasons over South Africa.

1.7. Summary

The southern Africa region is characterized by significant climate variability on a range of temporal and spatial scales. The variability of rainfall makes southern Africa vulnerable to extreme climate events. The most severe impacts of climate on human society and the natural environment over southern Africa are as a result of droughts and floods. There are a number of distinct large-scale atmospheric and synoptic systems, namely, ENSO, TTTs, ITCZ, MJO and SSTs that influence the characteristics of climate variables in southern Africa. Climate predictions can be achieved by using the GCMs, however their coarse resolution limits their ability to provide the detailed climate information at regional time scale. In order to address this problem GCM simulations need to be downscaled to generate the required higher resolution data. There are two main downscaling techniques that are widely used, namely statistical downscaling and dynamical downscaling. Although seasonal rainfall and temperature forecasts are currently produced in South Africa, these forecasts does not give detailed information to address some of the specific needs of the users. These forecasts need to also include a reliable estimation of intra-seasonal climate characteristics that may benefit decision making in agricultural and other user communities. This study seek to investigate the skill of both the coupled and uncoupled GCMs in predicting seasonal rainfall totals and number of rainfall days exceeding 1mm, 5mm, 10mm, 20mm, 30mm, 40mm and 50mm within OND, NDJ, DJF and JFM seasons as well as the onset months of the rainy seasons over South Africa.

CHAPTER 2

Data and Methodology

2.1. Observed rainfall data

Quality controlled observed daily rainfall data from 563 selected rainfall stations distributed across South Africa obtained from SAWS are used. The climate databank of SAWS collates, maintains and runs a quality control process of South Africa's meteorological and climate data. Only rainfall stations with no missing data from 1982 to 2009 are considered in this study. The station rainfall data are used to calculate monthly and 3-month seasonal rainfall totals as well as indices of the number of rainfall days exceeding 1mm, 5mm, 10mm, 15mm, 20mm, 25mm, 30mm, 35mm, 40mm, 45mm and 50mm threshold values for OND, NDJ, DJF and JFM seasons. Figure 2.1 show the climatological seasonal rainfall totals calculate from stations distributed across South Africa. The climatological seasonal rainfall totals show that most parts of the country receives more rainfall during summer months, mostly the eastern half of the country, whereas the south coast receiving the highest rainfall during winter. The number of rainfall days exceeding 1mm, 5mm, 10mm, 15mm, 20mm and 30mm rainfall thresholds within OND, NDJ, DJF and JFM seasons are depicted in Figure 2.2, Figure 2.3, Figure 2.4 and Figure 2.5, respectively. The rainfall frequency show that most of the summer rains is received from days with lower threshold values.

2.2. GCM output data

The 850hPa geopotential height fields of the fourth generation of the ECHAM4.5 atmospheric general circulation model (AGCM, Roeckner *et al.*, 1996; Beraki *et al.*, 2015) developed at the Max Planck Institute for Meteorology (MPIM) in Hamburg, Germany is used in this study. The ECHAM evolve originally from the spectral weather prediction model of the European Centre for Medium Range Weather Forecasts (ECMWF; Simmons *et al.*, 1989). The model is configured at a triangular spectral truncation 42 (T42) and at a resolution of about 2.8 degrees latitude and longitude with 19 vertical layers. The 850hPa geopotential height fields of the ocean-atmosphere coupled general circulation model (OAGCM) developed in partnership between South Africa and

the International Research Institute for Climate and Society (IRI), referred to as SAWS Coupled Model (SCM, Beraki *et al.* 2014) is also used. The AGCM feeds the ocean model (OGCM) called modular oceanic model version 3 (MOM3) with heat, momentum, freshwater, and surface solar flux. In turn, the OGCM feeds the AGCM with SST information.

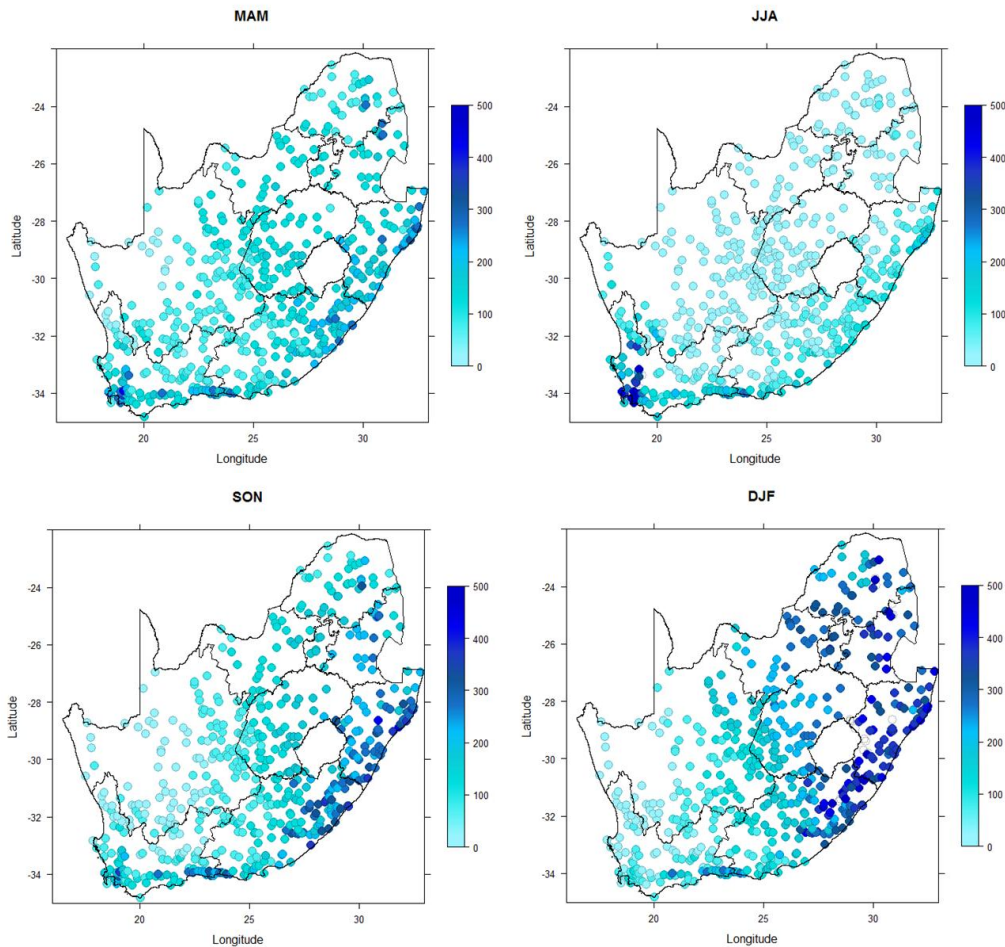


Figure 2.1. Climatological seasonal rainfall totals for MAM, JJA, SON and DJF over South Africa from 1982 to 2009.

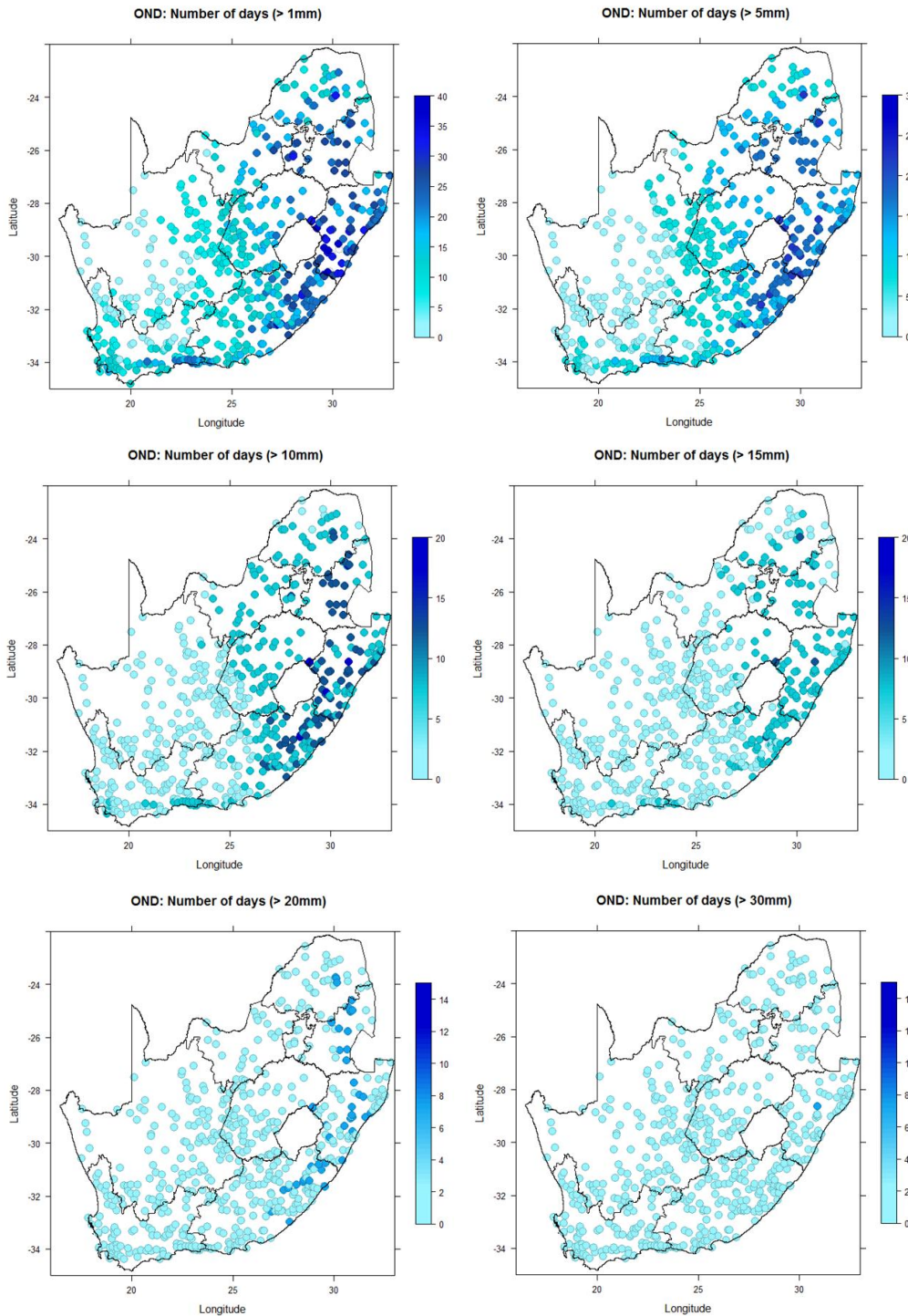


Figure 2.2. Number of days exceeding 1mm, 5mm, 10mm, 15mm, 20mm and 30mm rainfall threshold values for OND seasons over South Africa from 1982 to 2009.

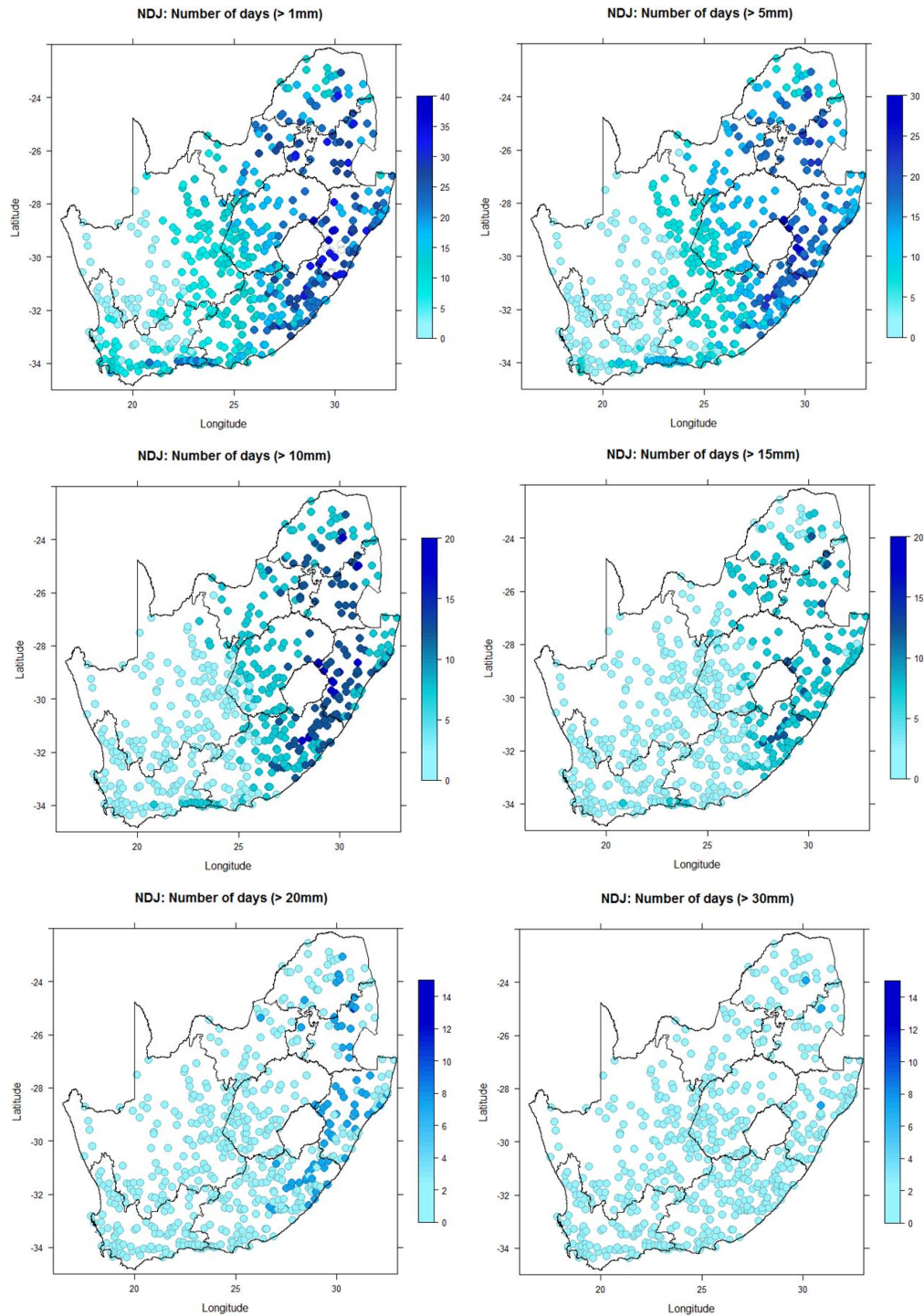


Figure 2.3. As in Figure 2.2, but for NDJ seasons.

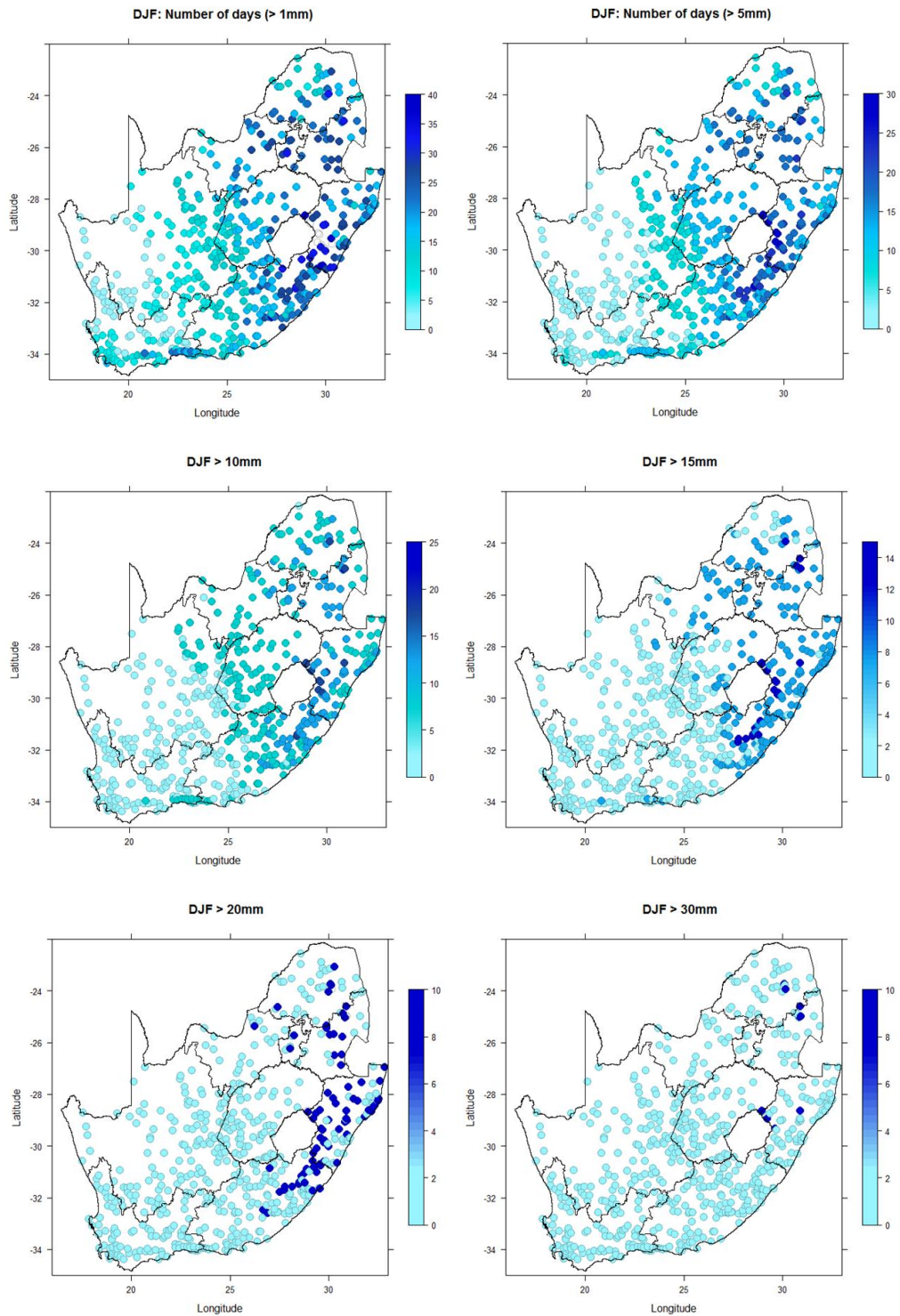


Figure 2.4. As in Figure 2.3, but for DJF seasons.

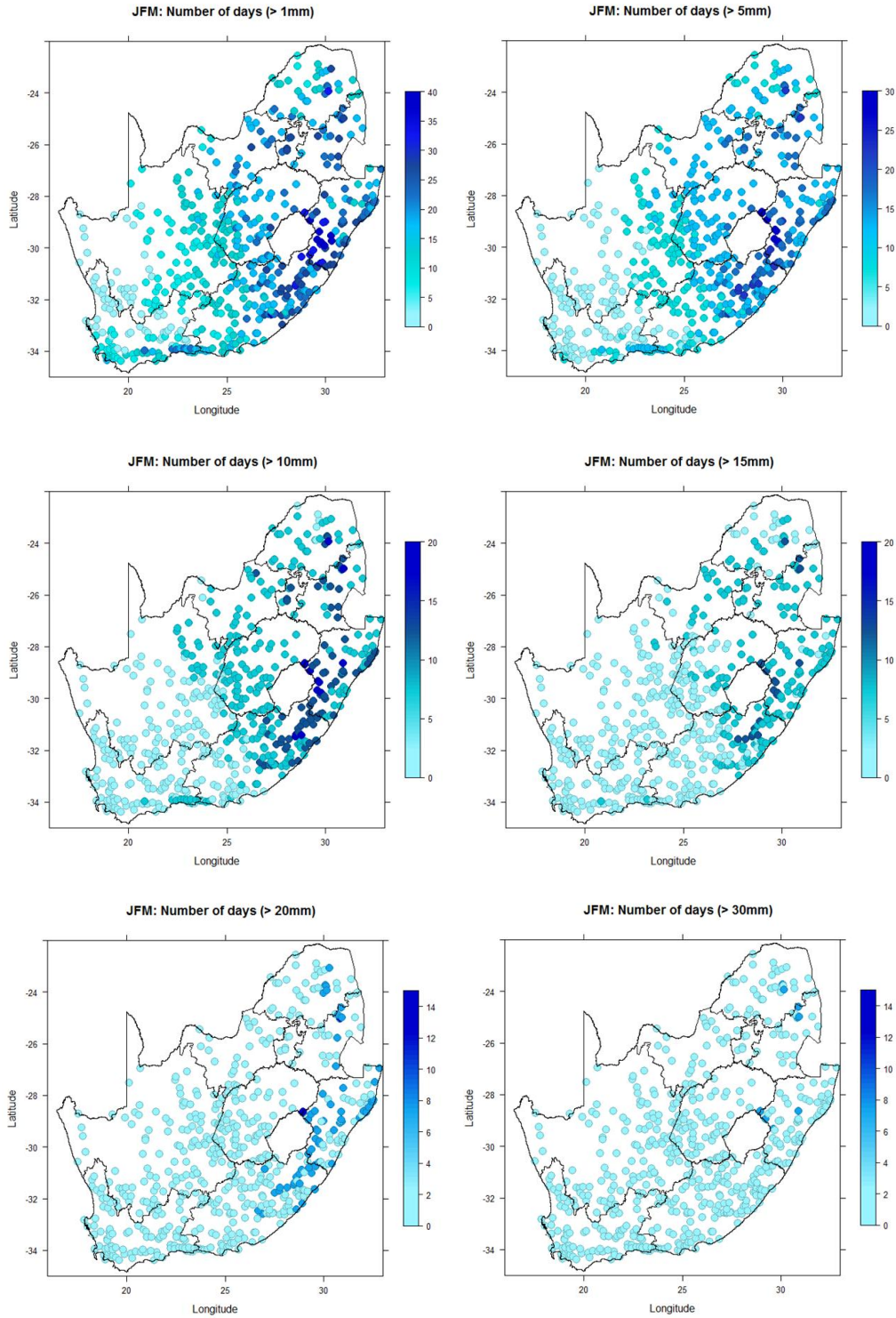


Figure 2.5. As in Figure 2.4, but for JFM seasons.

Large-scale 850hPa geopotential height fields of both the OAGCM and the AGCM from 1982 to 2009 are used as predictor fields. The 850hPa geopotential heights are used in this study because they are found to be a good predictor of seasonal rainfall over South Africa (e.g. Landman and Goddard, 2002; Landman and Beraki, 2012; Landman *et al.*, 2012, 2014). A number of various large-scale parameters as predictors in MOS downscaling has been tested before and found that 850hPa geopotential heights are the single field predictor providing marginally better forecast skill for rainfall over southern Africa (Landman and Goddard, 2002). This result has been used in a number of follow-up papers that successfully demonstrated the use of this variable as predictor (Landman and Beraki 2012, Landman *et al.* 2012, 2014). The reason why this variable is so successfully applied in statistical downscaling is because the circulation at this atmospheric level is effectively surface circulation over our region.

Both the two-tiered or uncoupled and coupled GCMs covers the global domain, however for the purpose of this study the domain used for statistical downscaling is set to 10N-50S latitudes and 20W-70E longitudes. The hindcast fields of both the GCMs are initialized at different lead-times for OND, NDJ, DJF and JFM seasons. For a 1-month lead-time for the two-tiered system, there are about 3 weeks from the issuance of the forecast to the beginning of the forecast season, meaning that a 0-month lead-time forecast for the DJF season is produced at the beginning of December, 1-month lead-time forecast in early November, 2-month lead-time forecast in early October, 3-month lead-time forecast in early September, and so on (Landman *et al.*, 2012). For the coupled system, there are at least 4 weeks between the production of the forecast and the first month of the forecast season (Landman *et al.*, 2012). For example, DJF forecasts at a 0-month lead-time are produced near the end of November, 1-month lead-time forecast at the end of October, 2-month lead-time forecast at the end of September, 3-month lead-time forecasts at the end of August, 4-month lead-time forecasts at the end of July, and so forth.

2.3. Model Output Statistics

Due to the relatively low spatial resolution of GCMs downscaling of the global model output to a higher resolution to capture local observations through the correction of systematic deficiencies in the global model is required (Landman and Beraki, 2012). Using the canonical correlation analysis (CCA) option of the Climate Predictability Tool (CPT) developed at the IRI (<http://iri.columbia.edu>) the hindcast outputs of both the AGCM and the OAGCM are statistically

recalibrated and downscaled to the observed seasonal rainfall totals and number of rainfall days exceeding 1mm, 5mm, 10mm, 15mm, 20mm, 30mm, 40mm and 50mm rainfall threshold values as well as onset months of the rainy seasons over South Africa by using the model output statistics (MOS). MOS is a multiple linear regression technique in which predictands are related to one or more predictors. CCA is a multivariate statistical technique to determine optimal linear combination of two sets of data (predictors and predictands) that are highly correlated and is also used to build statistical downscaling models (Landman *et al.*, 2009). MOS equations are developed to correct systematic biases in weather forecasts, as well as statistically correct climate model biases (Landman and Beraki, 2012; Wong *et al.*, 2014). It must be noted that in this work we did not run the models, but only done statistical downscaling. A schematic diagram on how downscaling has been done can be found in Bartman *et al.* (2003).

For climate models, MOS infers a correction function between model simulations and the corresponding observations and applies this correction function to a future simulation with the same model (Wong *et al.*, 2014). In constructing the CCA model, the empirical orthogonal function (EOF) analysis is performed because the predictor and the predictand fields contain a large number of highly correlated variables and few observations (Landman *et al.*, 2001; 2009). EOF analysis provides a set of orthogonally-based vectors to convert a data set containing a large number of variables into a set containing fewer new variables. These new variables are linear combinations of the original ones, which are chosen to represent a larger fraction of the variability contained in the original data. The number of EOF modes to be retained in the analysis is determined using cross-validation forecast skill sensitivity tests. The combination producing the highest area-average correlation is used as the best estimate of the number of predictor and predictand modes. The first CCA pair gives the maximum correlation between the two parameters, followed by the second CCA pair, and so on. CCA has the main advantage of selecting pairs of spatial patterns that are optimally correlated, making a physical interpretation of the connection between the observations and the retroactive forecasts or hindcasts possible (Busuioc *et al.*, 2001).

The CPT tool have two options to train the MOS models, namely cross-validation and retro-active options. The cross-validation is performed to determine the relation between the forecasts (predictor) and the observed (predictand) at each location over the domain of interest. The cross-validation procedure applied here is as follows: firstly leave the first year out of the training sample;

secondly reconstruct the model using the new smaller training sample, i.e., without the omitted year; thirdly forecast the omitted year; and lastly repeat by omitting subsequent years until a forecast has been made for each year of the training sample. In this study for a training sample from 1982 to 2009, firstly the 1982 year is left out and an initial training period of 1983 to 2009 is used to construct a model and predict the 1982 year. The 1983 year is omitted and the 1984 to 2009 including 1982 is used as training period and to reconstruct a model as well as to predict the 1983 year. The process is repeated until a forecast of each year has been made. However cross-validation has a tendency of overestimating forecast skill (Landman *et al.*, 2001).

On the other hand, retro-active forecast validation is a robust method to assess forecast model performance and give unbiased skill levels (Landman *et al.*, 2001). The retro-active procedure is as follows: firstly usually half of the training sample is used as training period; secondly reconstruct the model using that training period; thirdly forecast the year that follows the last year of the training period; lastly repeat the process by adding one year to the training period and then predict subsequent year until a forecast has been made for each year of the training sample. For this study an initial training period of 14 years from 1982 to 1995 out of a training sample of 28 year from 1982 to 2009 is used to construct the model and to forecast the 1996 year. A training period of 1982 to 1996 is used to reconstruct a model and forecast the 1997 year. The process is repeated for each of the subsequent years until a forecast of each year has been made.

2.4. Verification of forecasts

Forecast verification is the process of determining the quality of a forecast through assessment of the degree of similarity between that forecast and the observed conditions (Mandal *et al.*, 2007). Verification of forecasts is mostly performed to check if there is a strong relationship between the forecasts and the observations and if the results provide an accurate indication of how good or bad subsequent forecast will be (Mason, 2008). For verifying seasonal probabilistic forecasts relative operating characteristics (ROC) and reliability or attribute diagrams are mostly used (e.g. Landman *et al.*, 2012; Landman and Beraki, 2012)

2.4.1. ROC

ROC is based on signal detection theory and seeks to measure the signal and noise contained in the forecast information in the form of hits to misses ratios when measured against performance level (Zhang and Casey, 2000). The idea of ROC comes from quality control and signal detection theory where the quality of performance is assessed by the correlation between hit and false alarm rates as the decision criterion varies (Zhang and Casey, 2000). The graph in Figure 2.6 shows a typical ROC curve diagram for a skillful model. The ROC curve has the following properties as in Zhang and Casey (2000) as follows: A perfect model locates at the point (0, 1) in the coordinates of false alarm rate and hit rate; The worst forecasting model locates at the point (1, 0) in which the model gives either 0% or 100% probabilistic forecasts but no correct forecasts against observations. Constant value forecasts and random forecasts will locate on the no skill line (diagonal line). The shape of the ROC curve gives a total description of the skill of the model forecasts at all probability thresholds. A model with good skill will have its ROC curve located above and to the left of the diagonal line and a model with no skill compared with the random or constant forecast will be located below and to the right of the diagonal. ROC can be quantified by calculating the area beneath the ROC curve. The larger the area, the better the model skill. If the area is equal to or less than 0.5 of the whole (unit area), then the model is less skillful than a random or constant forecast.

2.4.2. Reliability Diagrams

The Reliability Diagram explain the resolution and reliability attributes which together determine the usefulness of probabilistic forecast systems (e.g. Brocker and Smith, 2007). Resolution measures the ability of a forecast system to resolve situations in which the observed frequency of the event is different to the climatological frequency, while reliability is a measure of the bias in predicted probabilities for the event, relative to the verified event frequency. A forecast with a good reliability is closer to the perfect reliability line (diagonal line) as in Figure 2.7. A forecast with good resolution has a wide range of frequency of observations corresponding to forecast probabilities. Resolution is considered the more fundamental of the two attributes, because reliability may generally be improved by calibration of the forecast probabilities, while resolution cannot. A forecast system that underestimate (overestimate) forecasts will have the forecast line positioned above (below) the perfect reliability line. The line halfway between climatology and perfect reliability is the no skill line and that is where the reliability and resolution are equal and

the brier skill score goes to zero. The histogram of forecasts in each probability bin shows the sharpness of the forecast.

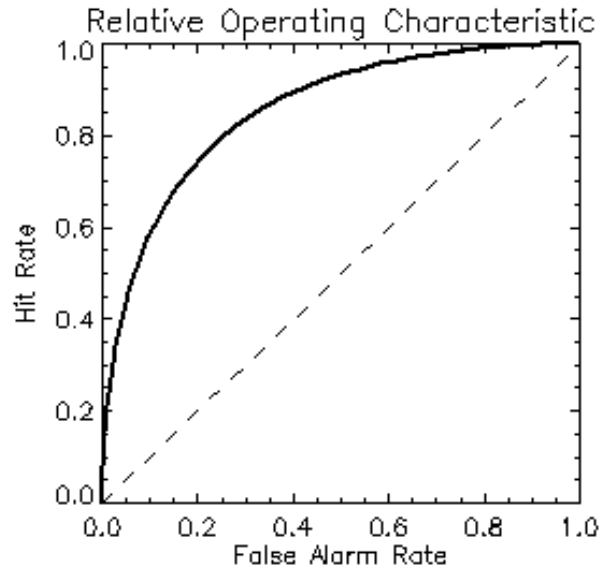


Figure 2.6. ROC curve diagram showing the hit rate and false alarm rate (adapted from www.cawcr.gov.au/projects/verification).

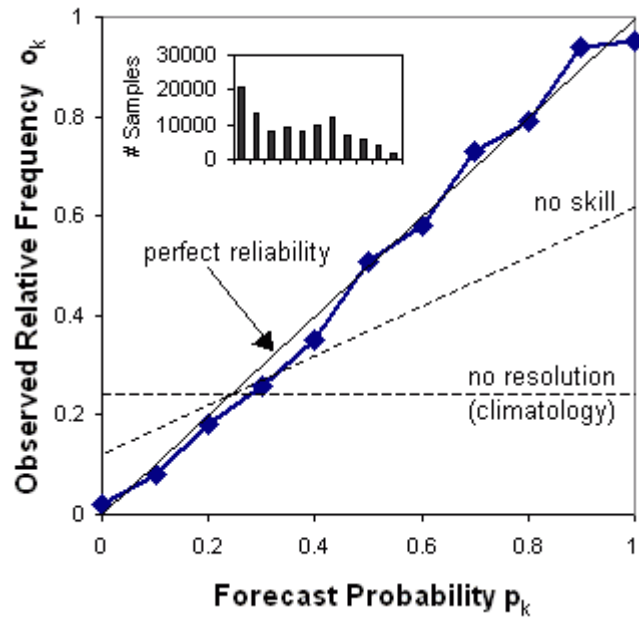


Figure 2.7. Reliability diagram (adapted from www.cawcr.gov.au/projects/verification).

2.4.3. Spearman's rank correlation

The Spearman's correlation coefficient is a statistical measure of the strength of a monotonic relationship between the independent variable (X) and the dependent variable (Y), and is computed as follows.

$$\rho = 1 - \frac{6 \sum d_i^2}{n(n^2 - 1)},$$

where n a sample size and $d_i = x_i - y_i$, is the difference between ranks.

The sign of the Spearman correlation indicates the direction of association between X and Y. If Y tends to increase when X increases, the Spearman correlation coefficient is positive, whereas if Y tends to decrease when X increases, the Spearman correlation coefficient is negative. A Spearman correlation of zero indicates that there is no tendency for Y to either increase or decrease when X increases. The Spearman correlation increases in magnitude as X and Y becomes close to being perfect monotone functions of each other. When X and Y are monotonically related, the Spearman correlation coefficient becomes 1. A perfect monotone increasing relationship implies that for any pairs of data values X_i, Y_i and X_j, Y_j , that X_i minus X_j and Y_i minus Y_j always have the same sign. A perfect monotone decreasing relationship implies that these differences always have opposite signs.

2.5. CCA pattern analysis

CCA is a way of measuring the linear relationship between two multidimensional variables. CCA can be defined as the problem of finding two sets of basis vectors, one for x and the other for y, such that the correlations between the projections of the variables onto these basis vectors are mutually maximized. The purpose of performing CCA is to construct a model based on a truncated subset of EOF coefficients instead of using the original fields. The benefits of this truncation include reducing the amount of noise in the problem by eliminating the higher EOF modes, which poorly represent small-scale features of the fields, as well as using orthogonal functions to simplify to the mathematics. CCA pattern analysis is performed here to determine the relationship between the atmospheric circulation pattern and the observed variable of interest (e.g. rainfall).

The CCA analysis is achieved using the following formula,

Physical fields = Spatial pattern x Time scores

The sign of the product of spatial pattern and time scores (positive or negative) determine the relationship between the circulation pattern and the observed variable. For example, when using geopotential heights to predict rainfall, if the product sign of the geopotential heights and the time scores is positive (negative) and the product sign of the rainfall and time scores is negative (positive). It imply that when there are high (low) pressure systems over a domain of interest there are tendency of an area of interest to receive less (more) rainfall.

2.6. Synopsis

This chapter described the data and methodology that are going to be used in the verification of results and a discussion thereof. The ROC, the reliability diagrams and the Spearman's correlation will be used to verify the forecasting systems. In addition to the verification of the forecasting system, CCA pattern analysis will be used to determine the relationship between the atmospheric circulation patterns and the observed variables. The following chapter presents a thorough details of the results of the predictability of seasonal rainfall totals over South Africa.

CHAPTER 3

PREDICTABILITY OF SEASONAL RAINFALL TOTALS FOR SUMMER SEASONS

This chapter describes the verification results for both the OAGCM and the AGCM administered at SAWS in predicting 3-months seasonal rainfall totals for OND, NDJ, DJF and JFM over South Africa. The predictions are a result of statistical downscaling the low-level circulation (i.e. the 850hPa geopotential heights fields) of the models to rainfall stations distributed across South Africa. The models' forecast skill levels are assessed using ROC scores and reliability diagrams, as well as the Spearman's correlations. Although the aim of this research is to evaluate the models in predicting intra-seasonal rainfall characteristics over South Africa, in this chapter the models are first evaluated in predicting seasonal rainfall totals to determine whether the results of this study are comparable with previous studies. By doing this part of the work first it will subsequently be shown that the model configurations have been set up properly and from these configurations additional properties of the season may be predicted. In addition to the forecast verification, CCA pattern analysis is also performed in order to determine the dominating atmospheric circulation systems predicted to be controlling rainfall totals for the summer seasons.

3.1. Probabilistic forecast skill

3.1.1. ROC scores

Using the predicted 850hPa geopotential heights of both the OAGCM and the AGCM at 0- to 4-month lead-times the ROC scores in downscaling the rainfall stations for OND, NDJ, DJF and JFM seasons over South Africa are calculated. A model that has acceptable forecast skill must have a ROC score of above 0.5, with a score close to 1 the better. The ROC scores values for the OAGCM and the AGCM are shown in Table 1 and Table 2, respectively. Both models show to have skill in predicting both the above-normal (wet conditions) and below-normal (dry conditions) at different lead-times. For the OAGCM prediction system, highest scores are found during NDJ and DJF seasons, with lowest scores found during OND and JFM seasons (Figure 3.1). In predicting wet conditions highest scores are found at 3- and 4-month lead-times during NDJ seasons as well as at 2-month lead-time during DJF seasons. When predicting dry conditions highest scores are found at 3-month and 0-month lead-times during NDJ and DJF, respectively.

The lowest score of less than 0.5 are found at 1- and 3-month lead-times in predicting wet conditions for OND seasons as well as at 3-month lead-time for JFM seasons. When predicting dry conditions lowest scores are found at 3- and 4-month lead-times during OND seasons.

For the AGCM prediction system, highest ROC scores in predicting wet conditions are found at 3-month lead-time during the NDJ seasons and at 0-, 2-, 3- and 4-month lead-times during DJF seasons as well as at 1-month lead-time during JFM seasons. When predicting dry conditions the highest scores are found at 2- and 3-month lead-times during NDJ as well as 4- and 1-month lead-times during DJF and JFM, respectively. The system is performing poorly when predicting wet conditions for OND at 1- to 3-month lead-times as well as for JFM at 3- and 4-month lead-times. In predicting dry conditions the lowest scores are found at 1- and 3-month lead-times for OND, whereas for JFM are found at 3- and 4-month lead-times.

Table 3.1. ROC scores of the OAGCM at 0- to 4-months lead-times in predicting seasonal rainfall totals for OND, NDJ, DJF and JFM over the 14 years retro-active forecasts from 1996 to 2009.

| ROC SCORES: OAGCM | | | | | |
|--------------------------------|----------------|----------------|----------------|----------------|----------------|
| ABOVE-NORMAL CATEGORIES | | | | | |
| SEASONS | 0-MONTH | 1-MONTH | 2-MONTH | 3-MONTH | 4-MONTH |
| OND | 0.506 | 0.490 | 0.502 | 0.478 | 0.510 |
| NDJ | 0.581 | 0.625 | 0.637 | 0.677 | 0.650 |
| DJF | 0.639 | 0.562 | 0.662 | 0.623 | 0.615 |
| JFM | 0.502 | 0.596 | 0.518 | 0.479 | 0.560 |
| BELOW-NORMAL CATEGORIES | | | | | |
| SEASONS | 0-MONTH | 1-MONTH | 2-MONTH | 3-MONTH | 4-MONTH |
| OND | 0.531 | 0.517 | 0.552 | 0.405 | 0.494 |
| NDJ | 0.561 | 0.604 | 0.601 | 0.632 | 0.622 |
| DJF | 0.648 | 0.586 | 0.612 | 0.616 | 0.577 |
| JFM | 0.540 | 0.582 | 0.573 | 0.550 | 0.542 |

Table 3.2. As in Table 1, but for the AGCM.

| ROC SCORES: AGCM | | | | | |
|--------------------------------|----------------|----------------|----------------|----------------|----------------|
| ABOVE-NORMAL CATEGORIES | | | | | |
| SEASONS | 0-MONTH | 1-MONTH | 2-MONTH | 3-MONTH | 4-MONTH |
| OND | 0.518 | 0.429 | 0.481 | 0.459 | 0.561 |
| NDJ | 0.603 | 0.546 | 0.619 | 0.654 | 0.587 |
| DJF | 0.643 | 0.588 | 0.597 | 0.611 | 0.602 |
| JFM | 0.524 | 0.625 | 0.543 | 0.494 | 0.464 |
| BELOW-NORMAL CATEGORIES | | | | | |
| SEASONS | 0-MONTH | 1-MONTH | 2-MONTH | 3-MONTH | 4-MONTH |
| OND | 0.534 | 0.470 | 0.532 | 0.474 | 0.569 |
| NDJ | 0.584 | 0.552 | 0.605 | 0.622 | 0.551 |
| DJF | 0.597 | 0.562 | 0.567 | 0.534 | 0.613 |
| JFM | 0.533 | 0.607 | 0.563 | 0.471 | 0.405 |

Although both prediction systems have skill in predicting seasonal rainfall totals for stations across South Africa, the OAGCM outperforms the AGCM in predicting both wet and dry conditions. As anticipated OAGCM is superior to AGCM because the former is able to explain the feedback between the ocean and atmosphere, while the latter assumed that the atmosphere respond to SST but does not in turn affect the oceans (Landman *et al.*, 2012). In fact, Landman *et al.* (2012) also found that ocean-atmospheric climate models outperform atmospheric models when predicting austral summer rainfall seasons over South Africa.

The results of the ROC scores presented here in predicting seasonal rainfall over South Africa are in agreement with the results found in Landman *et al.* (2012). They also found the highest scores during NDJ and DJF with higher scores found when predicting wet seasons as compared to dry seasons over South Africa. According to Landman *et al.* (2012) most of the predictability is found during these two seasons because tropical influence start to dominate the atmospheric circulation across South Africa. They further indicated that there is almost no predictability during

austral spring because during this time the seasonal rainfall of South Africa is mostly influenced by transient weather systems. In fact, the ROC scores for OND seasons in this study are close to 0.5 for all the lead-times, especially for the AGCM. Such transient systems are usually not predictable at seasonal time scales. In addition, the seasonal forecast verification statistics of the IRI Climate Forecast Verification page (<http://iri.columbia.edu>) entirely based on AGCMs including ECHAM4.5 indicates that the season of highest rainfall predictability over South Africa is found during NDJ seasons (Landman *et al.*, 2012), which is in agreement with the results presented in this chapter.

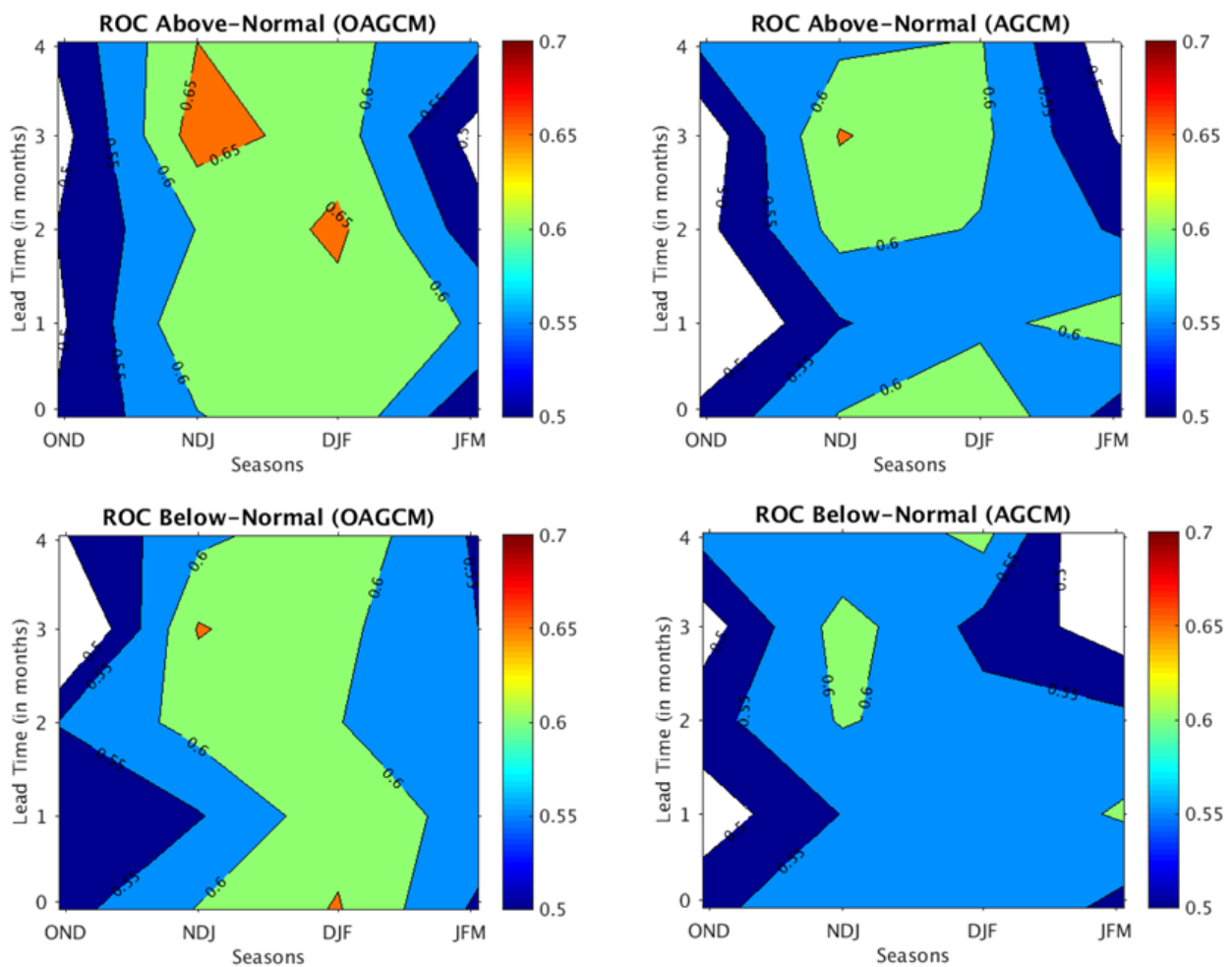


Figure 3.1: ROC scores of both the OAGCM (left panel) and the AGCM (right panel) at 0- to 4-month lead-times in predicting the seasonal rainfall for the summer rainy seasons over the 14 years retro-active forecasts from 1996-2009.

3.1.2. Reliability diagrams

Only the reliability diagrams for NDJ and DJF seasons are considered here since these two seasons have been found to be associated with the highest ROC scores. The reliability diagrams in Figure 3.2 indicates that when predicting wet conditions for NDJ seasons both the OAGCM and the AGCM at 0- to 3-month lead-times, the forecasts are generally over-confident, except that the OAGCM at 1- and 3-months lead-times as well as the AGCM at 3-month lead-time are under-confident. The forecasts for predicting wet conditions are reliable since the weighted least square regression lines are closer to the perfect reliability line as compared to predicting dry conditions. The frequency histograms indicates that the forecasts for both systems lack sharpness when predicting both wet and dry conditions. In general, the forecasts display a lack of sharpness because forecasts rarely deviate much from the climatological value of 33.3%. Low sharpness is common for South African rainfall prediction studies (Landman *et al.*, 2012, 2014).

When predicting both wet and dry conditions for DJF seasons the forecasts are also over-confident for both the systems, except for 2- and 3-month lead-times for the OAGCM and 3-month lead-time for the AGCM (Figure 3.3). The forecasts of both the systems show a high level of reliability when predicting wet conditions since the slopes of wet season regression lines are close to the slope of perfect reliability. In contrary, both the systems lack reliability when predicting dry conditions. The frequency histograms again indicate that both the systems lack sharpness when prediction both wet and dry conditions.

From the reliability diagrams presented here, it is evident that both the OAGCM and the AGCM systems are reliable when predicting wet conditions during DJF seasons. Generally forecasts for both the systems are under-confident (over-confident) when predicting wet (dry) conditions during DJF seasons. In fact, the climate models are over-confident when predicting dry conditions over South Africa. Forecasts display lack of sharpness when predicting rainfall over South Africa. Both the prediction systems predict DJF rainfall totals better as compared to NDJ, with the OAGCM outperforming the AGCM.

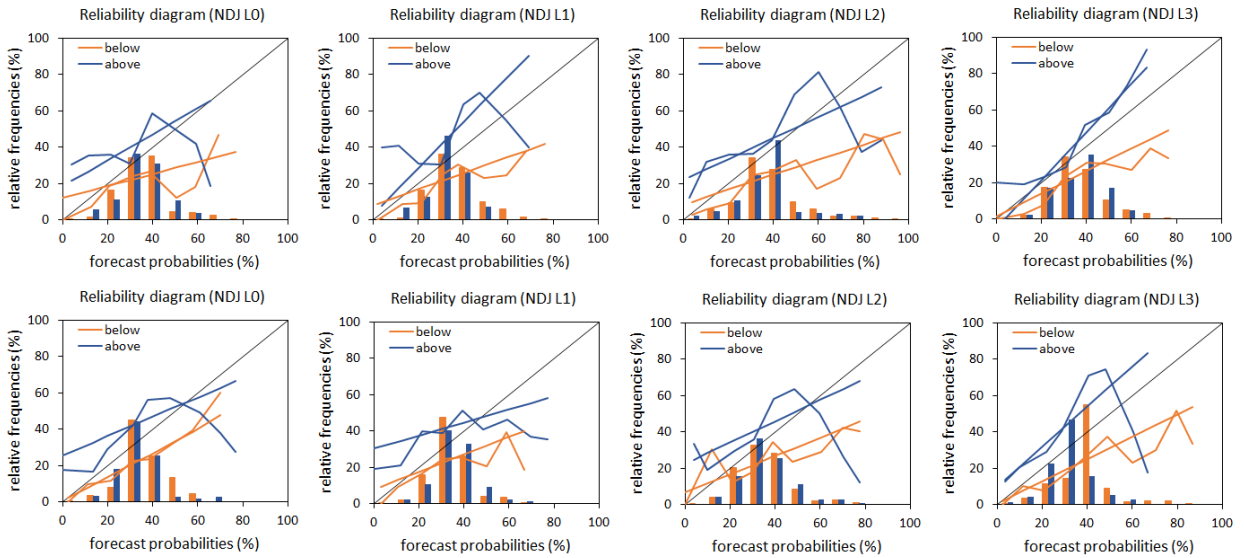


Figure 3.2. Reliability diagrams and frequency histograms for both the OAGCM (top panel) and the AGCM (bottom panel) at 0- to 3-months lead-time in predicting above- normal and below-normal rainfall totals for NDJ seasons.

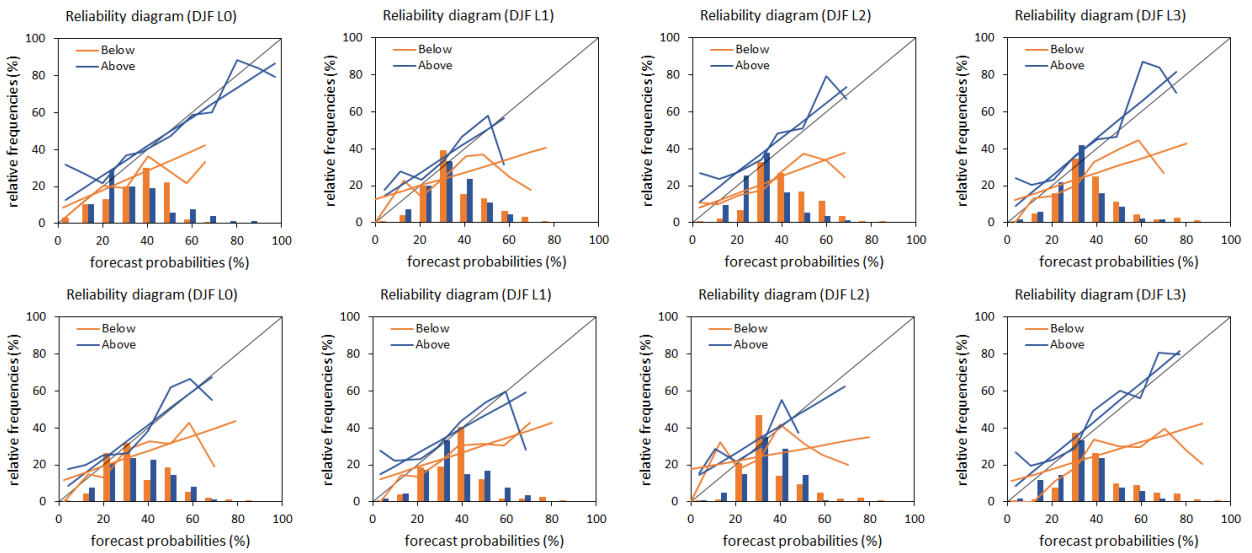


Figure 3.3. As in figure 3.2, but for DJF seasons.

3.2. Deterministic forecast skill

3.2.1. Spearman's rank correlations

Again only the Spearman's rank correlations for NDJ and DJF seasons are considered for the same reason that the two seasons have been found to be associated with highest ROC scores when predicting seasonal totals. The Spearman's correlations and their level of confidence for the stations distribution across South Africa in predicting NDJ rainfall totals at 0- to 3-month lead-times with retroactively downscaled forecasts for the OAGCM and the AGCM are shown in Figure 3.4 and Figure 3.5, respectively. For both models, positive highest correlations are found over the interior and towards the eastern parts of the country, as well as the southeastern parts. The lowest (negative) correlations are found over the northeastern and southwestern parts of the country. For the OAGCM, highest positive correlations are found when predicting rainfall totals during NDJ at 0- and 2-month lead-times, whereas for the AGCM, highest positive correlations are found at 0- and 1-month lead-times.

For DJF seasons, highest positive values are scattered across the country, except for the Western Cape and the South coast having highest negative correlations for both the OAGCM (Figure 3.6) and the AGCM (Figure 3.7). As compared to the NDJ seasons, positive values are extending into the northeastern parts of South Africa during DJF seasons. Once again the skill of the OAGCM system outperforms that of the AGCM, except for the 3-month lead-time where the AGCM correlations outscore the OAGCM during DJF seasons, especially over the central parts. Highest positive correlations are found at 0- and 3-month lead-times for the OAGCM and the AGCM, respectively, during DJF seasons.

The Spearman's rank correlation maps presented here show that both the prediction systems have high skill in predicting seasonal rainfall totals during DJF seasons as compared to NDJ seasons over South Africa. The high skill over the northeastern interior, east coast and part of the central as well as western interior during DJF seasons are in agreement with the results found by Landman *et al.* (2012). Both the models seem to have no skill over the Western Cape during NDJ and DJF seasons for all the lead-times.

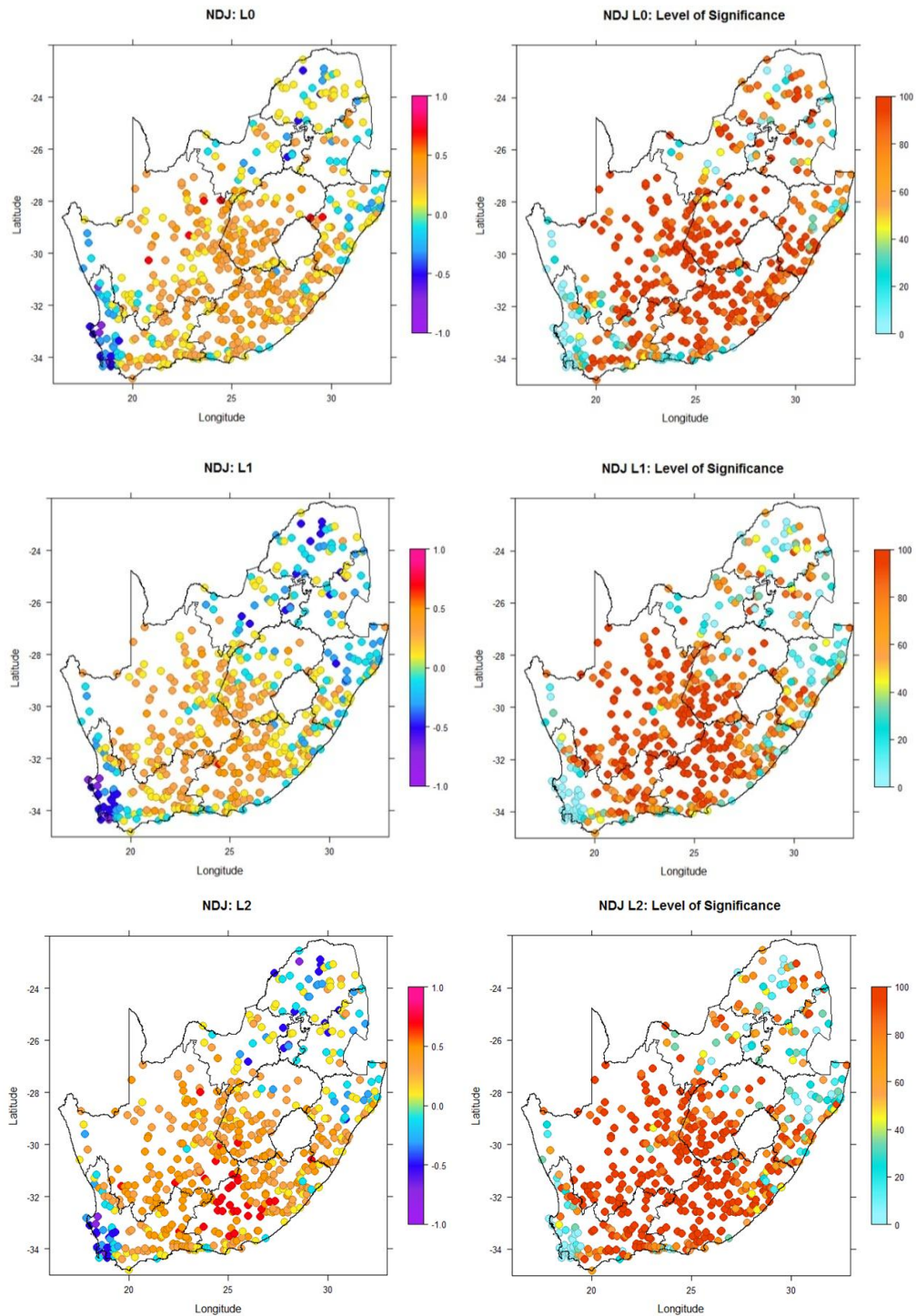


Figure 3.4. Spearman's rank correlations of the OAGCM (left panel) and their p-values level of significance (right panel) at 0- to 3-months lead-times (L0, L1, L2 and L3) for NDJ seasons over the 14 year retro-active forecasts from 1996 to 2009.

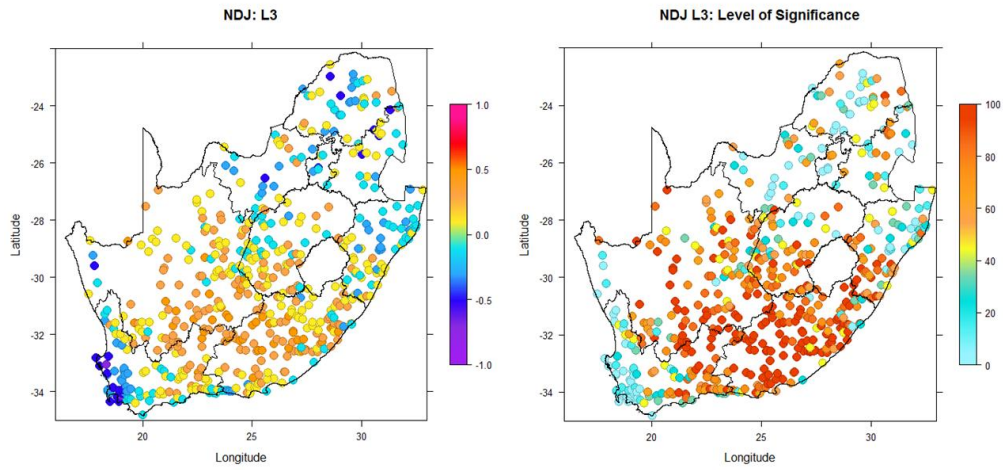
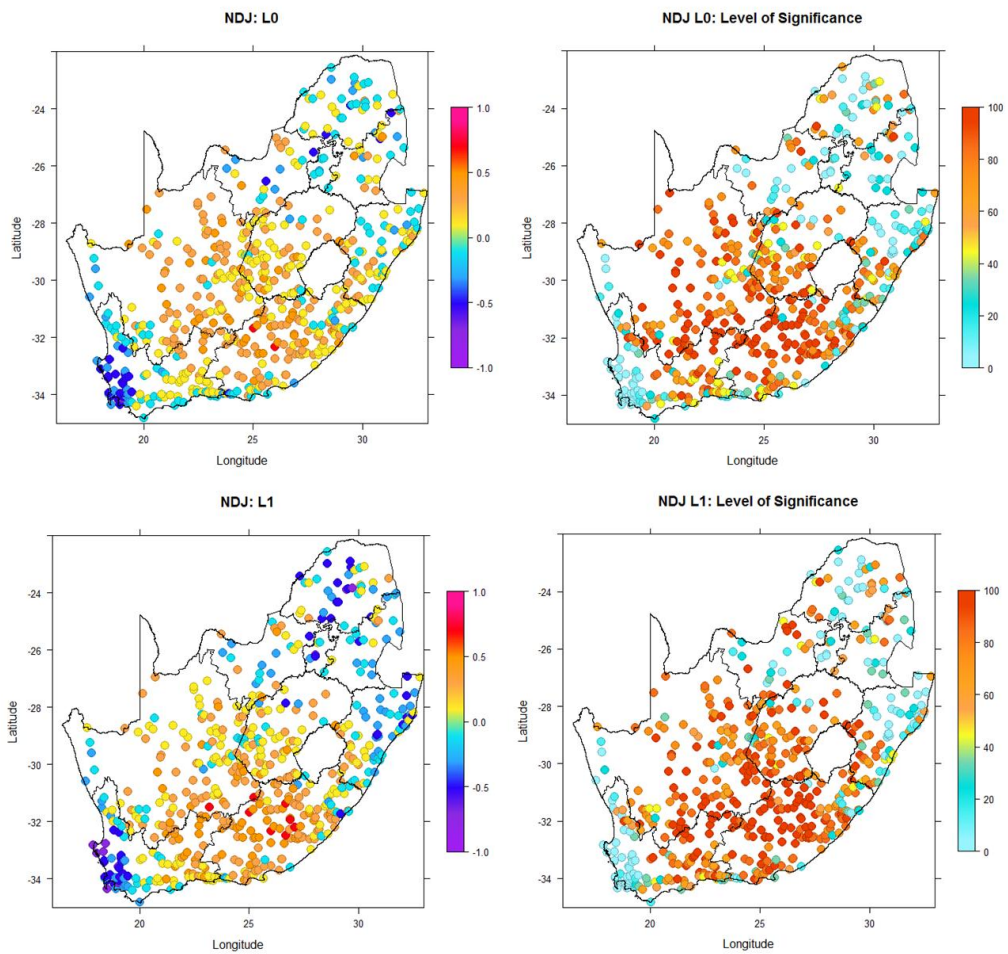


Figure 3.4. Continues.



3.5. As in Figure 3.4, but for the AGCM.

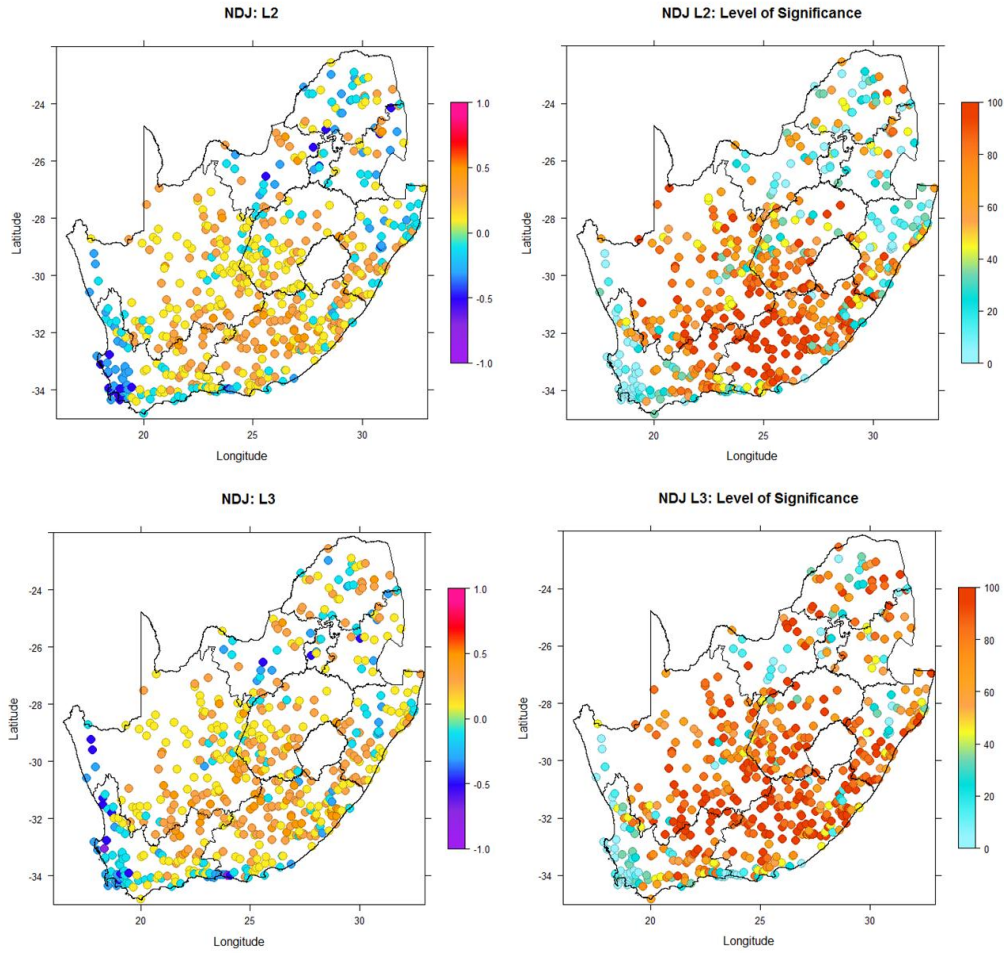


Figure 3.5. Continues.

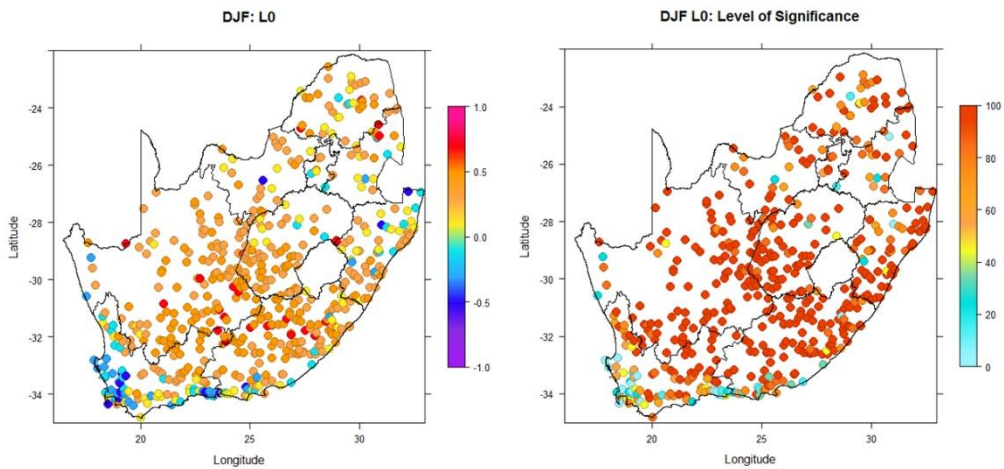


Figure 3.6. Spearman's rank correlations of the OAGCM (left panel) and their level of significance (right panel) at 0- to 3-months lead-times (L0, L1, L2 and L3) for DJF seasons over the 14 year retro-active forecasts from 1996 to 2009.

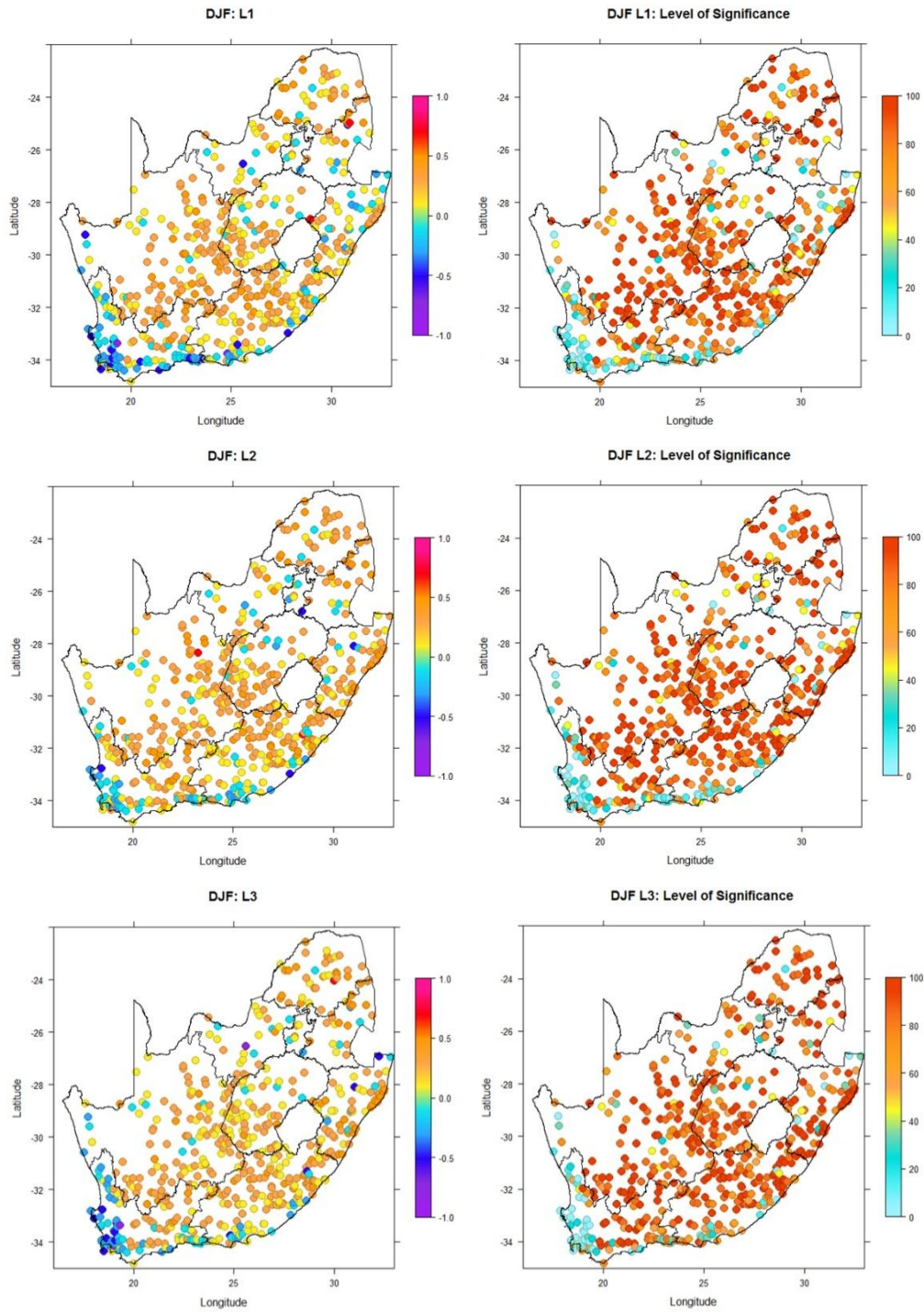


Figure 3.6. Continues.

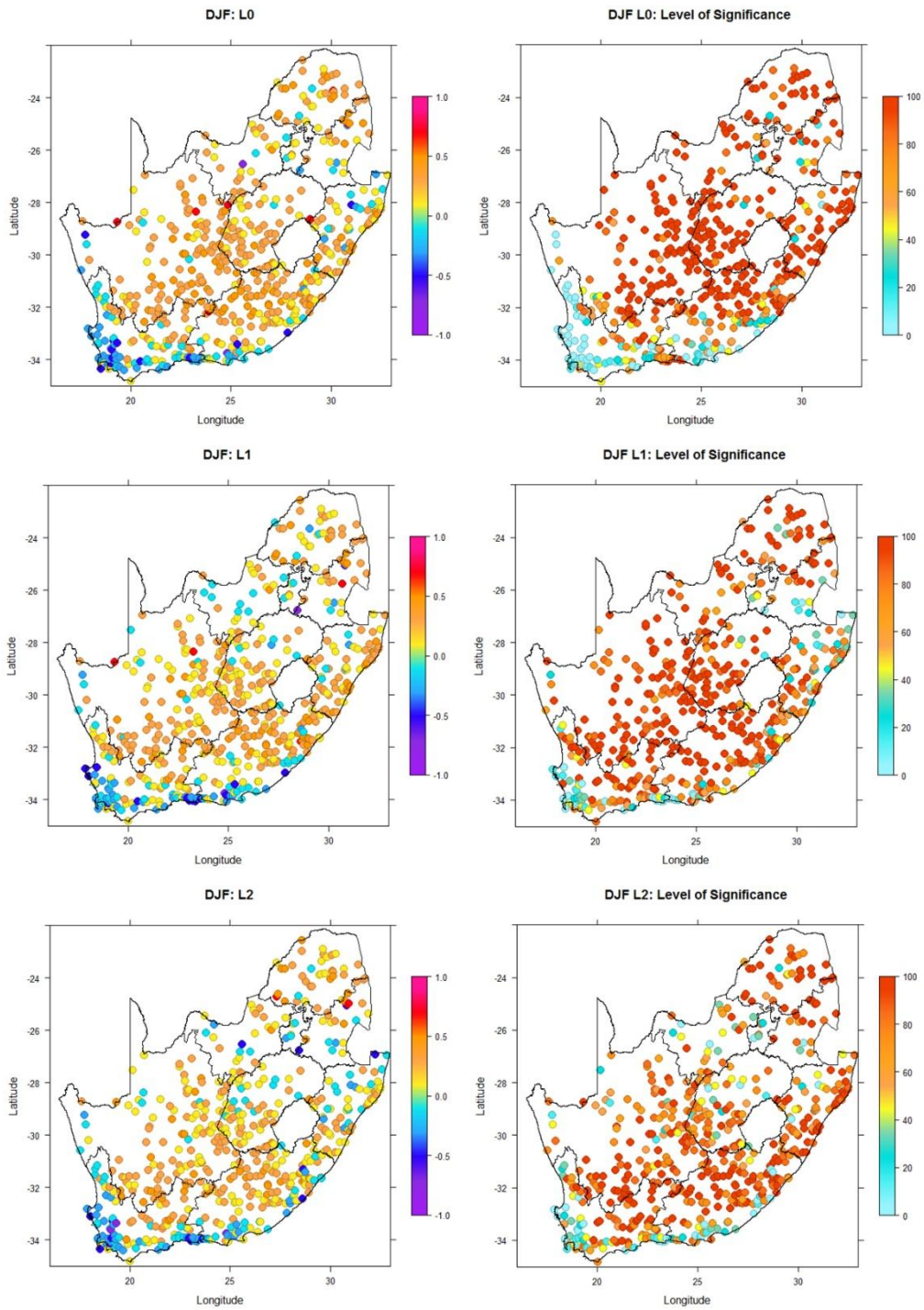


Figure 3.7. As in Figure 3.6, but for the AGCM.

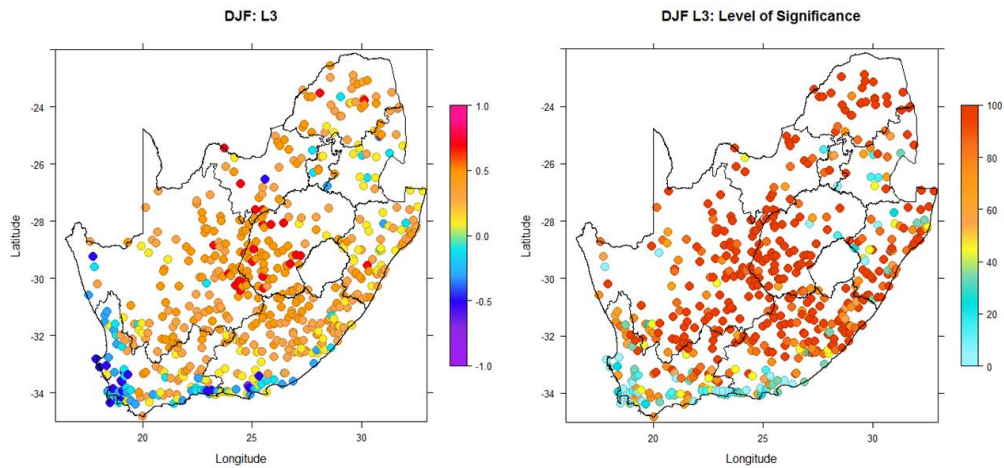


Figure 3.7. Continues.

3.3. CCA pattern analysis

When predicting climate variables such as rainfall, insight into the physical mechanism responsible for forecast skill is beneficial. In order to understand how the predicted atmospheric circulation patterns are configured so that skillful forecast can be made, several analysis methods such as cluster analysis, self-organizing maps (SOM) and canonical correlation analysis (CCA), among others, can be considered. In this study CCA pattern analysis is performed to investigate the relationship between the predicted 850hPa geopotential heights (predictors) for both the OAGCM and the AGCM at 1-month lead-time and the downscaled rainfall totals (predictands) for OND, NDJ, DJF and JFM, respectively. CCA maps for both the OAGCM and the AGCM indicate that in when there are anomalously negative (positive) 850hPa geopotential heights (x spatial loadings) over South Africa there are anomalously wet (dry) rainfall conditions (y spatial loadings) over South Africa for summer seasons as depicted in Figure 3.8 and Figure 3.9.

For NDJ and DJF seasons during 1982 and 2006, for example, the predictor's spatial loadings for both models are anomalously negative and the temporal scores are also negative as shown in Figure 3.8 (b and c) and Figure 3.9 (b and c), respectively. The product of the predictor's spatial loadings and the time scores is positive. During the same years over most parts of South Africa, the rainfall spatial loadings are positive and the temporal scores are negative, and their product is negative. This result implies that when there are anomalously positive 850hPa geopotential

heights over South Africa there are anomalously dry conditions over South Africa. In fact, when there is a high pressure system over the interior of South Africa it draws out the moist air out of the country and usually the country remain dry.

For both the OAGCM and the AGCM during NDJ and DJF seasons but this time during 1999 and 2007 there are anomalously negative predictor's spatial loadings over South Africa and the time scores are positive, and their product is negative. During the same years the rainfall spatial loadings over most parts of South Africa are anomalously positive and the time scores are positive. The product of rainfall spatial loadings and the time scores is positive. Likewise this implies that when there are anomalously negative 850hPa geopotential heights over South Africa there are anomalously wet conditions over most parts of South Africa. Usually when there is a low pressure system over the interior of South Africa during summer seasons, it advects the moist air into the country and usually results in rainfall events.

During most of the El Niño years, e.g. 1982, 1986, 1991, 1994, 2003 and 2006 (http://www.cpc.ncep.noaa.gov/products/analysis_monitoring/ensostuff/ensoyears.shtml) during NDJ and DJF seasons for both the OAGCM and the AGCM there were high pressure systems over South Africa, which suppressed rainfall and results in dry conditions over the country. This results support the notion that during most of the El Niño episodes South Africa tend to be drier than normal. Most notably, during the strong events of 1982 and 1991 where South Africa experienced severe droughts. It must be noted however that during the 1997 and 2009 El Niño events most parts of South Africa was not dry as anticipated. In fact, most parts received above-normal rainfall.

On the other hand, during most of the La Niña years, namely, 1984, 1988, 1995, 1999 and 2007 (http://www.cpc.ncep.noaa.gov/products/analysis_monitoring/ensostuff/ensoyears.shtml) also during NDJ and JFM seasons for both the OAGCM and the AGCM there were low pressure systems over South Africa which draw moist air into the country resulting in wet conditions. This results also agrees with the fact that during La Niña events South Africa mostly experience wet conditions than normal. For example, the 1999 event left most of the summer rainfall areas of South Africa wetter than normal, including floods in some areas.

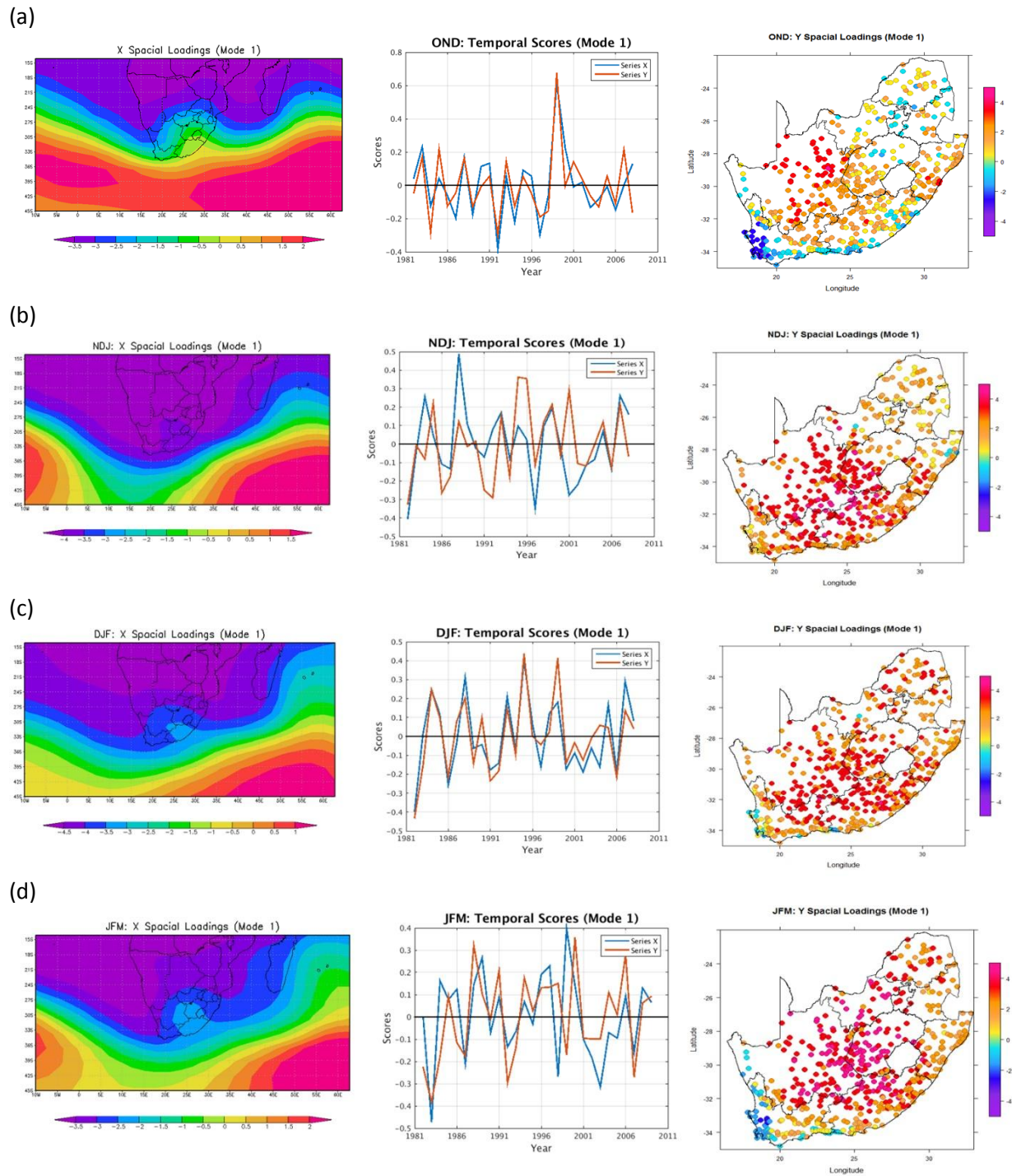


Figure 3.8. Mode 1 CCA maps of the 850hPa geopotential heights of the OAGCM and the downscaled seasonal rainfall totals for (a) OND, (b) NDJ, (c) DJF, and (d) JFM. The X spatial loadings and the Y spatial loadings maps are for the predictors and the predictands, respectively.

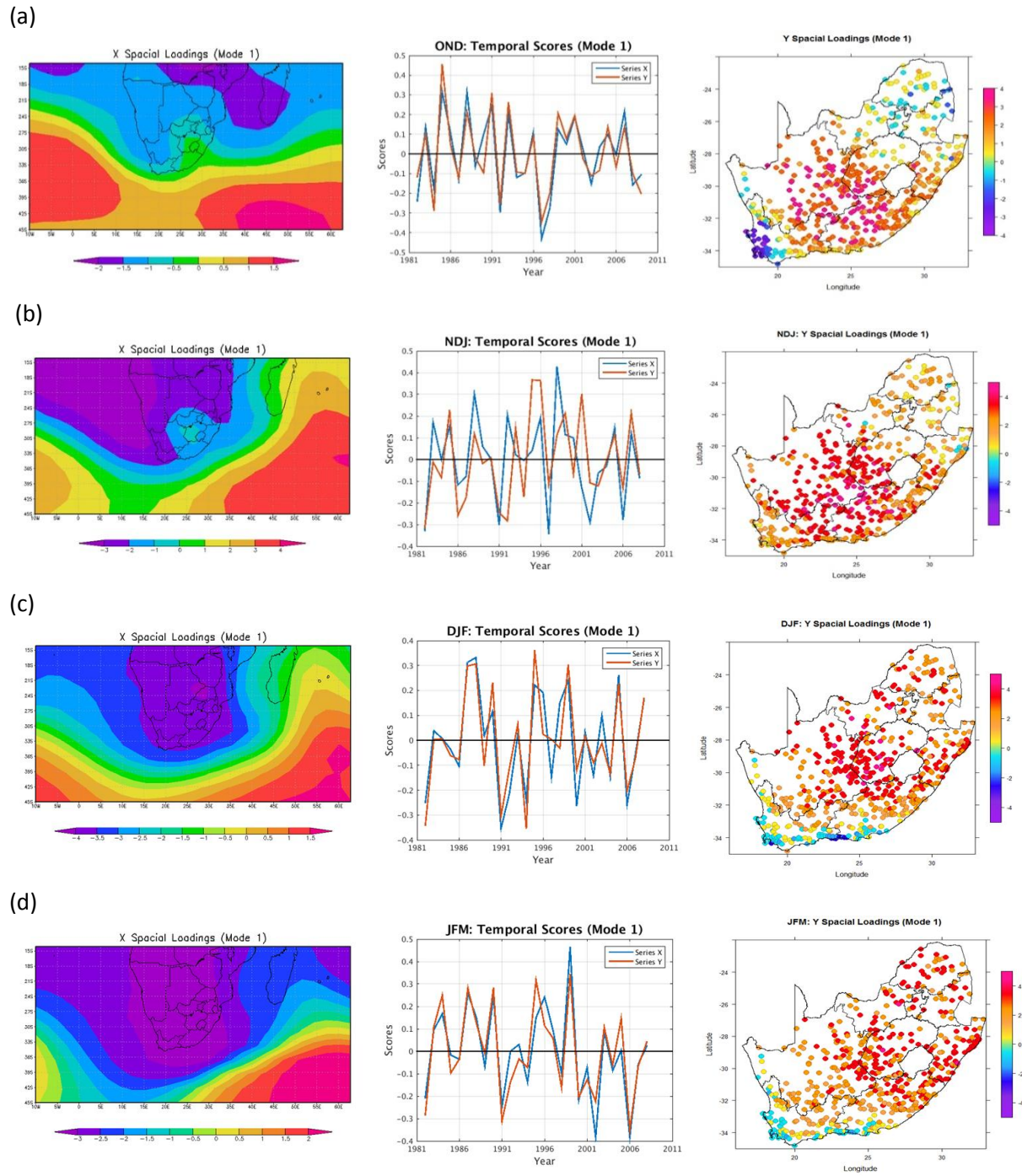


Figure 3.9. As in Figure 3.8, but for the AGCM.

3.4. Synopsis

In this chapter the skill levels of both the OAGCM and the AGCM in predicting the 3-month seasonal rainfall totals for OND, NDJ, DJF and JFM over South Africa are evaluated. The ROC scores show that both the models have skill in predicting seasonal rainfall totals over South Africa, especially during NDJ and DJF seasons. The coupled model seem to outperform the uncoupled one. The reliability diagrams indicate that the predicted 850hPa geopotential heights of both the models are over-confident (under-confident) when predicting dry (wet) conditions during NDJ seasons. For the DJF seasons the reliability diagrams indicate that both models are reliable in predicting wet conditions, however the forecasts for both systems are always over-confident when predicting dry conditions. The Spearman's rank correlation coefficients also indicate that the OAGCM outperforms the AGCM in predicting the seasonal rainfall totals during NDJ and DJF seasons, and both models predict DJF rainfall better as compared to NDJ rainfall. CCA pattern analysis results presented here suggest that same physical mechanism of atmospheric circulation patterns are responsible for rainfall during summer seasons. It was found that when there are anomalously negative (positive) predicted 850hPa geopotential heights over South Africa it is associated with anomalously wet (dry) conditions for most parts of South Africa. In addition ENSO episodes have significant influence in rainfall of South Africa, with the El Niño associated with dry seasons and La Niña with wet seasons. In fact, the results presented in this chapter are in agreement with previous studies of seasonal rainfall predictions in South Africa and subsequently it shows that the model configurations have been set up properly and from these configurations additional properties of the season can be predicted. The following chapter presents the results of the predictability of number of rainfall days exceeding pre-defined threshold values over South Africa.

CHAPTER 4

PREDICTABILITY OF RAINFALL DAYS EXCEEDING PRE-DEFINED THRESHOLD VALUES WITHIN SUMMER RAINY SEASONS

In this chapter the verification results of both the OAGCM and the AGCM in predicting intra- (within) seasonal rainfall characteristics are presented. For this purpose the number of predicted rainfall days exceeding 1mm, 5mm, 10mm, 15mm, 20mm, 30mm, 40mm and 50mm threshold values for the six run-on seasons of OND, NDJ, DJF and JFM over South Africa are verified. The predictions are a result of retro-active statistical downscaling the 850hPa geopotential height fields of the global models to the number of rainfall days exceeding the above mentioned thresholds for the rainfall stations distributed across South Africa. Like in the previous chapter, the downscaled skill levels are assessed using ROC scores and reliability diagrams, as well as the Spearman's rank correlations. CCA pattern analysis is once again performed in order to determine the dominating atmospheric circulation systems predicted to be controlling rainfall and in turn the number of rainfall days exceeding the pre-defined threshold values for the various seasons considered.

4.1. ROC scores

The predicted 850hPa geopotential heights of both the OAGCM and the AGCM at 1-month lead-time are downscaled to the number of rainfall days exceeding the pre-defined threshold values for OND, NDJ, DJF and JFM seasons over South Africa. ROC scores for high- and low-number of rainfall days exceeding threshold values are then calculated for both the GCMs. As mentioned in the previous chapter the ROC scores higher than 0.5 are considered skillful. Table 1 and Table 2 show ROC score values for the OAGCM and the AGCM, respectively, in predicting the statistically downscaled threshold values. Both models have skill because the scores are higher than 0.5.

The skill is high during NDJ and DJF seasons for the OAGCM system as compared to OND and JFM seasons, with highest skill found in predicting 1mm and 5mm during DJF as well as 10mm during NDJ (Figure 4.1). In fact, the forecast skill of the OAGCM in predicting the high-number of rainfall days is limited to 30mm. However, it must be noted that in predicting the number of days exceeding 5mm threshold the ROC score is less than 0.5 for NDJ seasons. Furthermore, the skill is decreasing with higher threshold values when predicting the high-number of rainfall days. On the other hand, the skill in predicting the low-number of rainfall days is increasing with higher threshold values. The increasing of skill is due to the fact that there are fewer low-number of rainfall days to count for higher thresholds.

For the AGCM prediction system, the highest scores is found when predicting the high-number of rainfall days exceeding 1mm and 5mm during NDJ and DJF, respectively, as well as 10mm during JFM seasons (Figure 4.1). As with the OAGCM, the skill of the AGCM in predicting the high-number of rainfall days is limited to 30mm and is also decreasing with higher threshold values as well as increasing with higher threshold values when predicting low-number of rainfall days. Like the OAGCM, the AGCM perform poorly with ROC score of less than 0.5 in predicting the 5mm threshold during NDJ seasons.

Although both prediction systems have skill in predicting the number of rainfall days exceeding the pre-defined threshold values over South Africa, the OAGCM seem to outperform the AGCM in predicting both the high- and low-number of rainfall days. As mentioned in the previous chapter the OAGCM outperforms the AGCM because the former is able to explain the feedback between the ocean and atmosphere, while the latter assumed that the atmosphere respond to SST but does not in turn affect the oceans. The OAGCM is thus a better description of reality than the AGCM.

The ROC scores results presented here indicate that the predicted 850hPa geopotential heights for both the OAGCM and the AGCM can be used to predict the number of rainfall days exceeding the pre-defined thresholds. However, both models seem to predict better lower threshold values as compared to higher thresholds. In fact, both models can only be use to predict thresholds less than 30mm. Accurate predictions of high and low number of rainfall days exceeding threshold values can add value to seasonal rainfall predictions, since it provides detailed information on the

number rainy days within the season of interest. In fact, it can be deduced that a season with high (low) number of rainfall days is likely to receive above (below) normal rainfall, in turn wet (dry) spells. According to Tennant and Hewitson (2002) wet seasons generally have higher number of heavy rainfall days (> 20mm), suggesting that wet seasons are mostly dominated by heavier rainfall events as compared to numerous light rain events.

Table 4.1. ROC scores of the OAGCM at 1-month lead-time in predicting number of days exceeding seasonal rainfall totals for OND, NDJ, DJF and JFM over the 14 years retro-active forecasts from 1996 to 2009.

| ROC SCORES: OAGCM | | | | | | | | |
|-------------------------------------|-----------------|-----------------|------------------|------------------|------------------|------------------|------------------|------------------|
| HIGH-NUMBER OF RAINFALL DAYS | | | | | | | | |
| SEASONS | > 1mm | > 5mm | > 10mm | > 15mm | > 20mm | > 30mm | > 40mm | > 50mm |
| OND | 0.557 | 0.545 | 0.507 | 0.479 | 0.452 | 0.435 | 0.354 | 0.327 |
| NDJ | 0.612 | 0.453 | 0.656 | 0.583 | 0.578 | 0.501 | 0.429 | 0.359 |
| DJF | 0.682 | 0.657 | 0.632 | 0.590 | 0.548 | 0.499 | 0.448 | 0.394 |
| JFM | 0.637 | 0.636 | 0.629 | 0.589 | 0.546 | 0.472 | 0.405 | 0.333 |
| LOW-NUMBER OF RAINFALL DAYS | | | | | | | | |
| SEASONS | > 1mm | > 5mm | > 10mm | > 15mm | > 20mm | > 30mm | > 40mm | > 50mm |
| OND | 0.542 | 0.588 | 0.561 | 0.537 | 0.541 | 0.624 | 0.721 | 0.790 |
| NDJ | 0.589 | 0.496 | 0.604 | 0.609 | 0.605 | 0.647 | 0.696 | 0.724 |
| DJF | 0.643 | 0.633 | 0.636 | 0.614 | 0.601 | 0.624 | 0.669 | 0.766 |
| JFM | 0.637 | 0.643 | 0.639 | 0.628 | 0.620 | 0.675 | 0.714 | 0.751 |

Table 4.2. ROC scores of the AGCM at 1-month lead-time in predicting number of days exceeding seasonal rainfall totals for OND, NDJ, DJF and JFM over the 14 years retro-active forecasts from 1996 to 2009.

| ROC SCORES: AGCM | | | | | | | | |
|------------------------------|-------|-------|--------|--------|--------|--------|--------|--------|
| HIGH-NUMBER OF RAINFALL DAYS | | | | | | | | |
| SEASONS | > 1mm | > 5mm | > 10mm | > 15mm | > 20mm | > 30mm | > 40mm | > 50mm |
| OND | 0.564 | 0.557 | 0.539 | 0.547 | 0.503 | 0.437 | 0.347 | 0.329 |
| NDJ | 0.660 | 0.401 | 0.611 | 0.585 | 0.559 | 0.485 | 0.429 | 0.367 |
| DJF | 0.642 | 0.653 | 0.627 | 0.576 | 0.549 | 0.502 | 0.468 | 0.444 |
| JFM | 0.642 | 0.587 | 0.669 | 0.612 | 0.592 | 0.492 | 0.443 | 0.397 |
| LOW-NUMBER OF RAINFALL DAYS | | | | | | | | |
| SEASONS | > 1mm | > 5mm | > 10mm | > 15mm | > 20mm | > 30mm | > 40mm | > 50mm |
| OND | 0.554 | 0.568 | 0.569 | 0.583 | 0.546 | 0.615 | 0.696 | 0.772 |
| NDJ | 0.628 | 0.497 | 0.608 | 0.619 | 0.646 | 0.681 | 0.707 | 0.801 |
| DJF | 0.588 | 0.605 | 0.608 | 0.608 | 0.616 | 0.613 | 0.666 | 0.759 |
| JFM | 0.631 | 0.595 | 0.696 | 0.636 | 0.636 | 0.619 | 0.703 | 0.804 |

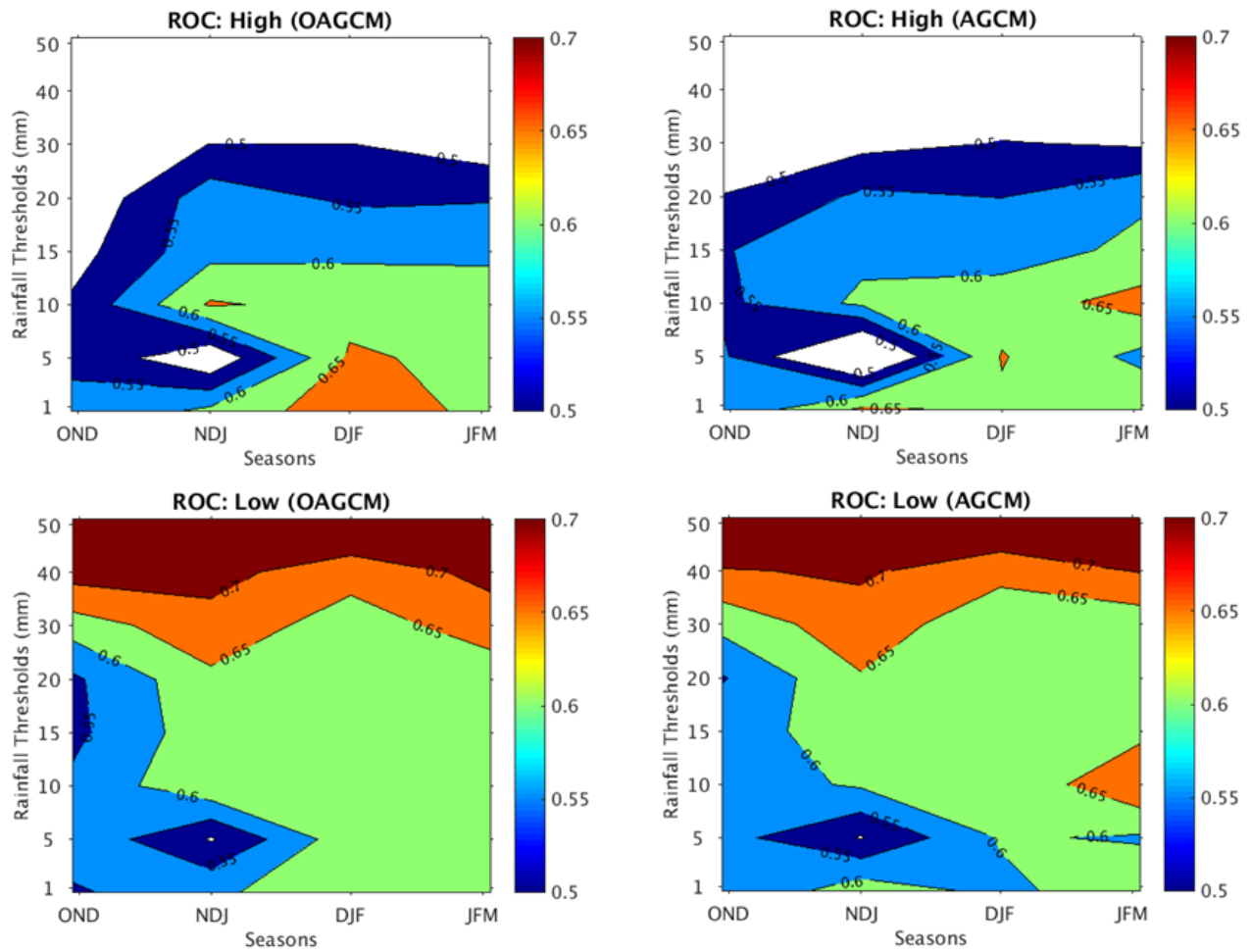


Figure 4.1: ROC scores for both the OAGCM and the AGCM at 1-month lead-time in predicting high- and low-number of rainfall days exceeding different threshold values over the 14 years retrospective forecasts from 1996 to 2009.

4.2. Reliability diagrams

Only the reliability diagrams for NDJ, DJF and JFM seasons are considered here since these three seasons have been found to be associated with the highest ROC scores. The reliability diagrams for the OAGCM (Figure 4.2) and the AGCM (Figure 4.3) indicate that when using the predicted 850hPa geopotential heights to predict the high (low) number of rainfall exceeding 1mm, 5mm, 10mm, 15mm, 20mm, 30mm, 40mm and 50mm within the NDJ seasons, the forecasts are generally under-confident (over-confident). The forecasts for all the above mentioned thresholds lack reliability since the weighted least square regression lines are far apart from the perfect reliability lines. In fact, for days with 5mm and heavier rainfall (> 20mm) the forecasts have no skill and no resolution. As mentioned in the previous chapter the forecasts display a lack of sharpness because the forecasts rarely deviate much from the climatological value of 33.3%.

The reliability diagrams in Figure 4.4 and Figure 4.5 for the OAGCM and the AGCM, respectively, show that forecasts are over-confident in predicting the high- and low-number of rainfall days exceeding the pre-defined threshold values for the DJF seasons. However, as compared to predicting the low-number of rainfall days, the high-number of rainfall days are more reliably as they are close to the perfect reliability line, especially for 1mm and 5mm threshold values. Again for the days with heavier rainfall (> 20mm) both the GCMs show to have no skill and no resolution. The frequency histograms included in the reliability diagrams indicate that the forecasts lack sharpness, for the same reason mentioned in previous paragraph.

When predicting the high-number of rainfall days exceeding 1mm, 5mm, 10mm, 15mm and 20mm for the JFM seasons the forecasts for both the global models are highly reliable as depicted in Figure 4.6 and Figure 4.7, respectively. In contrast, the forecasts for thresholds greater than 20mm have no skill and no resolution as well as lacking sharpness. From the reliability diagrams presented here, it is evident that both the models have some level of reliability in predicting the high- and low-number of rainfall days for the lower thresholds for the seasons considered. In fact, both the models are reliable in predicting the high-number of rainfall days less than or equal to 20mm during DJF and JFM seasons as compared to predicting the low-number of rainfall days. In addition, the OAGCM generally outperforms the AGCM, specifically during DJF and JFM seasons.

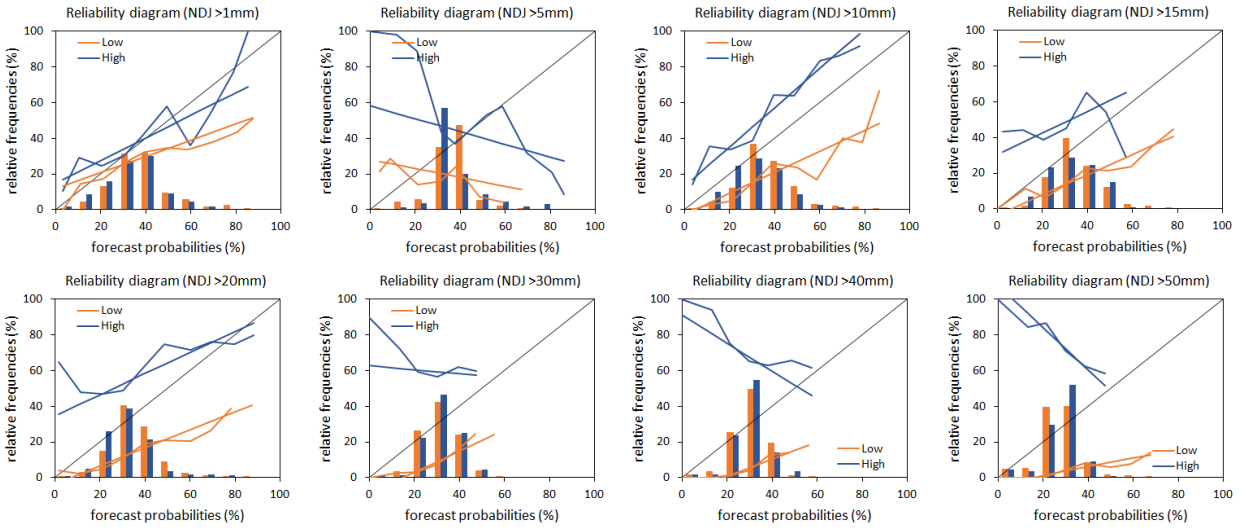


Figure 4.2. Reliability diagrams of the OAGCM at 1-month lead-time in predicting low (orange) and high (blue) number of rainfall days exceeding pre-defined threshold values within NDJ seasons.

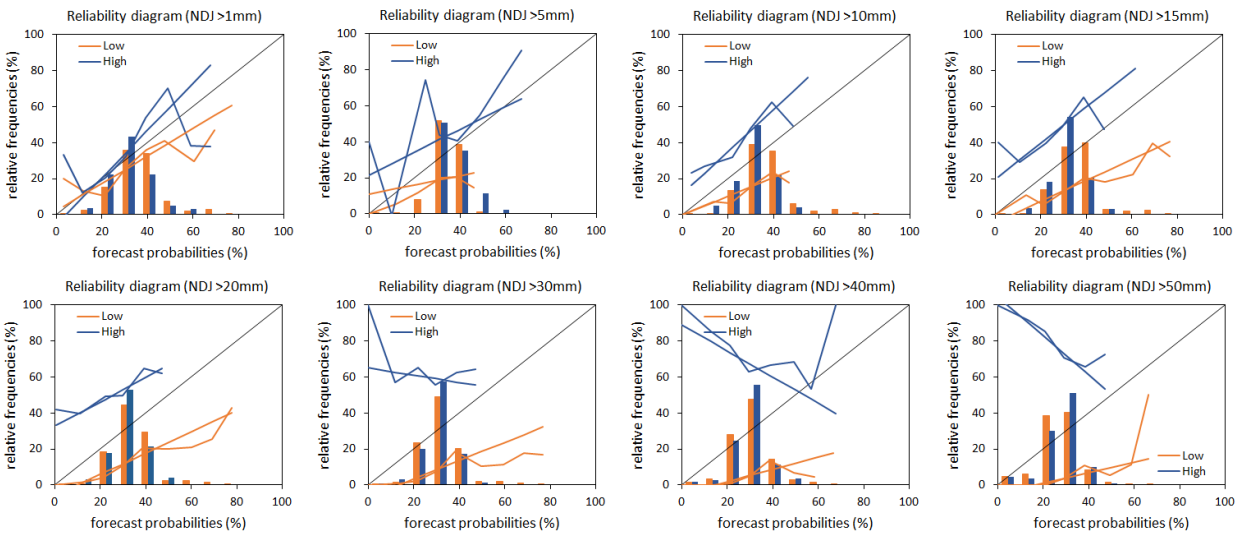


Figure 4.3. As in Figure 4.2, but for AGCM.

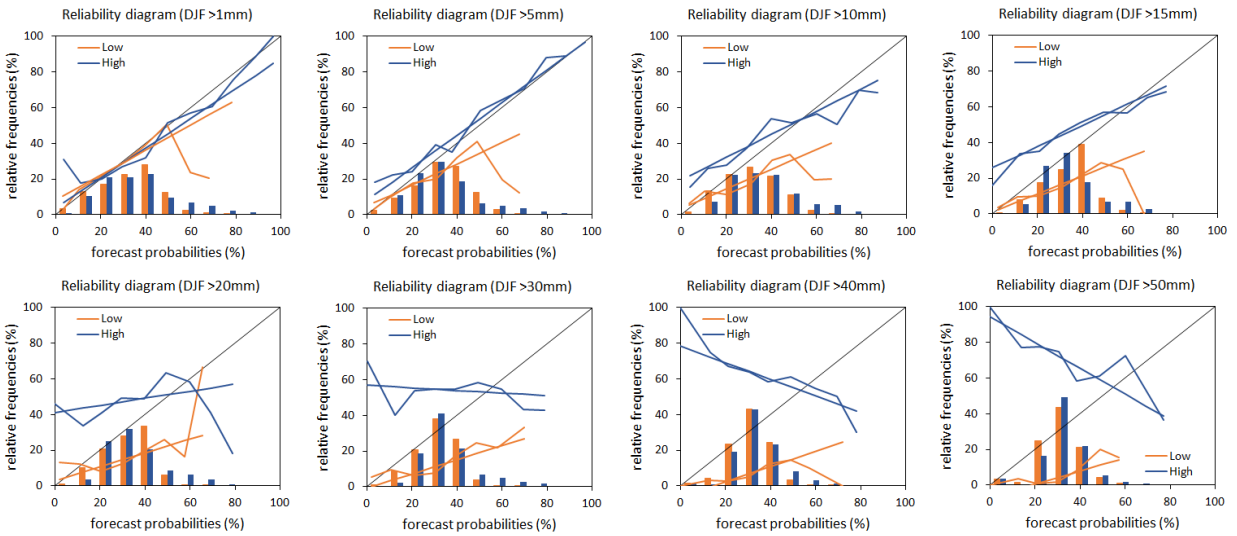


Figure 4.4. Reliability diagrams of the OAGCM at 1-month lead-time in predicting low (orange) and high (blue) number of rainfall days exceeding pre-defined threshold values within DJF seasons.

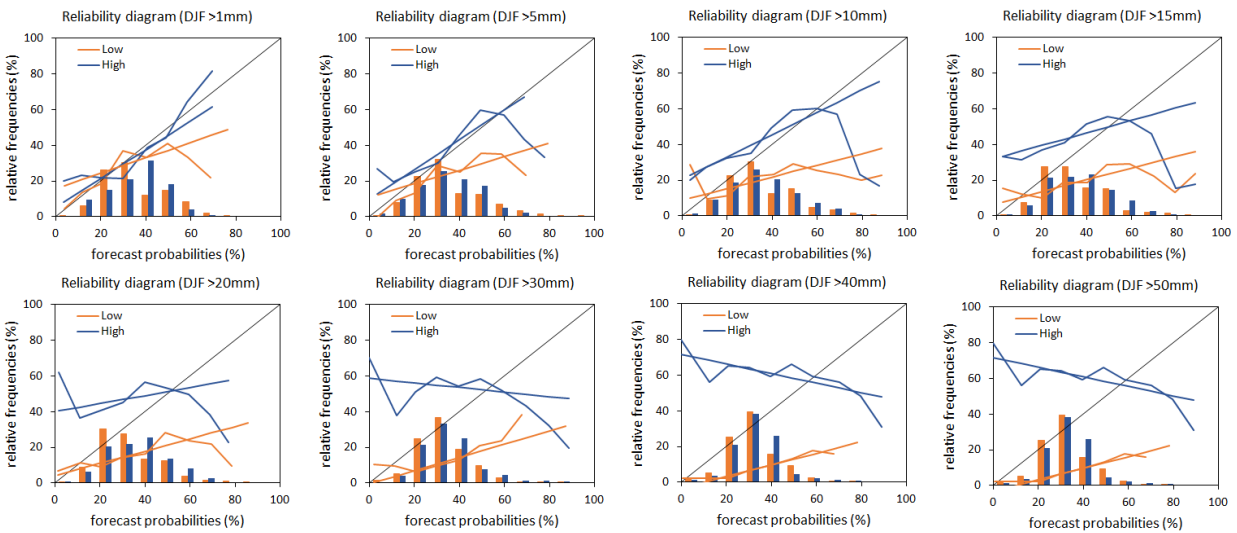


Figure 4.5. As in Figure 4.4, but for AGCM.

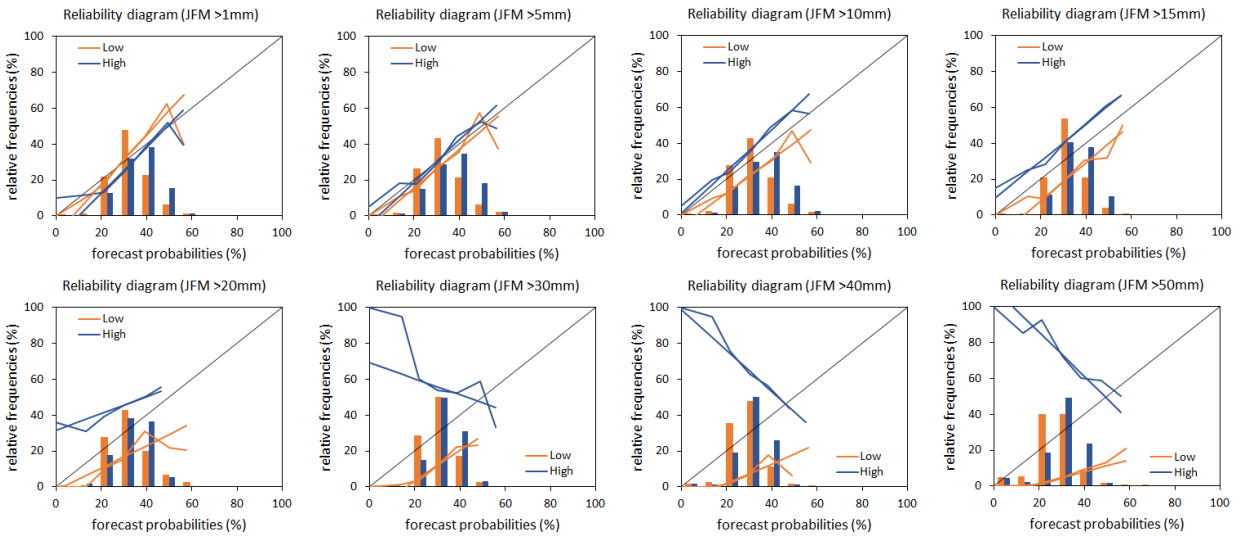


Figure 4.6. Reliability diagrams of the OAGCM at 1-month lead-time in predicting low (orange) and high (blue) number of rainfall days exceeding pre-defined threshold values within JFM seasons.

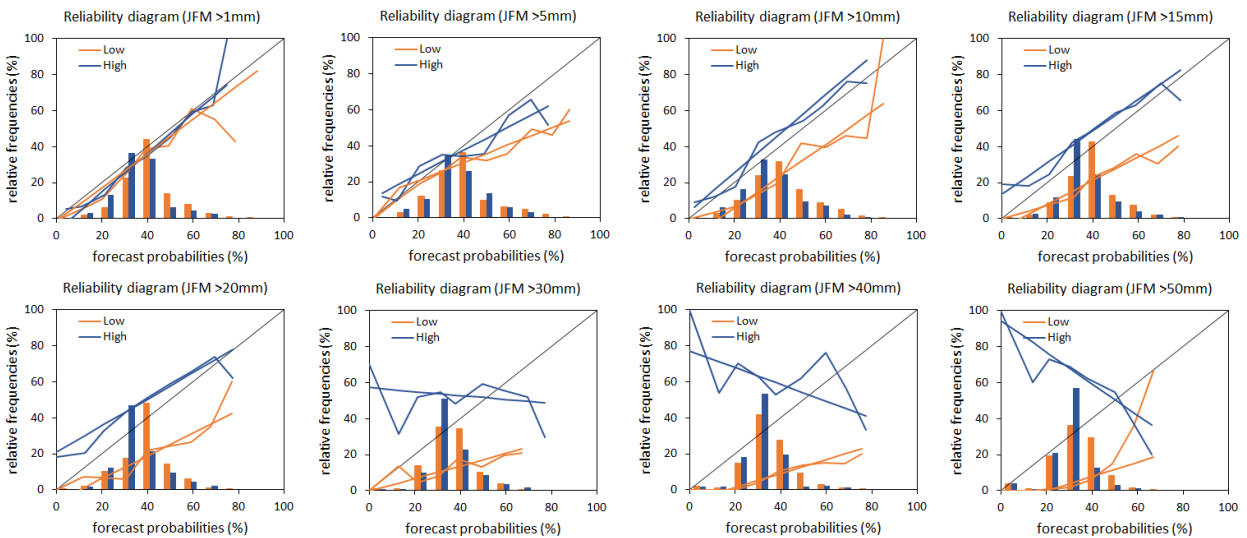


Figure 4.7. As in Figure 4.6, but for AGCM.

4.3. Spearman's rank correlations

Only the Spearman's rank correlation for threshold values less than or equal to 20mm for the NDJ, DJF and JFM seasons are considered since higher thresholds display a lack of reliability. The Spearman's correlations for both the OAGCM (Figure 4.8) and the AGCM (Figure 4.9) in predicting the number of rainfall days exceeding 1mm, 10mm and 20mm for stations distribution across South Africa during the NDJ seasons. For both models significant skill (positive correlations at 95% level of significance) is found over the interior and towards the eastern parts of the country, as well as the southeastern parts when predicting number of rainfall days exceeding 1mm and 10mm. The lowest (negative) correlations are found over the northeastern and southwestern parts of South Africa.

For both models during the DJF seasons, the Spearman's correlations show that the highest positive correlations for the OAGCM (Figure 4.10) and the AGCM (Figure 4.11) are scattered across the country, except for the Western Cape and the South coast having highest negative correlations. As compared to the NDJ seasons, the positive correlations extend into the northeastern parts of South Africa during DJF seasons. The highest skill (positive correlations at 95% level of confidence) is found when predicting 1mm, 5mm and 10mm for both the OAGCM and the AGCM during DJF seasons.

The Spearman's correlation maps indicate that both the OAGCM (Figure 4.12) and the AGCM (Figure 4.13) have skill (positive correlations at 95% level of confidence) in predicting the number of rainfall days exceeding the pre-defined threshold values during JFM seasons. The positive correlations are distributed across the country, except for the Western Cape and the southern coast where negative correlations are found. The distribution of the skill during JFM is almost the same as that of DJF, however, DJF skill is in general higher than that of JFM. In fact, DJF seasons are highly predictable as compared to the NDJ and JFM. This results indicate that the predicted 850hPa geopotential height fields can be used to predict the number of days exceeding threshold values up to 20mm during DJF and JFM seasons.

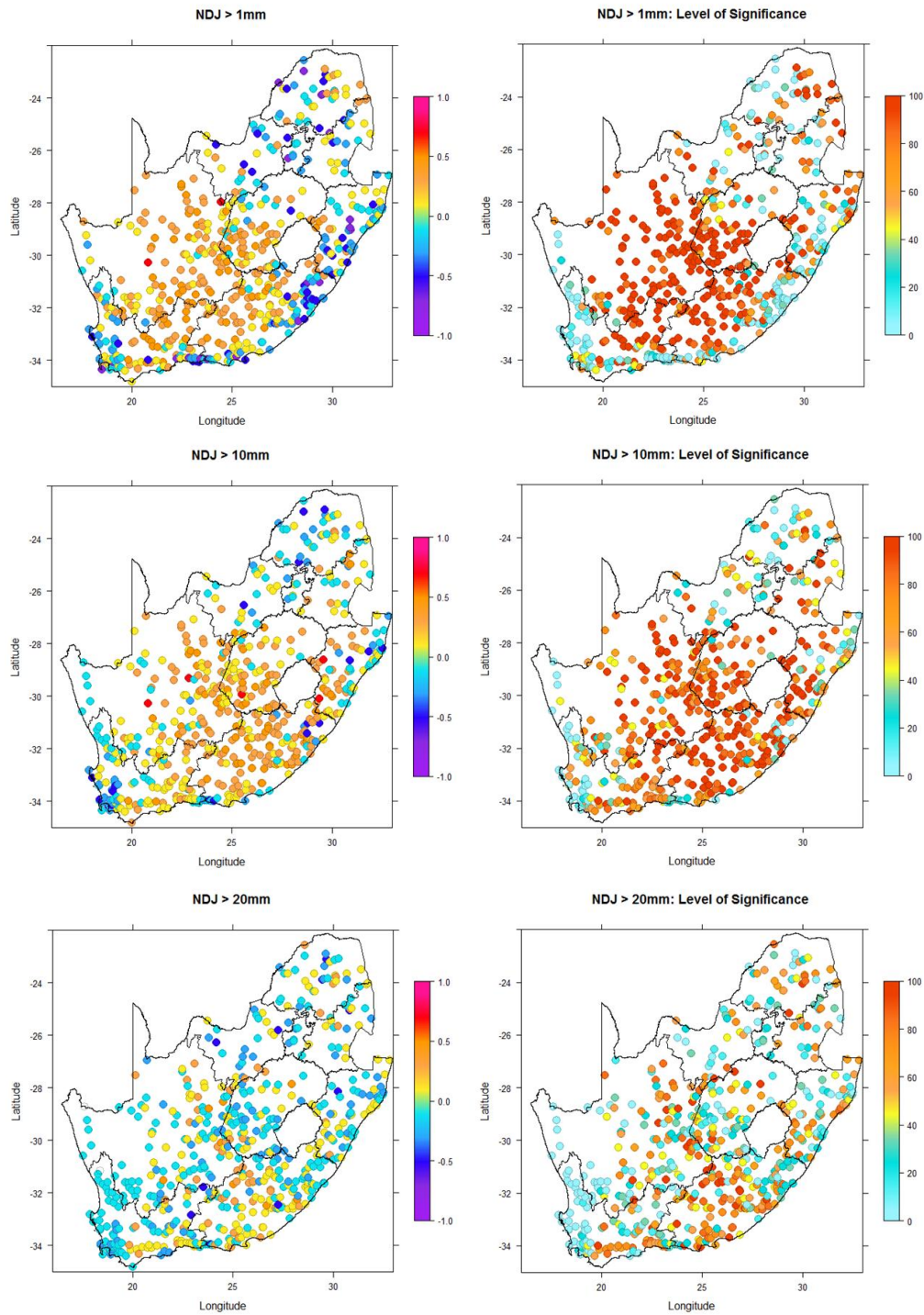


Figure 4.8. Spearman's rank correlations of the OAGCM (left panel) and their p-values level of significance (right panel) at 1-month lead-time for NDJ seasons over the 14 year retro-active forecasts from 1996 to 2009.

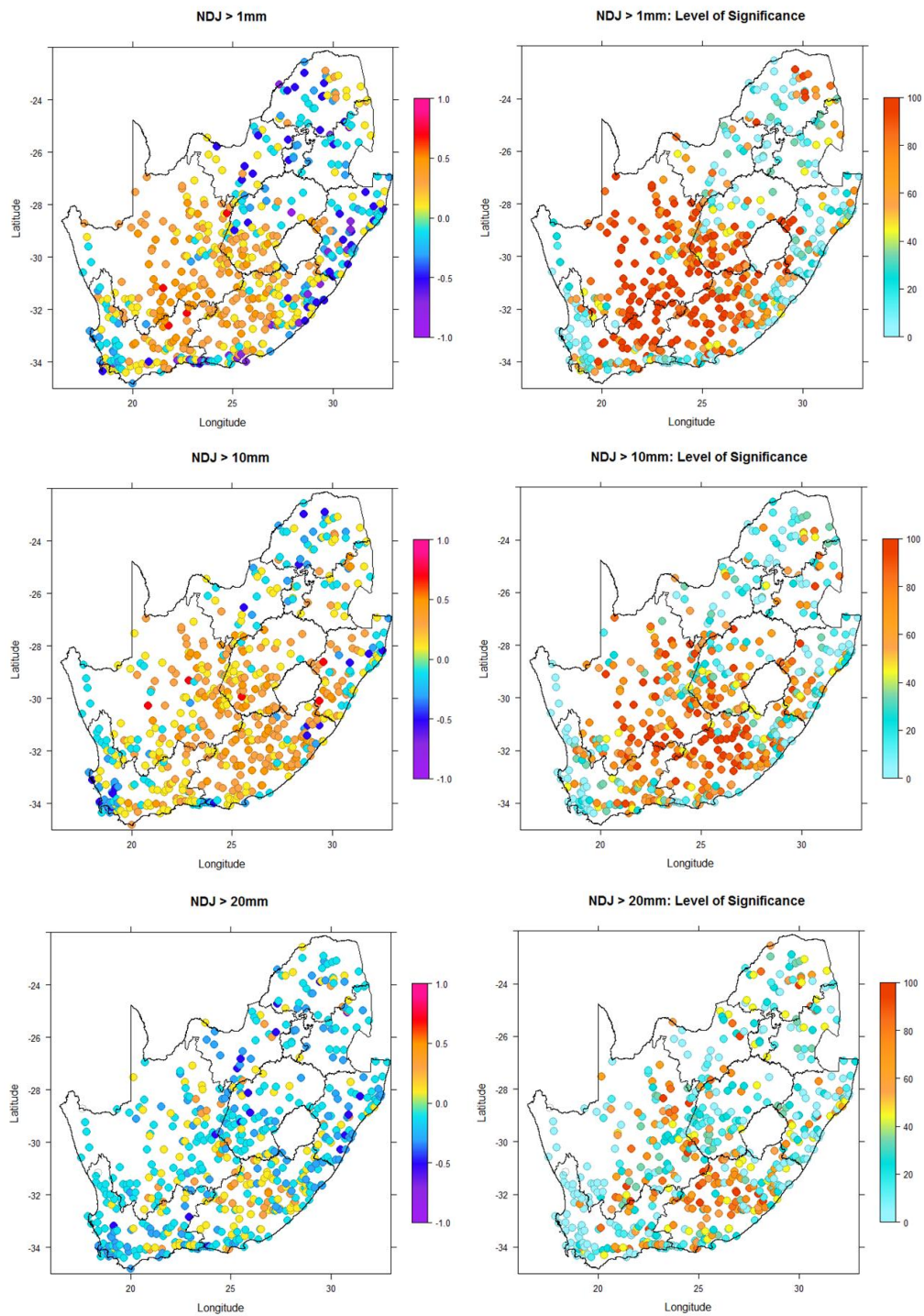


Figure 4.9. As in Figure 4.8, but for the AGCM.

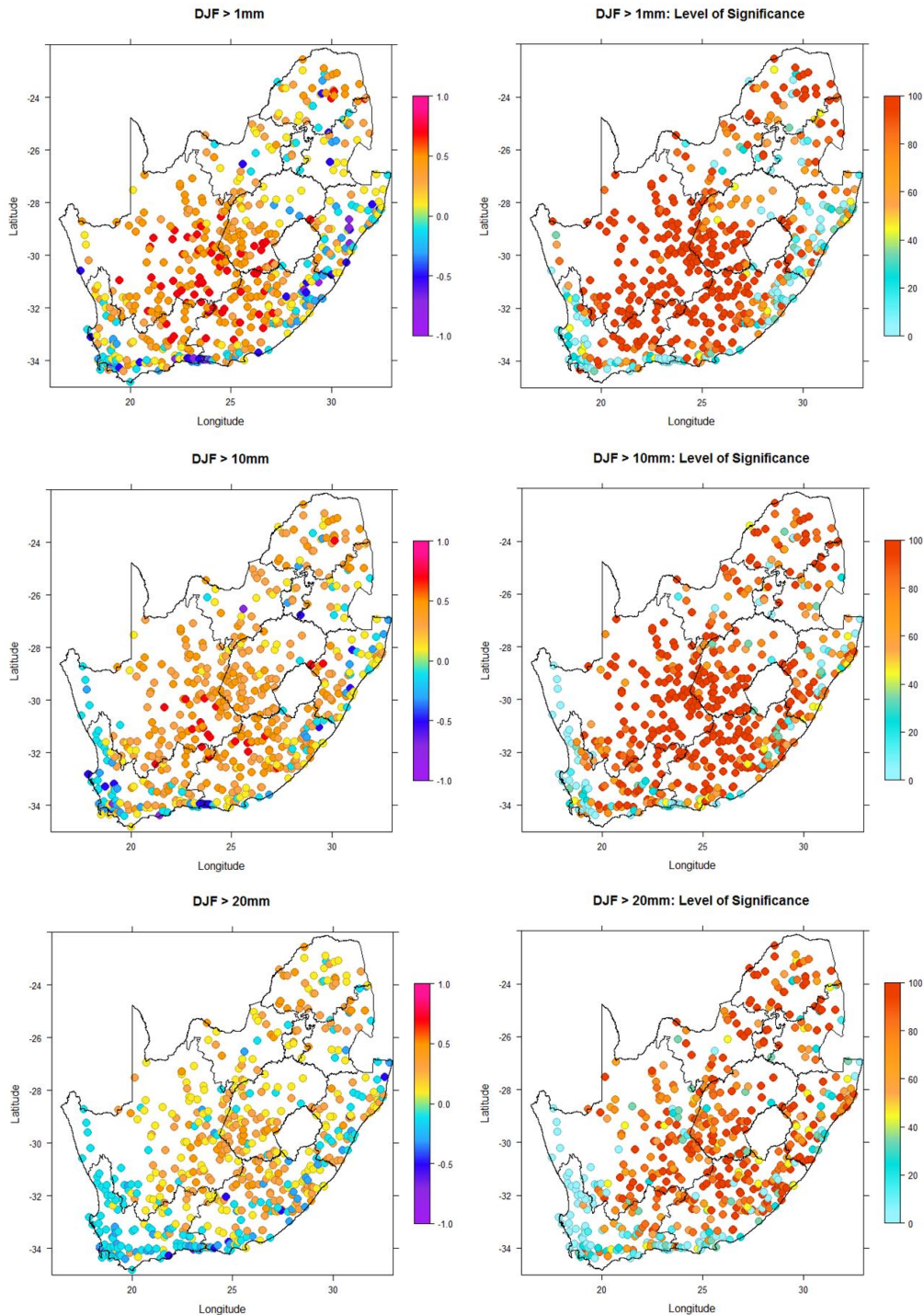


Figure 4.10. Spearman's rank correlations of the OAGCM (left panel) and their p-values level of significance (right panel) at 1-month lead-time for DJF seasons over the 14 year retro-active forecasts from 1996 to 2009.

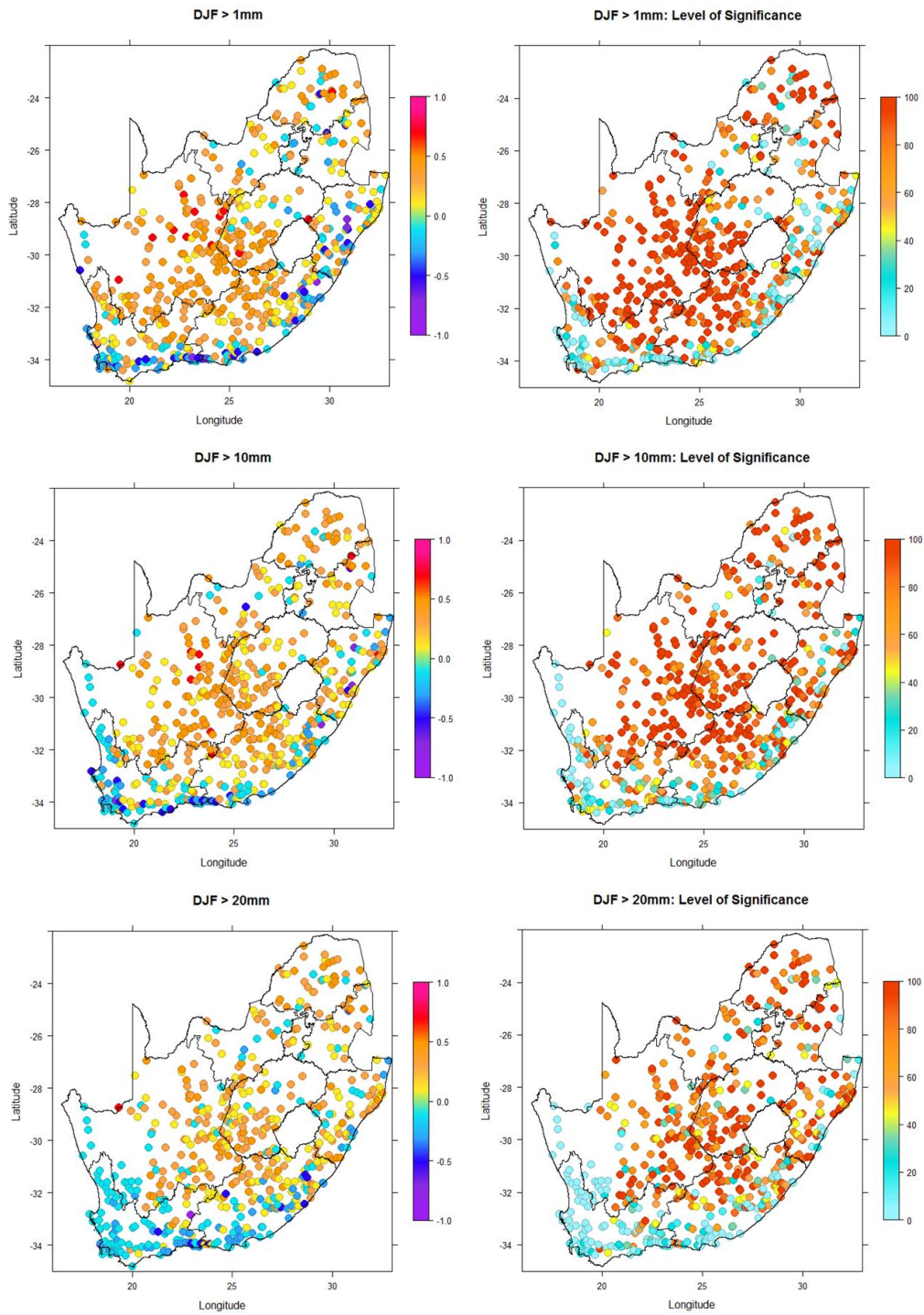


Figure 4.11. As in Figure 4.10, but for the AGCM.

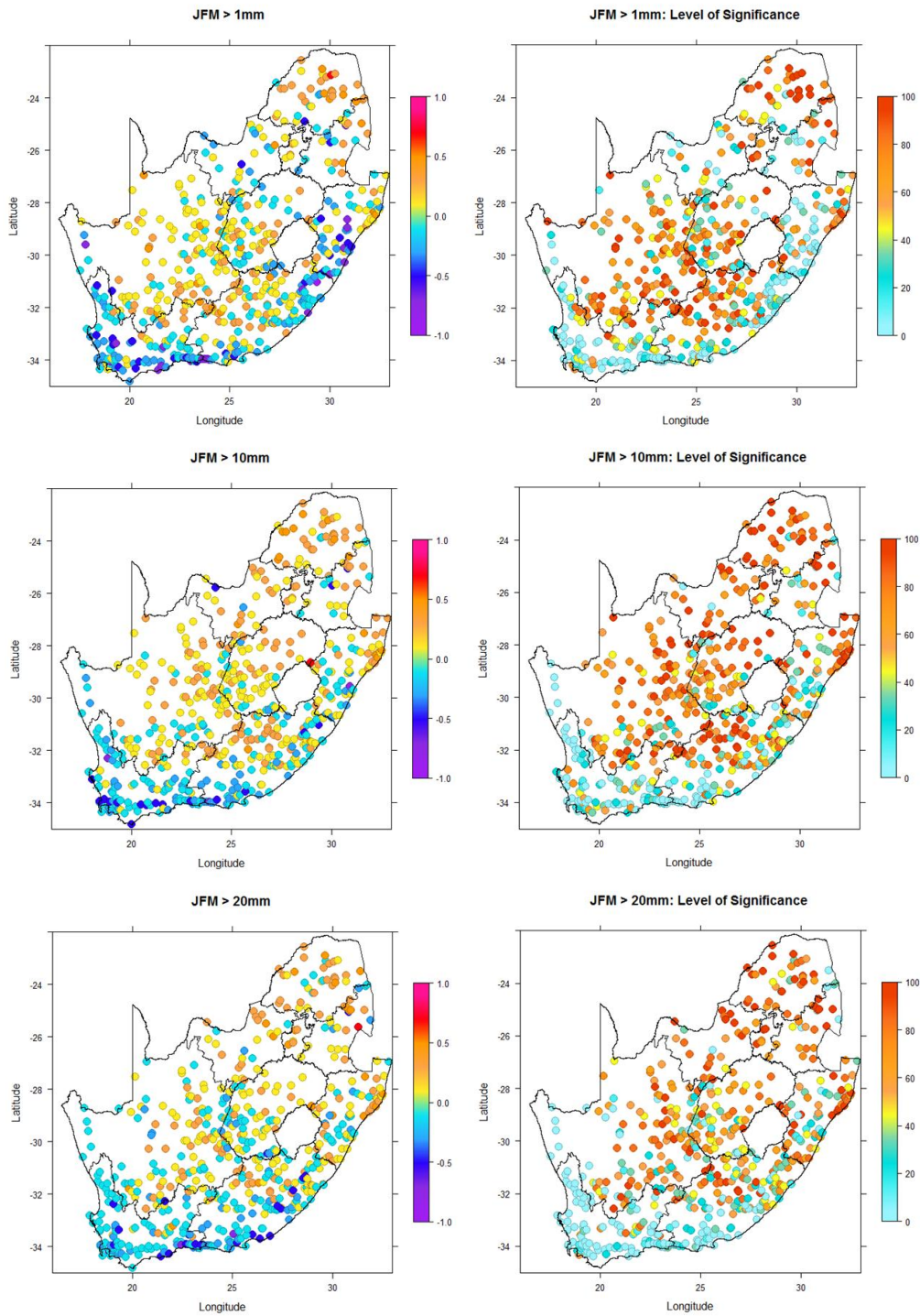


Figure 4.12. Spearman's rank correlations of the OAGCM (left panel) and their p-values level of significance (right panel) at 1-month lead-time for JFM seasons over the 14 year retro-active forecasts from 1996 to 2009.

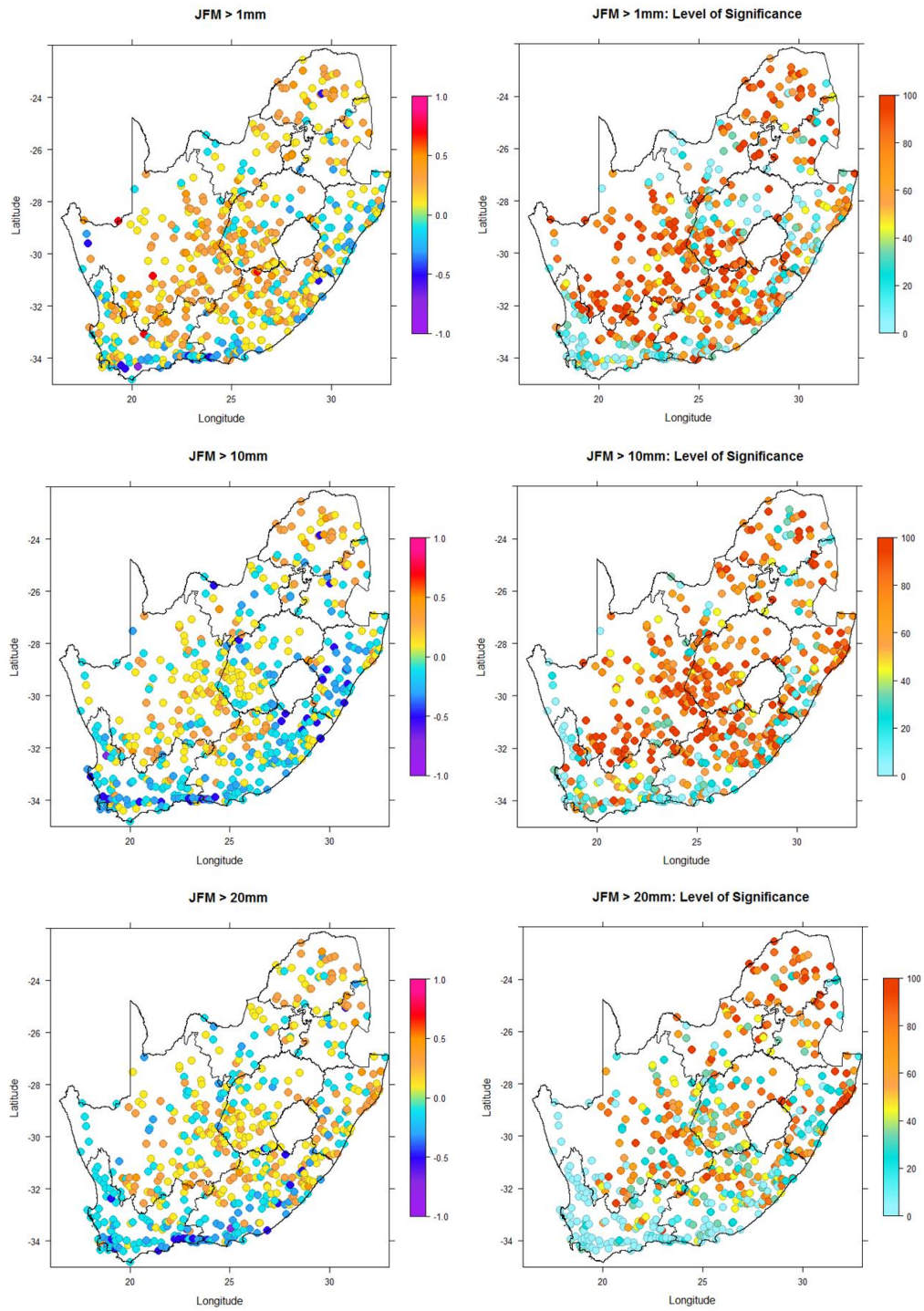


Figure 4.13. As in Figure 4.12, but for the AGCM.

4.4. CCA pattern analysis

The CCA pattern analysis is performed here to investigate the relationship between the predicted 850hPa geopotential heights of both the OAGCM and the AGCM at 1-month lead-time and the downscaled number of rainfall days exceeding 1mm, 10mm, 20mm and 30mm threshold values for NDJ, DJF and JFM seasons, respectively. The CCA maps (mode 1) for both the OAGCM and the AGCM indicate that when there are anomalously negative (positive) 850hPa geopotential heights over South Africa there are anomalously high (low) number of rainfall days exceeding the mentioned threshold values over South Africa for NDJ (Figure 4.14 (OAGCM) and Figure 4.15 (AGCM)), DJF (Figure 4.16 (OAGCM) and Figure 4.17 (AGCM)) and JFM (Figure 4.18 (OAGCM) and Figure 4.19 (AGCM)) seasons.

Only CCA pattern analysis for DJF seasons are discussed here since the results are similar to that of NDJ and JFM seasons. For DJF seasons during 1982, 1986, 1991, 1994 and 2006, for example, the predicted 850hPa geopotential heights for both the OAGCM and the AGCM are anomalously negative and their temporal scores are also negative as shown in Figure 4.16 and Figure 4.17, respectively. The product of the predictor loadings and their time scores is positive. During the same years over South Africa, the downscaled number of rainfall days exceeding 1mm, 10mm, 20mm and 30mm for both the OAGCM and the AGCM are positive and their temporal scores are negative. The product of the spatial loadings and their scores is negative. This results implies that when there are anomalously positive 850hPa geopotential heights over South Africa there are anomalously low number of rainfall days exceeding the mentioned threshold values over South Africa. This in turn implies that when there is a high pressure system over South Africa during DJF seasons, it draws out the moist air of the country and usually the country remain dry, resulting in low number of rainfall days.

For both models during DJF seasons, but this time during 1984, 1988, 1993, 1999 and 2007, CCA pattern analysis maps indicate that there are anomalously negative predictor's loadings over South Africa and their corresponding time scores are positive. The product of the spatial loadings and the scores is negative. The predictand spatial loadings are anomalously positive over most parts of South Africa and their temporal scores are positive. The product of the spatial loadings

and their scores is positive. This again implies that when there are anomalously negative 850hPa geopotential heights over South Africa there are anomalously high number of rainfall days exceeding the pre-defined threshold values over South Africa. In fact, when there is a low pressure system over South Africa it advects the moist air into the country usually results in rainfall events, in turn leading to high number of rainfall days.

The years that are associated with low number of rainfall days are actually El Niño years and usually during El Niño years large part of South Africa receives below-normal rainfall, sometimes even drought. Most notably, during the events of 1982 and 1991 South Africa experienced severe droughts. This implies that for DJF seasons during these El Niño events there were high pressure systems over the country suppressing rainfall activities and reducing the number of rainfall days. In contrast, during the La Niña events large part of South Africa receive above-normal rainfall as well as floods at times. For example, the 1999 and 2010 events left most of the summer rainfall areas of South Africa wetter than normal, including floods in some areas. In fact during the 1984, 1988, 1995, 1999 and 2007 La Niña events there were low pressure systems and associated ridging highs bringing moist air into the country resulting in wet conditions, in turn leading to high number of rainfall days.

CCA analysis results presented in this chapter show that the atmospheric circulation patterns responsible for rainfall totals (shown in Chapter 3, Figures 3.6 and 3.7) are similar to the analysis for the number of rainfall days during NDJ, DJF and JFM seasons (e.g. Figures 4.13 and 4.14). For both the GCMs systems during NDJ, DJF and JFM seasons most of the El Niño years produced low-number of rainfall days exceeding pre-defined threshold values, resulting in dry seasons as well as drought in some cases over the summer rainy season areas of South Africa. On the other hand, for both models during NDJ, DJF and JFM seasons most of the La Niña years produced high number of rainfall days exceeding different threshold values, resulting in wet seasons leading to flooding in some areas.

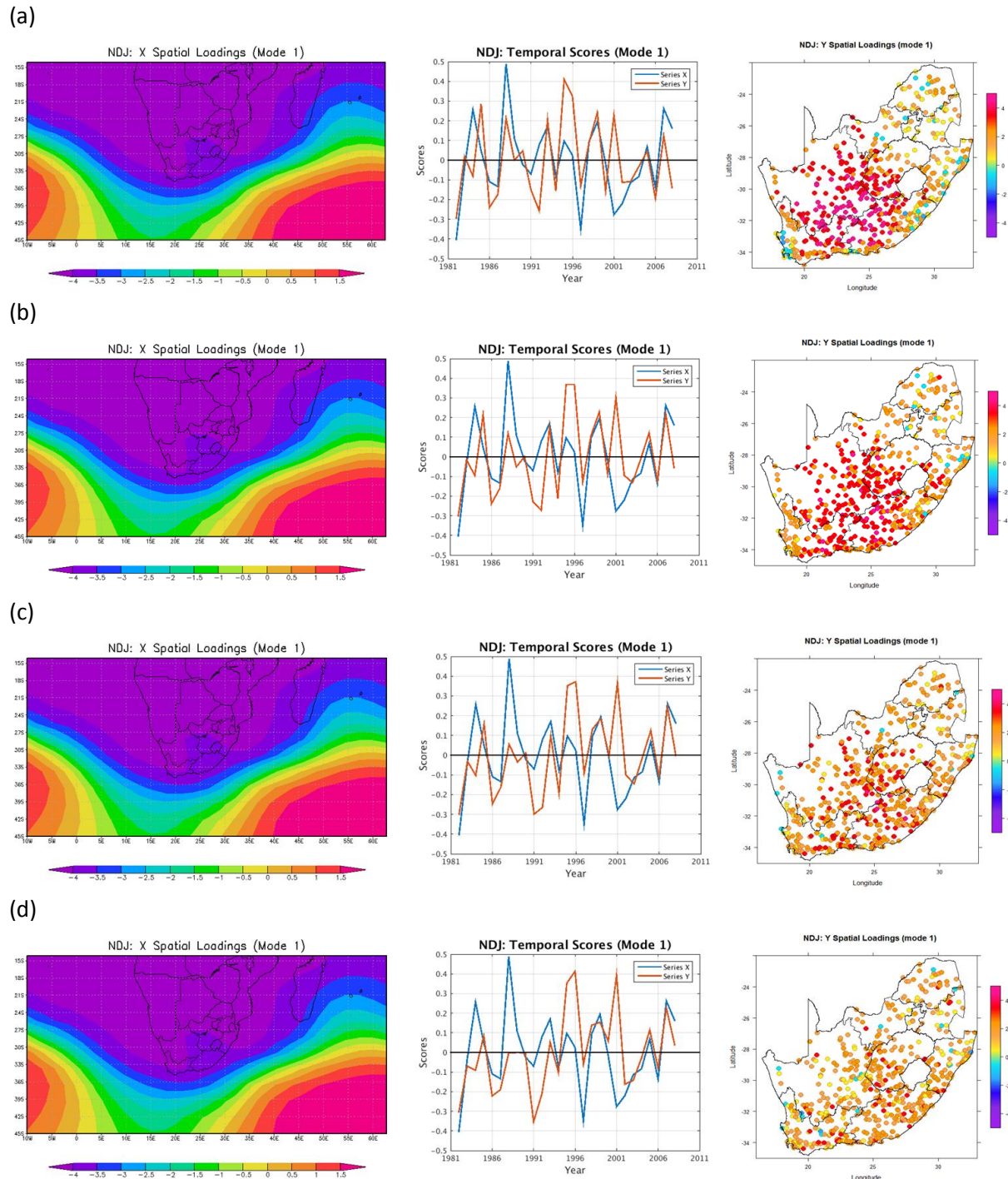


Figure 4.14. Mode 1 CCA maps of the 850hPa geopotential heights of the OAGCM and the number of rainfall days exceeding 1mm (a), 10mm (b), 20mm c) and 30mm (d) for NDJ seasons. The X and Y are the spatial loadings of the predictors and predictands, respectively.

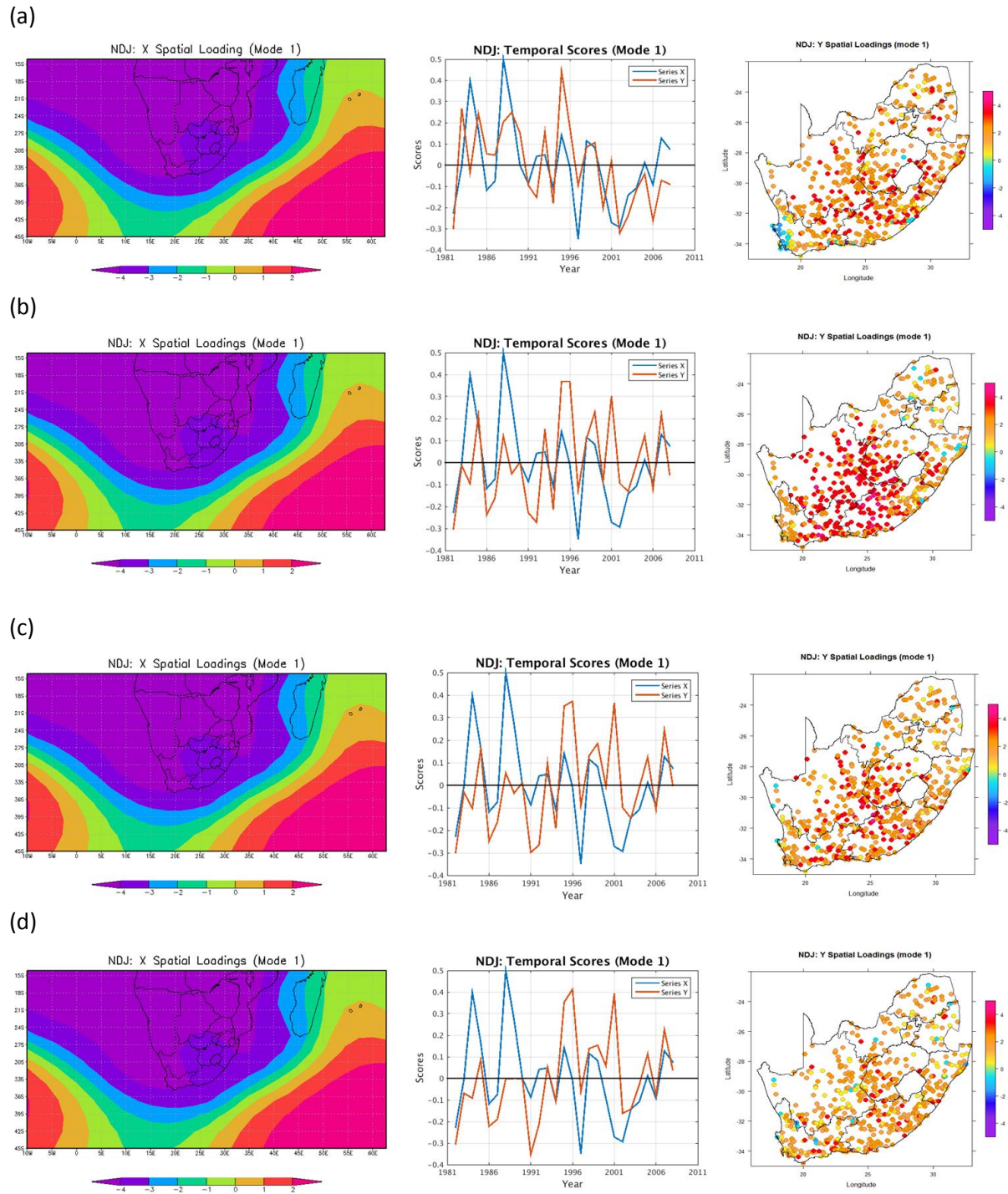


Figure 4.15. As in Figure 4.14, but for the AGCM.

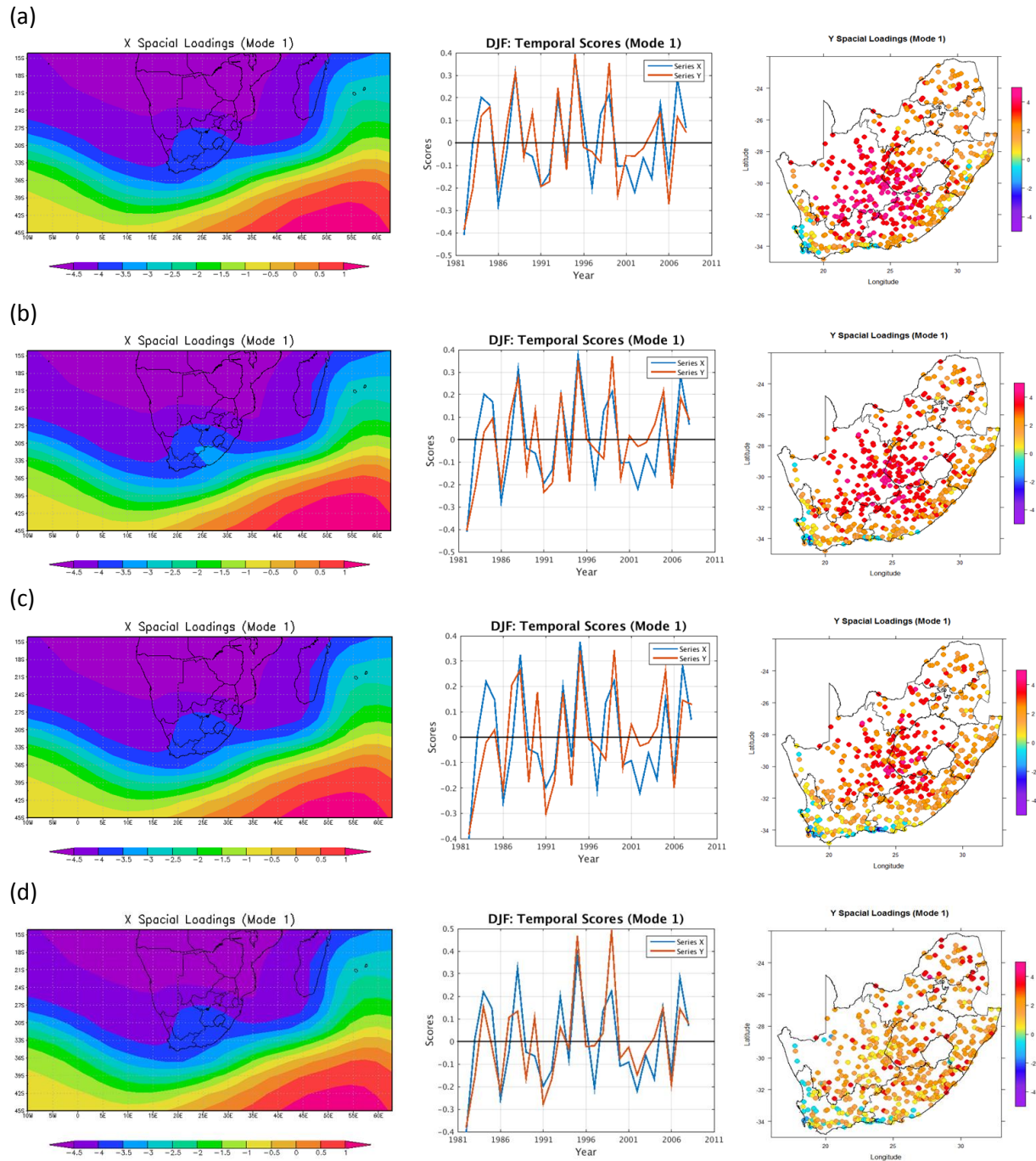


Figure 4.16. Mode 1 CCA maps of the 850hPa geopotential heights of the OAGCM and the number of rainfall days exceeding 1mm (a), 10mm (b), 20mm (c) and 30mm (d) for DJF seasons. The X and Y are the spatial loadings of the predictors and predictands, respectively.

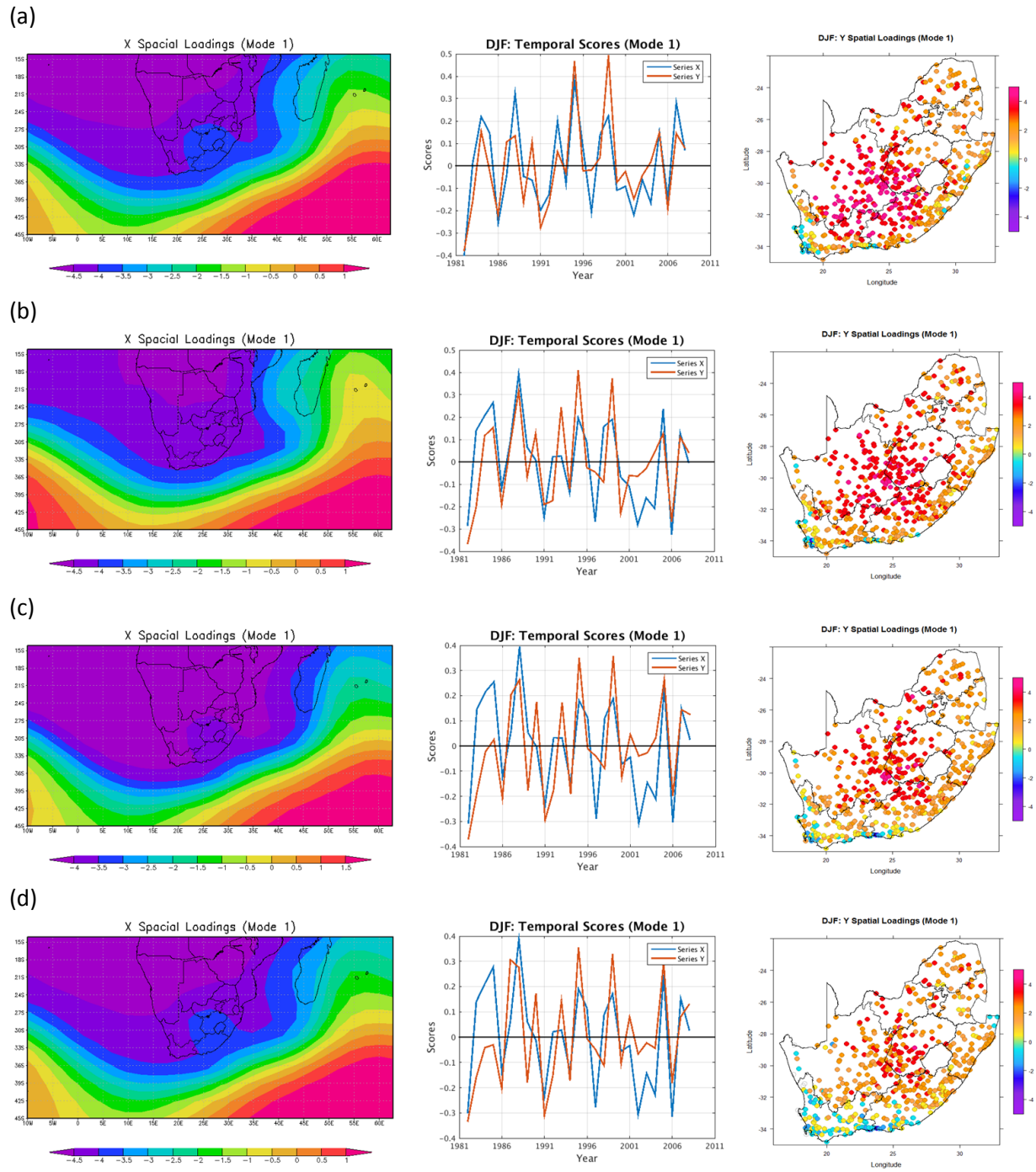


Figure 4.17. As in Figure 4.16, but for the AGCM.

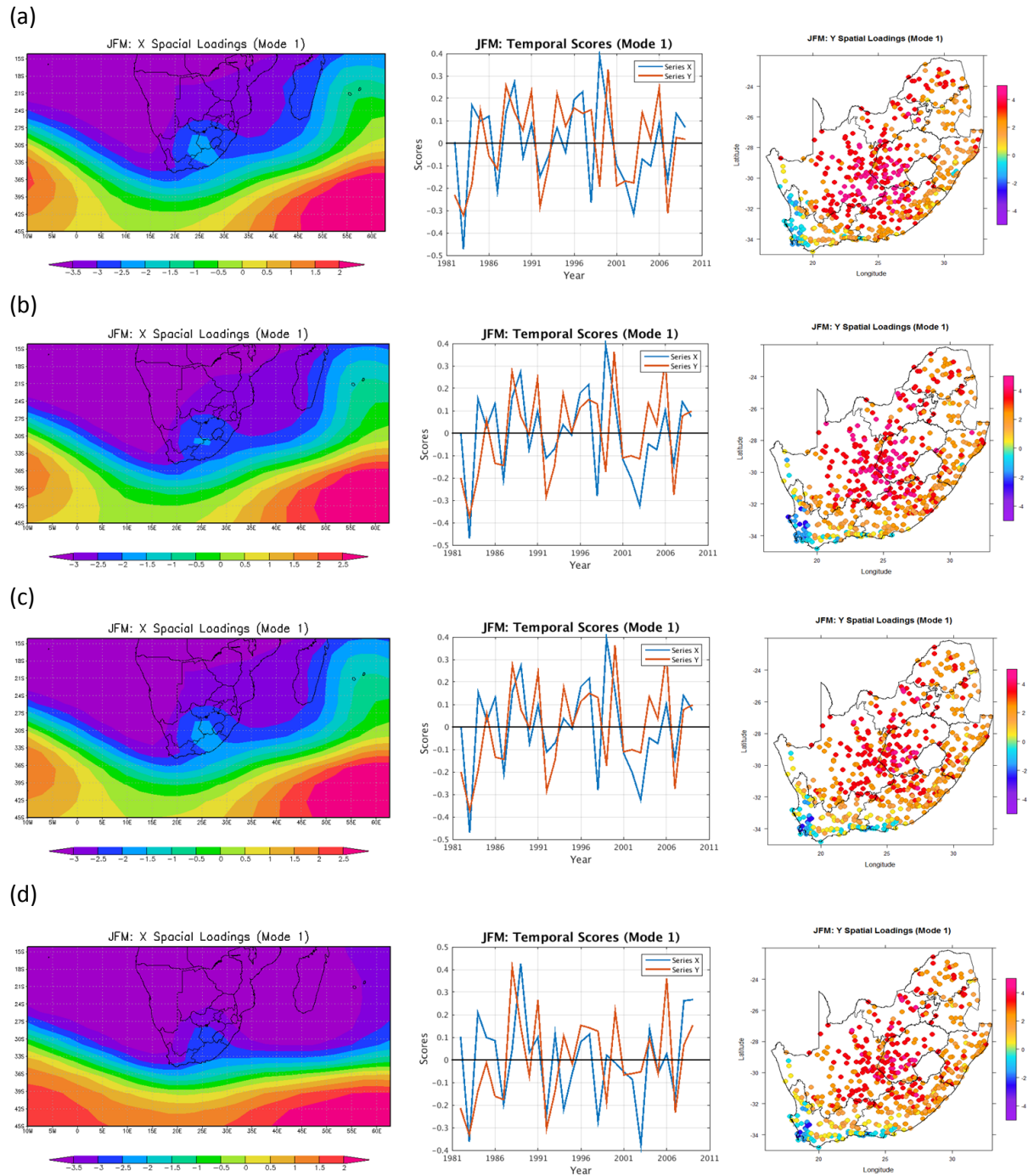


Figure 4.18. Mode 1 CCA maps of the 850hPa geopotential heights of the OAGCM and the number of rainfall days exceeding 1mm (a), 10mm (b), 20mm c) and 30mm (d) for JFM seasons. The X and Y are the spatial loadings for the predictors and predictands, respectively.

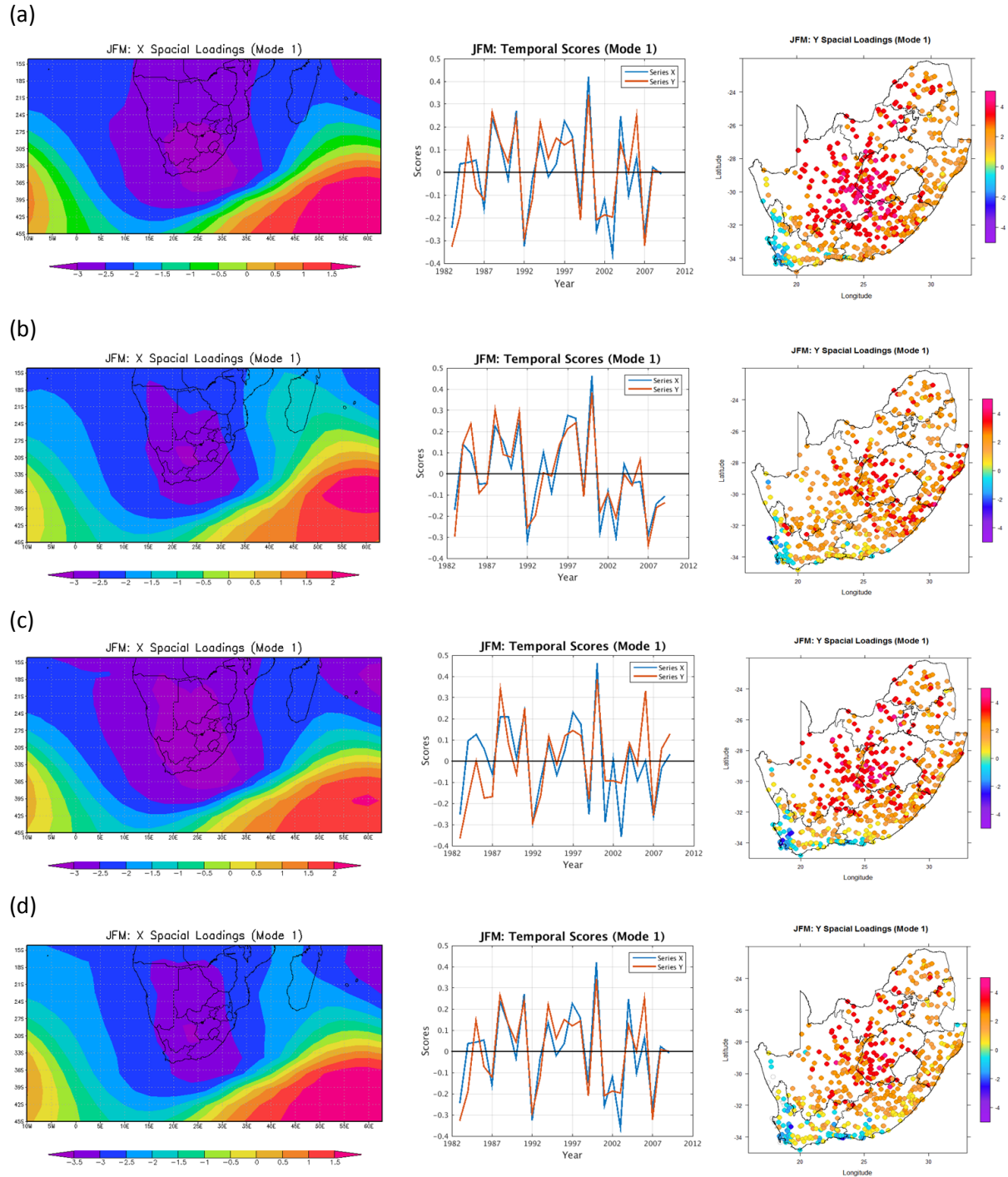


Figure 4.19. As in Figure 4.18, but for the AGCM.

4.5. Synopsis

This chapter evaluated the skill levels of both the OAGCM and the AGCM in predicting the number of rainfall days exceeding 1mm, 5mm, 10mm, 15mm, 20mm, 30mm, 40mm and 50mm threshold values over South Africa. The ROC scores show that both models have the attribute of discrimination in predicting the number of days exceeding threshold values less than or equal to 20mm. The highest ROC scores are found during NDJ and DJF for the OAGCM system and during DJF and JFM for the AGCM system. The reliability diagrams also indicate that both systems can reliably predict number of rainfall exceeding thresholds less or equal to 20mm, especially during DJF and JFM seasons. The Spearman's correlations also show that both systems have skill (positive correlations at 95% level of significance) in predicting number of rainfall days, especially during DJF seasons. The ROC scores, the reliability diagrams and the Spearman's correlations have shown that the OAGCM outperforms the AGCM in predicting number of rainfall days exceeding the pre-defined threshold values over South Africa. CCA analysis showed that when there are anomalously negative (positive) predicted 850hPa geopotential heights over South Africa there are anomalously high (low) number of rainfall days exceeding the pre-defined threshold values for NDJ, DJF and JFM seasons over most parts of South Africa. Such configuration is also found for modelling seasonal rainfall totals (Chapter 3). The next chapter presents the results of the predictability of the onset of the rainy seasons over South Africa.

CHAPTER 5

PREDICTABILITY OF ONSET OF THE RAINY SEASONS

This chapter presents the verification results for both the OAGCM and the AGCM in predicting the onset of the rainy seasons across eight homogeneous rainfall regions over South Africa (Landman *et al.*, 2009). Firstly the onset of the rainy seasons is defined. The models' forecast skill levels are again evaluated using ROC scores and reliability diagrams, as well as Spearman's rank correlations. As with previous chapters, CCA pattern analysis is performed in order to determine the dominating atmospheric circulation systems predicted to be controlling rainfall and subsequently the onset of the main rainfall seasons.

5.1. Definition of the onset of the rainy seasons

The onset is defined here as the first month of a three month season on condition that the season consists of the wettest consecutive three months of the year as calculated over several decades (climatological values). According to this definition of onset, the onset month for Region 1 is May, October for Region 2 and 3, November for Region 4, 5 and 6, December and January for Region 7 and 8, respectively and are indicated with black arrows on the climatological annual rainfall circles (Figure 5.1).

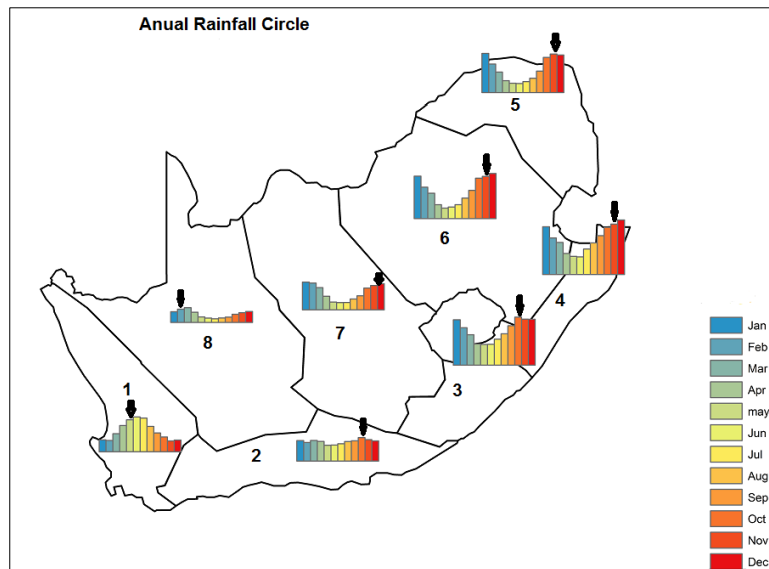


Figure 5.1. The eight homogeneous rainfall regions calculated using cluster analysis and their annual rainfall cycles from 1982 to 2009.

5.2. ROC scores

The 850hPa geopotential heights of both the OAGCM and the AGCM at 1-month lead-time are statistically downscaled to the rainfall totals of the onset months for the eight homogeneous rainfall regions of South Africa. The ROC scores for above-normal rainfall (wet conditions) and below-normal rainfall (dry conditions) for the onset months are then calculated for both models (Table 5.1 and Table 5.2). It was found from the ROC scores that both models have a variation of skill distributed across all eight rainfall regions when predicting wet and dry conditions for the onset months. All the ROC scores are greater than 0.5 for all the onset months for the two models.

The ROC scores bar graphs in Figure 5.2 indicate that the OAGCM is more skillful in predicting dry conditions as compared to wet conditions for the onset months of Region 1, Region 3, Region 4, Region 5 and Region 8. The highest ROC scores are found when predicting dry conditions for the onset months for Region 1 (May), Region 4 (November) and Region 8 (January). On the other hand highest scores in predicting wet conditions for the onset months are found in Region 8 and Region 7, followed by Region 1 and Region 5. In fact the OAGCM system is more skillful when predicting dry conditions as compared to wet conditions.

The AGCM system also has skill in predicting both wet and dry conditions for all the onset months of the rainfall regions (Figure 5.3). The AGCM seem to have high ROC scores when predicting wet conditions as compared to dry conditions of the onset months. The highest scores are found when predicting wet conditions for the onset months for Region 5 (November) followed by Region 4 (November) and Region 1 (May), whereas in predicting dry conditions highest scores are found in Region 2 (October), Region 3 (October), Region 5 (November) and Region 8 (February). In contrast to the OAGCM, the AGCM is more skillful when predicting wet conditions as compared to dry conditions.

The findings of the ROC scores presented here indicate that the 850hPa geopotential heights at 1-month lead-time of both the OAGCM and the AGCM can be used to predict the onset months for the eight homogeneous rainfall regions of South Africa. The skill for summer rainfall regions is due to the fact that there is rainfall-ENSO teleconnection for those areas (Landman *et al.*, 2001). For the austral winter rainfall region (i.e. Region 1), it was found that when the winter season includes May there is rainfall-ENSO teleconnection (Philippon *et al.*, 2011). Possible that is the reason for the high skill for the May onset months of Region 1. Although both prediction systems

have skill in predicting wet and dry conditions for the onset months, the AGCM seems to outperform the OAGCM in predicting wet conditions. The OAGCM, on the other hand seem to be more skillful in predicting dry conditions as compared to wet conditions. However, the level of skill distributed across the eight rainfall regions varies for the two models.

Table 5.1. ROC scores of the forecasts downscaled from the OAGCM 1-month lead-time in predicting above-normal and below-normal rainfall totals of the onset months for the eight homogeneous rainfall regions of South Africa over the 14 year retro-active forecasts from 1996 to 2009.

| REGION | ONSET MONTH | ABOVE-NORMAL | BELOW-NORMAL |
|--------|-------------|--------------|--------------|
| 1 | May | 0.590 | 0.708 |
| 2 | October | 0.574 | 0.556 |
| 3 | October | 0.545 | 0.630 |
| 4 | November | 0.563 | 0.754 |
| 5 | November | 0.580 | 0.594 |
| 6 | November | 0.574 | 0.547 |
| 7 | December | 0.601 | 0.592 |
| 8 | January | 0.618 | 0.676 |

Table 5.2. As in Table 5.1, but for the AGCM.

| REGION | ONSET MONTH | ABOVE-NORMAL | BELOW-NORMAL |
|--------|-------------|--------------|--------------|
| 1 | May | 0.607 | 0.598 |
| 2 | October | 0.553 | 0.612 |
| 3 | October | 0.578 | 0.645 |
| 4 | November | 0.629 | 0.603 |
| 5 | November | 0.682 | 0.614 |
| 6 | November | 0.578 | 0.540 |
| 7 | December | 0.564 | 0.534 |
| 8 | January | 0.564 | 0.636 |

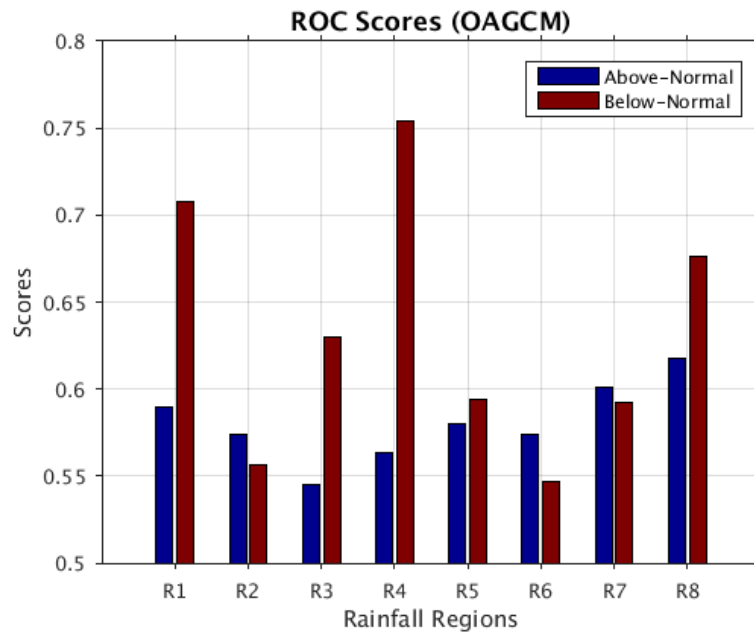


Figure 5.2. ROC scores of the forecasts downscaled from OAGCM 1-month lead-time in predicting above-normal and below-normal rainfall totals of the onset months for the eight homogeneous rainfall regions of South Africa over the 14 year retro-active forecasts from 1996 to 2009.

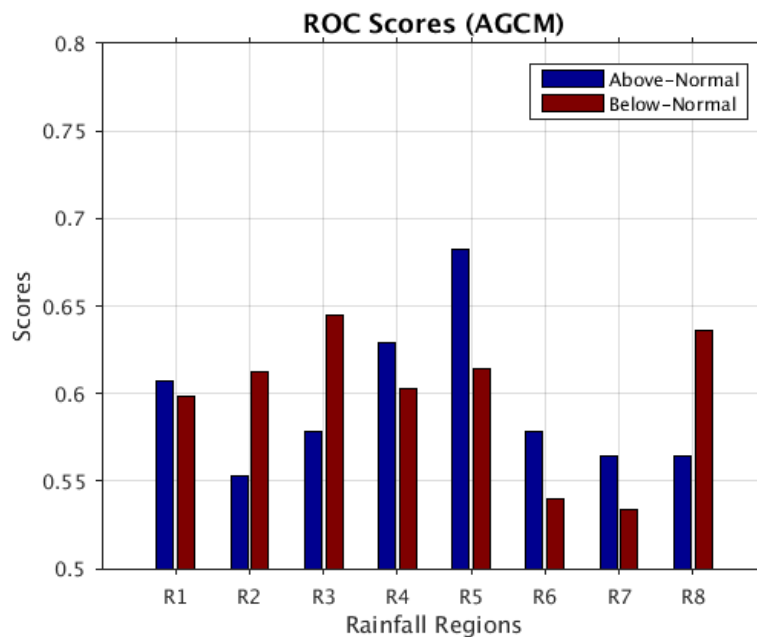


Figure 5.3. As in Figure 5.2, but for the AGCM.

5.3. Reliability diagrams

The reliability diagrams (Figure 5.4) show that the forecasts of both the OAGCM and the AGCM 1-month lead-time are over-confident when predicting both wet and dry conditions for Region 1 onset months. However, the forecasts are more reliable when predicting wet conditions since the weighted least square regression line is closer to the perfect reliability line. On the other hand, the forecasts for predicting dry conditions lack reliability. As with previous chapters, the frequency histograms included in the reliability diagrams indicate that the forecasts lack sharpness.

The OAGCM (AGCM) forecasts are over-confident (under-confident) in predicting dry conditions for Region 2 onset months (Figure 5.5), while both models are over-confident in predicting wet conditions. The forecasts for both models are reliable in predicting dry conditions as compared to predicting wet conditions for the onset months of Region 2. Again the frequency histograms show that in general the forecasts lack sharpness in predicting both dry and wet conditions for the onset months.

Forecasts for both the systems are over-confident in predicting both wet and dry conditions for the October onset months of Region 3 (Figure 5.6). As with Region 2, the forecasts for Region 3 are more reliable when predicting dry conditions as compared to predicting wet conditions. As indicated before the frequency histograms included in the reliability diagrams show that the forecasts display lack of sharpness in predicting both wet and dry conditions for Region 3 onset months.

The two systems are over-confident in predicting both dry and wet conditions for Region 4, 6, 7 and 8 (Figures 5.7, 5.9, 5.10 and 5.11) onset months. Both models seem to be more reliable in predicting wet conditions for the onset months as compared to predicting dry conditions for the onset months of the mentioned regions. As in previous paragraphs, the frequency histograms included in the reliability diagrams indicate that the forecasts lack sharpness in predicting both wet and dry conditions for the onset months of Region 4, 6, 7 and 8.

Figure 5.8 show that the OAGCM (AGCM) forecasting system is under-confident (over-confident) in predicting wet conditions for Region 5 onset months. On the other hand, both models are over-confident in predicting dry conditions. In fact, both models have some degree of reliability in predicting both wet and dry conditions for Region 5 onset months. The frequency histograms once again indicate that the forecasts lack sharpness.

From the reliability diagrams presented here, it is evident that both the OAGCM and the AGCM systems have some level of reliability in predicting both wet and dry conditions for the onset months for the eight homogeneous rainfall regions. In fact, both models seem to perform better when predicting wet conditions as compared to dry conditions. The two forecasting systems lack sharpness when predicting both wet and dry conditions for the onset months for the different rainfall regions over South Africa.

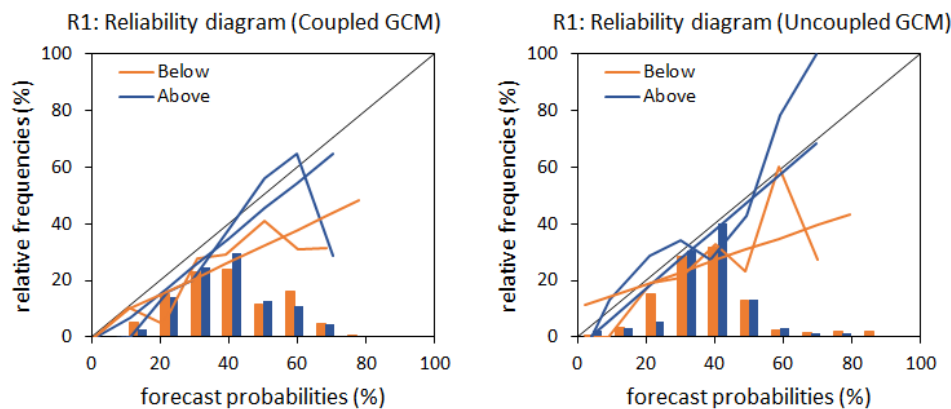


Figure 5.4. Reliability diagrams and frequency histograms for the downscaled forecasts produced by both the OAGCM (Coupled) and AGCM (Uncoupled) 1-month lead-time in predicting above-normal and below-normal rainfall totals of the onset month for Region 1 over 14 year retro-active forecasts from 1996 to 2009.

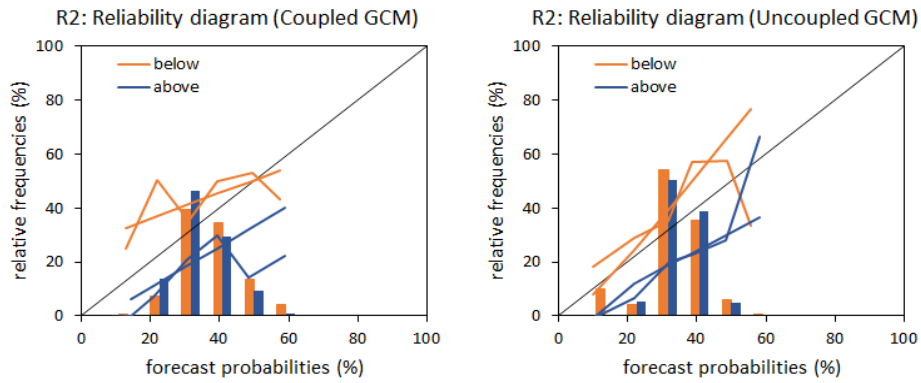


Figure 5.5. As in Figure 5.4, but for Region 2.

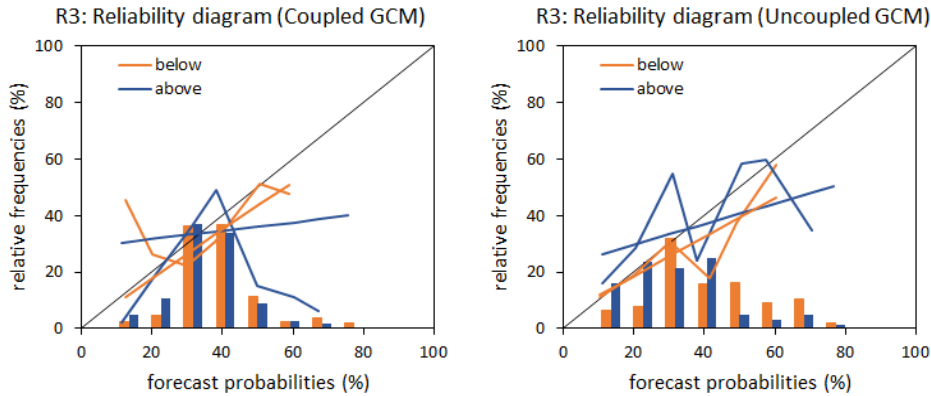


Figure 5.6. As in Figure 5.5, but for Region 3.

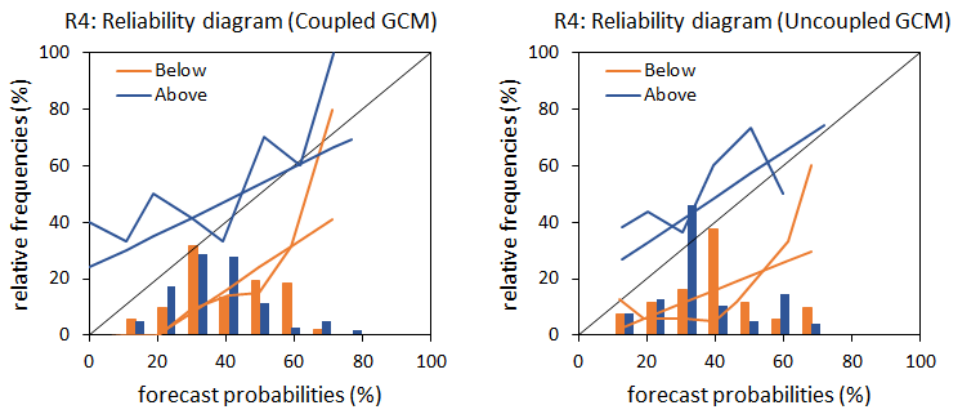


Figure 5.7. As in Figure 5.6, but for Region 4.

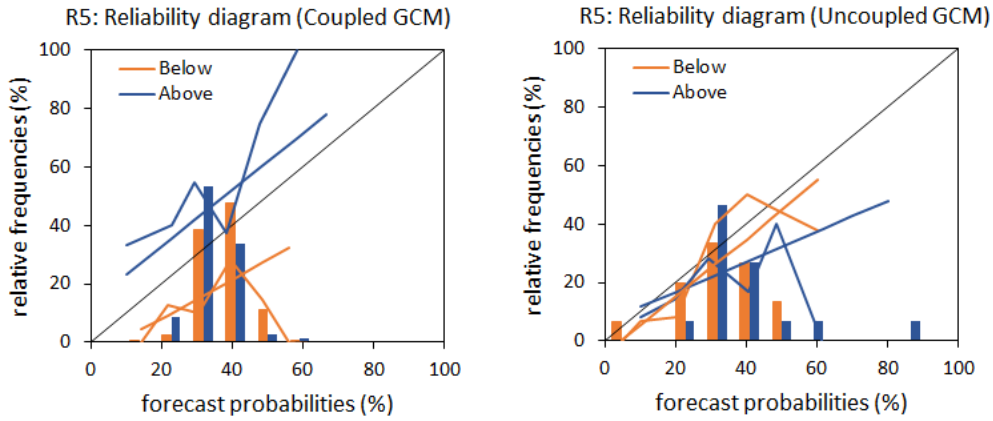


Figure 5.8. As in Figure 5.7, but for Region 5.

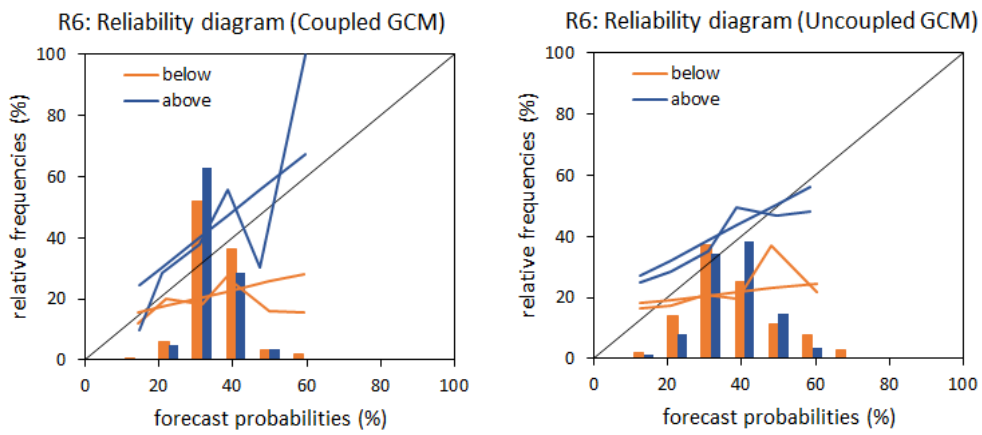


Figure 5.9. As in Figure 5.8, but for Region 6.

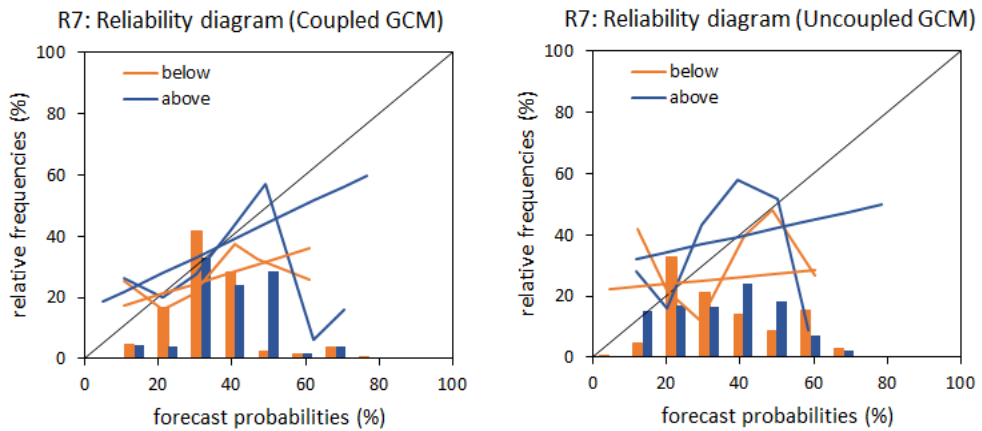


Figure 5.10. As in Figure 5.9, but for Region 7.

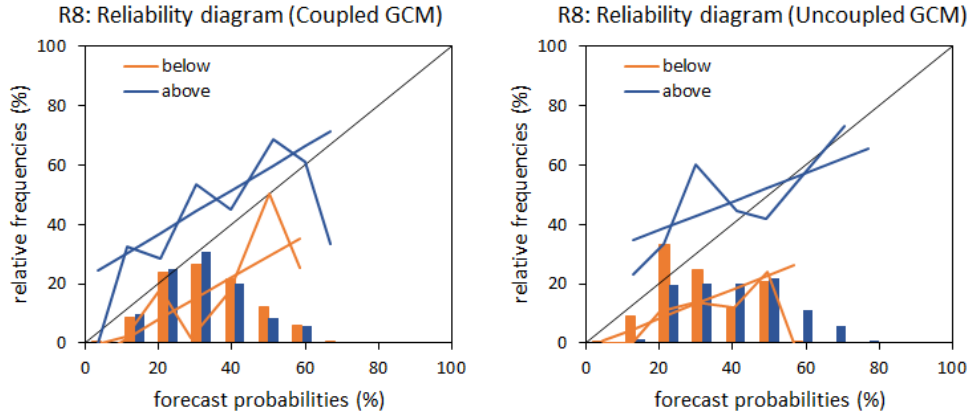


Figure 5.11. As in Figure 5.10, but for Region 8.

5.4. Spearman's rank correlations

ROC scores and reliability diagrams presented in this work explored how the models performed in terms of forecast skill. The Spearman's rank correlations is used here to estimate the spatial distribution of forecast skill. Figure 5.12 depicts the Spearman's rank correlations between the simulated rainfall totals from the two models at 1-month lead-time and the observed rainfall totals for the onset months as well as the correlations level of significance. The correlations of the distribution of skill in predicting rainfall totals for the onset months for all the regions varies for both the OAGCM and the AGCM. The variations of the distribution of skill is due to the fact that the onset months for rainfall regions differ. In fact, it been found that skill over South Africa is a function of time of the year and location (e.g. Landman *et al.* 2012).

The OAGCM system have positive correlations at different level of significance for all the eight rainfall regions, with the highest correlations (and high level of significance) found when predicting rainfall totals for the onset months of Region 1, Region 2, Region 4 and Region 5. In fact, the highest positive correlation is found when predicting rainfall totals for onset month of Region 1 and the lowest correlations are found for the onset months of Region 7, followed by Region 3. For the AGCM system positive correlations are found for the seven rainfall regions, except for Region 2 with negative correlation at a very low significant level. Furthermore, the highest positive correlations are found when predicting rainfall totals for the onset months for Region 1, Region 4, Region 5, Region 7 and Region 8. The lowest and negative correlation is found when predicting rainfall totals for onset months of Region 2.

The Spearman's rank correlations presented here indicates that the simulated rainfall from the two models are correlated with the observed rainfall totals for onset months for different rainfall regions of South Africa. However, the correlation varies across the rainfall regions. This in turn, imply that the forecast skill distributed across the regions varies for both the OAGCM and the AGCM systems. In fact the OAGCM have higher Spearman's correlations as compared to the AGCM.

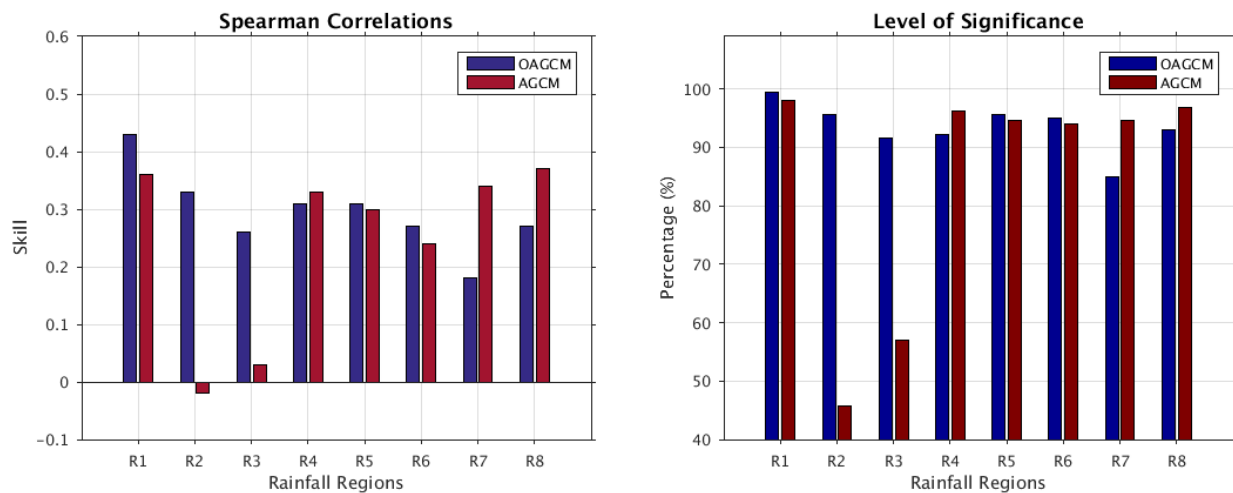


Figure 5.12. Spearman's rank correlations and their level of significance between simulated rainfall from both the OAGCM and the AGCM at 1-month lead-time and rainfall totals of the onset months for the eight homogeneous rainfall regions over the 14 year retro-active forecasts from 1996 to 2009.

5.5. CCA pattern analysis

5.5.1. OAGCM

The CCA maps in Figure 5.13 indicate that when there are anomalously negative (positive) 850hPa geopotential heights (predictor spacial loadings) for the OAGCM positioned southeast of South Africa there are anomalously dry (wet) conditions for Region 1 onset months. During 1983, 1998 and 2006 for example, the predictor spatial loadings are anomalously negative and their temporal scores are also negative. The product of the spatial loadings and their temporal scores is positive. The rainfall totals (predictand loadings) are anomalously negative and their temporal

scores are negative, and their product is positive. During 1982 and 2003 the predictor spatial loadings are anomalously negative and their temporal scores are positive, and their product is negative. The predictand loadings for the onset months are anomalously negative and their temporal scores are positive, and their product is negative. This result implies that when there is a strong low (high) pressure system at 850hPa situated southeast of South Africa the onset months for Region 1 tend to be drier (wetter) than normal.

It was found that when there are anomalously negative (positive) predictor spatial loadings south of South Africa there are anomalously wet (dry) conditions for Region 2, 3 and 4 (Figures 5.14, 5.15 and 5.16) onset months. For example, during 1998 and 2006 the predictor loadings are anomalously negative and their temporal scores are negative, and their product is positive. The predictand loadings are positive and their temporal scores are negative, and the product of the loadings and scores is negative. During 1985 and 1997 the predictor spatial loadings are anomalously negative and their temporal scores are positive, and their product is negative. The predictand loadings for onset months are positive and their temporal scores are positive, and their product is positive. This finding mean that when there is a strong high (low) pressure system at 850hPa situated south of South Africa the onset months for Region 2, 3 and 4 tend to be drier (wetter) than normal.

For Region 5, 6, 7 and 8 (Figures 5.17, 5.18, 5.19 and 5.20) when there are anomalously negative (positive) predictor spatial loadings over South Africa, there are anomalously wet (dry) conditions for onset months. During 1987 and 2006 the predictor spatial loadings are anomalously negative and their temporal scores are negative, and their product is positive. The predictand loadings are positive and their temporal scores are negative, and the product of the loadings and scores is negative. During 1983 and 1997 the predictor spatial loadings are anomalously negative and their temporal scores are positive, and their product is negative. The predictand loadings for onset months are positive and their temporal scores are positive, and their product is positive. This result implies that when there is a strong low (high) pressure system at 850hPa over South Africa the onset months for Region 5, 6, 7 and 8 tend to be wet (dry).

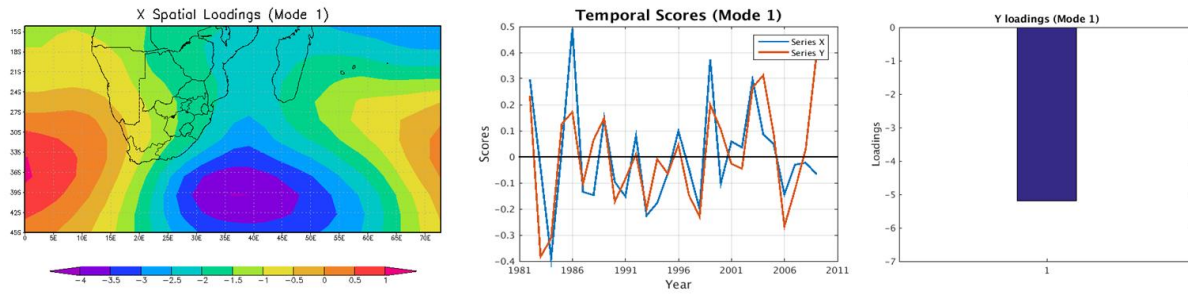


Figure 5.13. Mode 1 CCA maps for the 850hPa geopotential heights of the OAGCM 1-month lead-time and rainfall totals for onset months for Region 1 from 1982 to 2009.

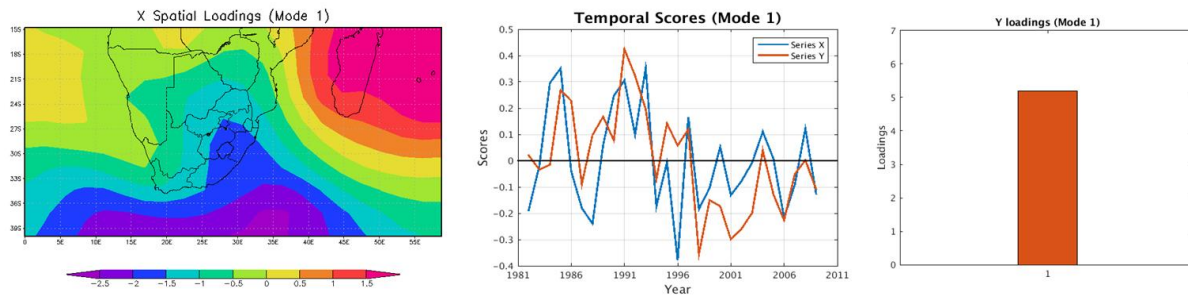


Figure 5.14. As in Figure 5.13, but for Region 2.

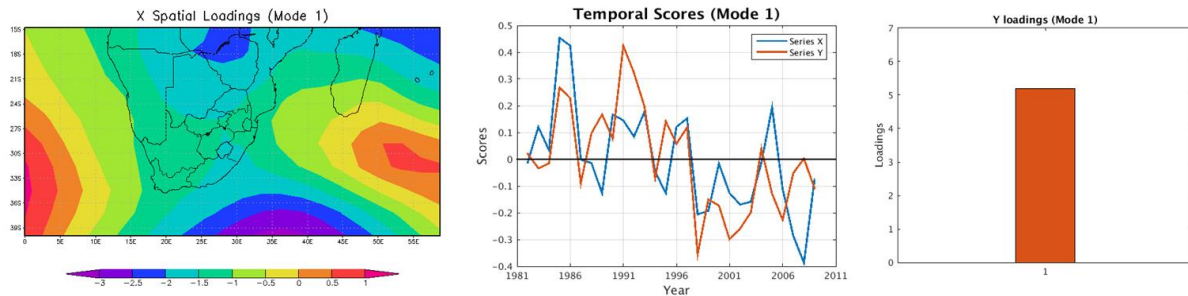


Figure 5.15. As in Figure 5.14, but for Region 3.

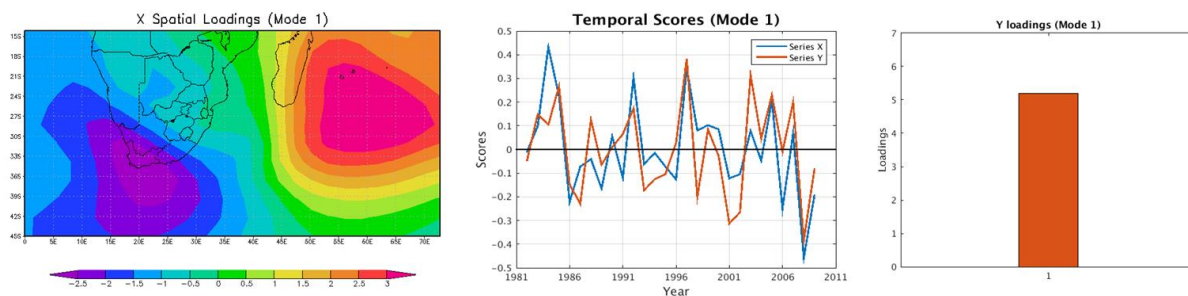


Figure 5.16. As in Figure 5.15, but for Region 4.

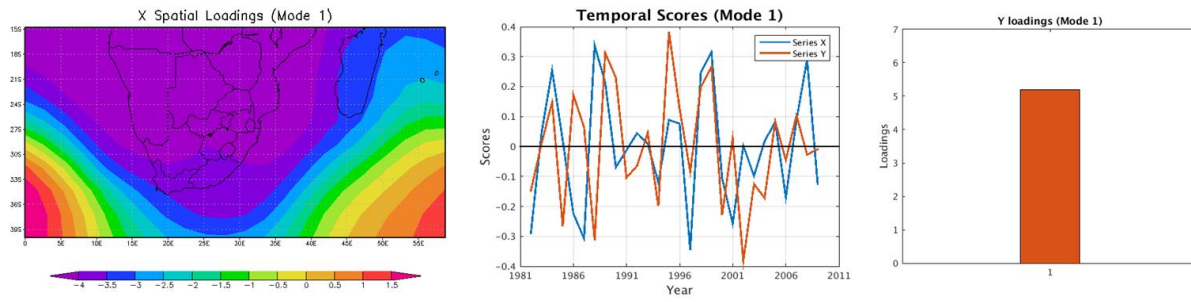


Figure 5.17. As in Figure 5.16, but for Region 5.

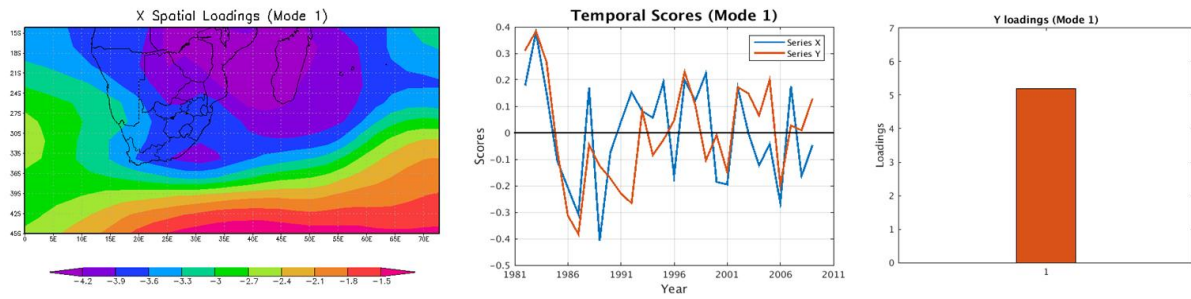


Figure 5.18. As in Figure 5.17, but for Region 6.

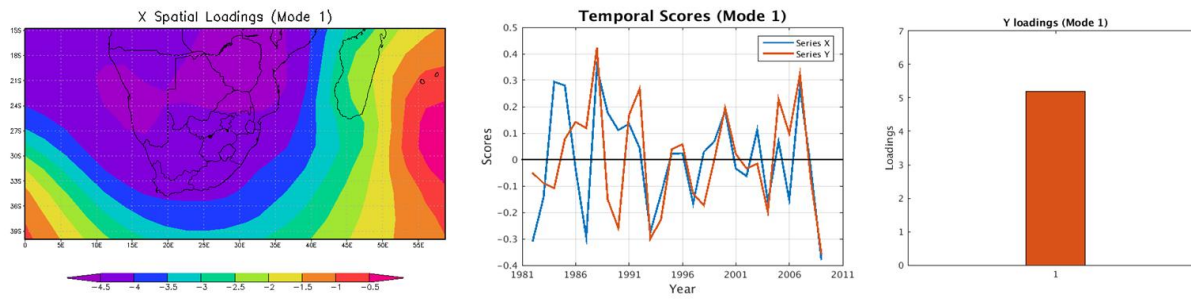


Figure 5.19. As in Figure 5.18, but for Region 7.

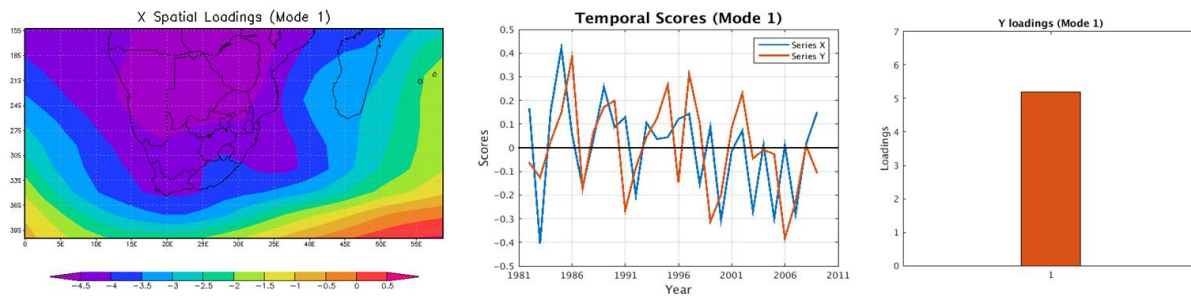


Figure 5.20. As in Figure 5.19, but for Region 8.

5.5.2. AGCM

Region 1 onset months tend to be wetter (drier) than normal when there are anomalously negative (positive) predictor spatial loadings for the AGCM positioned southwest of South Africa (Figure 5.21). During 1982 and 2003 for example, the predictor spatial loadings are anomalously negative and their temporal scores are also negative. The product of the spatial loadings and their temporal scores is positive. The predictand loadings are positive and their temporal scores are negative, and their product is negative. During 1984 and 2006 the predictor loadings are anomalously negative and their temporal scores are positive, and their product is negative. The predictand loadings are anomalously positive and their temporal scores are positive, and their product is positive. This finding imply that when there is a strong low (high) pressure system at 850hPa southwest of South Africa the onset months for Region 1 tend to be dry (wet).

Figure 5.22 depicts that when there are anomalously positive (negative) predictor spatial loadings southwest of South Africa there are anomalously dry (wet) conditions for the onset months for Region 2. For example, during 1985 and 1992 the predictor spatial loadings are anomalously positive and their temporal scores are negative, and their product is negative. The predictand loadings are negative and their temporal scores are negative, and the product of the loadings and time scores is positive. During 1998 the predictor spatial loadings are anomalously positive and their temporal scores are positive, and their product is positive. The predictand loadings are negative and their temporal scores are positive, and their product is negative. This result mean that when there is a strong high (low) pressure system at 850hPa situated southwest of South Africa the onset months for Region 2 tend to be dry (wet).

The CCA maps for Region 3 and 4 (Figures 5.23 and 5.24) show that when there are anomalously negative (positive) spatial loadings for the AGCM over of South Africa accompanied by positive (negative) anomalies east of the country there are anomalously wet (dry) conditions for the onset months. During 1986 the predictor spatial loadings are anomalously negative over South Africa and their temporal scores are negative, and their product is positive. The predictand loadings are positive and their temporal scores are negative, and the product of the loadings and scores is negative. During 1999 the predictor spatial loadings are anomalously negative and their temporal scores are positive, and their product is negative. The predictand loadings are positive and their temporal scores are positive, and their product is positive. This finding implies that when there is

a strong high (low) pressure system at 850hPa over South Africa accompanied by low (high) pressure system east of the country the onset months for Region 3 and 4 tend to be wetter (drier) than normal.

When there are anomalously negative (positive) predictor spatial loadings over South Africa extending to SWIO, there are anomalously wet (dry) conditions for the onset months of Region 5 and 6 (Figures 5.25 and 5.26). During 1982 and 2002 the predictor spatial loadings are anomalously negative and their temporal scores are negative, and their product is positive. The predictand loadings are positive and their temporal scores are negative, and their product is negative. During 1986 and 1999 the predictor loadings are anomalously negative and their temporal scores are positive, and their product is negative. The predictand loadings are positive and their temporal scores are positive, and their product is positive. This results mean that when there is a strong high (low) pressure system at 850hPa over South Africa extending to SWIO the onset months for Region 5 and 6 tend to be dry (wet).

For Region 7 the CCA maps (Figure 5.27) indicate that when there are anomalously negative (positive) predictor spatial loadings over South Africa there are anomalously wet (dry) conditions for the onset months. During 1993 and 2009 for example, the predictor spatial loadings are anomalously negative and their temporal scores are negative, and their product is positive. The predictand loadings are positive and their temporal scores are negative, and the product of the loadings and scores is negative. During 1988 and 2007 the predictor spatial loadings are anomalously negative and their temporal scores are positive, and their product is negative. The predictand loadings are positive and their temporal scores are positive, and their product is positive. This mean that when there is a strong high (low) pressure system at 850hPa over South Africa the onset months for Region 7 tend to be drier (wetter) than normal.

Figure 5.28 show that when there is a high (low) pressure system situated west of South Africa the onset months for Region 8 tend to be wet (dry). For example, during 1986 and 1998 the predictor spatial loadings are anomalously negative and their temporal scores are negative, and their product is positive. The predictand loadings are positive and their temporal scores are negative, and their product is negative. During 1985 and 1996 the predictor spatial loadings are anomalously negative and their temporal scores are positive, and their product is negative. The

predictand loadings are positive and their temporal scores are positive, and their product is positive. This finding implies that when there is a strong high (low) pressure system at 850hPa situated southwest of South Africa the onset months for Region 8 tend to be wet (dry).

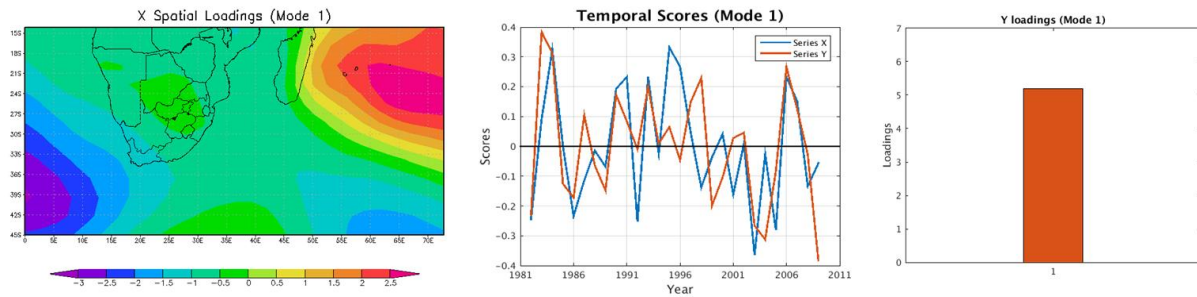


Figure 5.21. Mode 1 CCA maps for 850hPa geopotential heights of the AGCM at 1-month lead-time and rainfall totals of the onset months for Region 1 from 1982 to 2009.

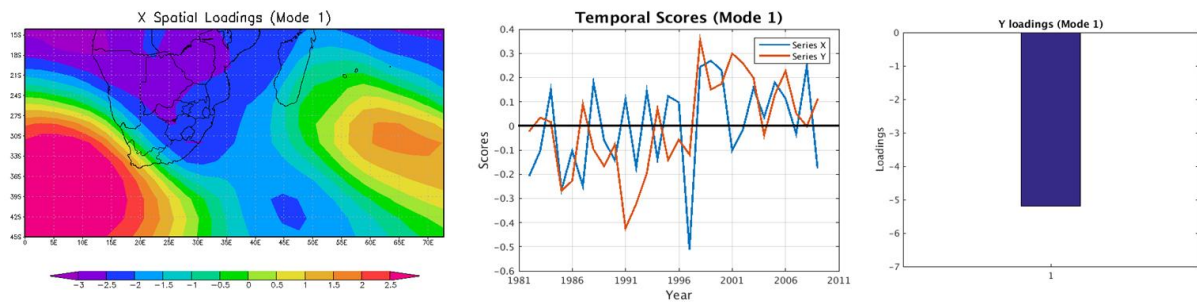


Figure 5.22. As in Figure 5.21, but for Region 2.

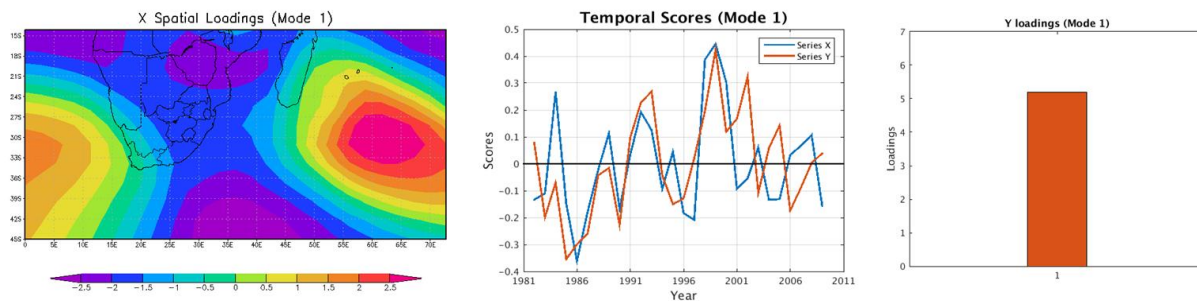


Figure 5.23. As in Figure 5.22, but for Region 3.

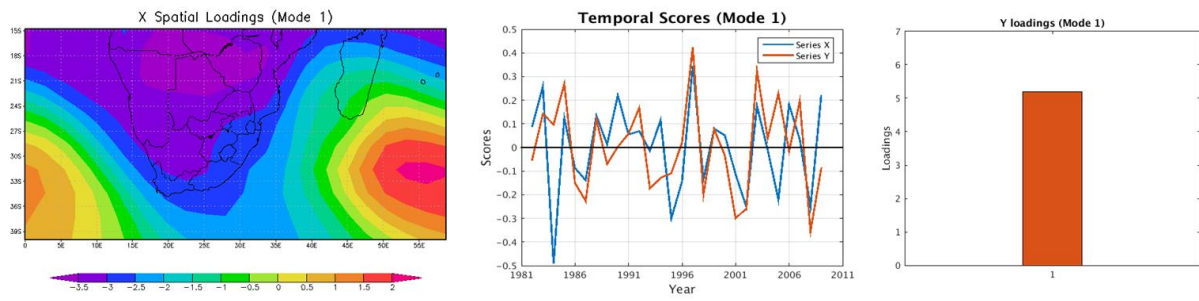


Figure 5.24. As in Figure 5.23, but for Region 4.

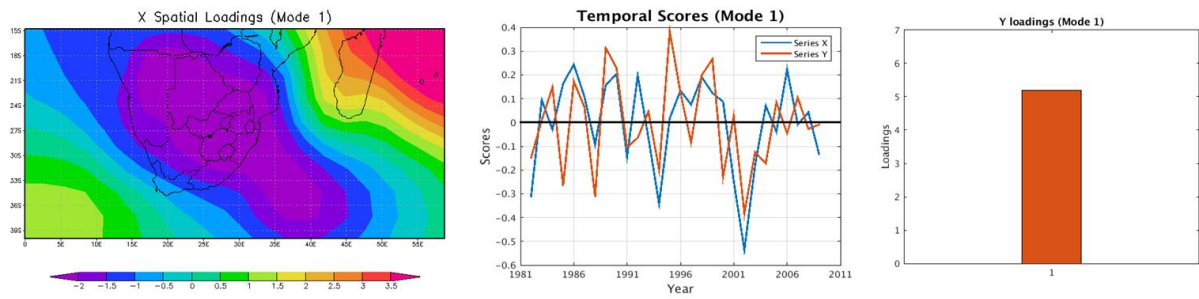


Figure 5.25. As in Figure 5.24, but for Region 5.

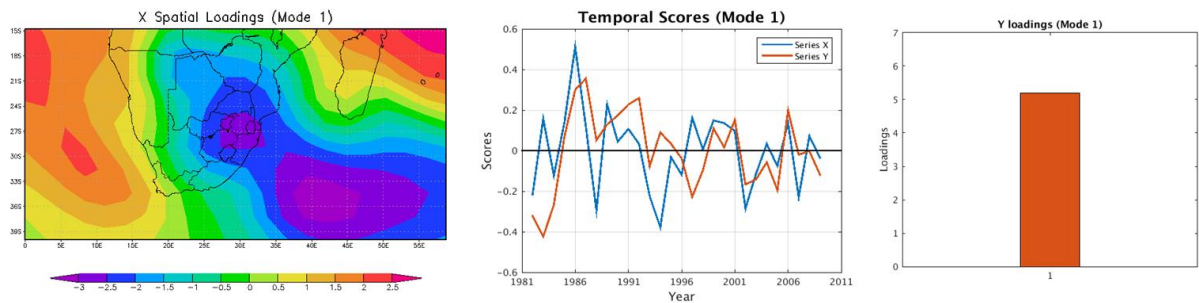


Figure 5.26. As in Figure 5.25, but for Region 6.

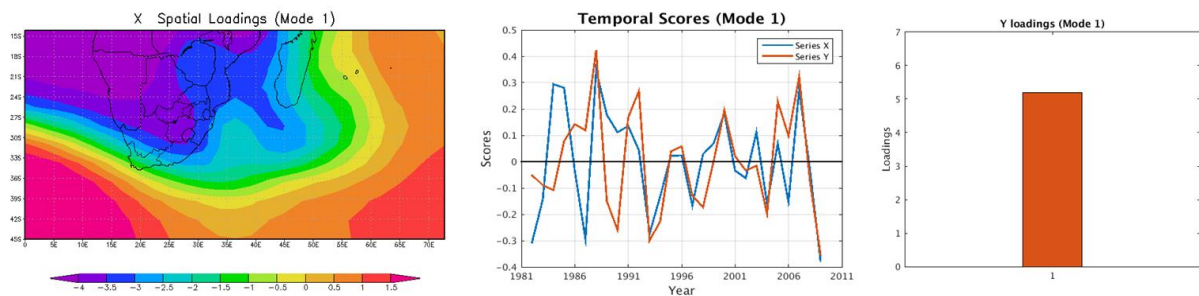


Figure 5.27. As in Figure 5.26, but for Region 7.

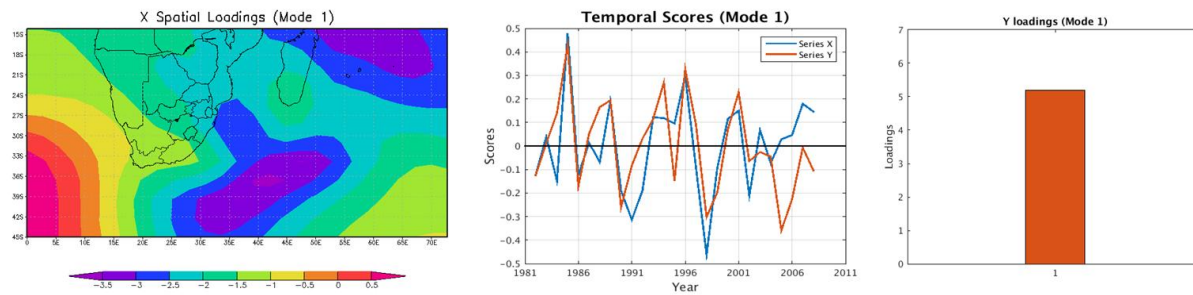


Figure 5.28. As in Figure 5.27, but for Region 8.

5.6. Synopsis

This chapter evaluated the skill levels of both the OAGCM and the AGCM in predicting rainfall totals for the onset months of the eight homogeneous rainfall regions of South Africa. The ROC scores have shown that the 850hPa geopotential heights at 1-month lead-time for both the models can be used to predict the onset months. The reliability diagrams also showed that both systems are reliable in predicting wet and dry conditions. However, both the prediction systems lack sharpness when predicting the onset months. The Spearman's rank correlations showed that the simulated rainfall of both the OAGCM and the AGCM are correlated with the observed rainfall totals for the onset months of the different rainfall regions. The skill of the forecasting systems in predicting summer rainfall region onset months is due to the already known fact that there is rainfall-ENSO teleconnection, more especially from November to February. For the austral winter rainfall region it was also found that when May is included in the season (i.e. May to September) there is rainfall-ENSO teleconnection, hence the May onset months of Region1 are predictable. The CCA pattern analysis showed that different atmospheric circulation systems are responsible for rainfall for most of the onset months. In fact, the atmospheric circulation systems controlling the individual onset months seem to be different from the systems responsible for the seasonal rainfall totals as well as the number of rainfall days exceeding pre-defined thresholds considered in this study. Furthermore, the circulation systems produced by the OAGCM are also different to the ones produced by the AGCM for most of the onset months.

CHAPTER 6

SUMMARY AND CONCLUSIONS

This study evaluates the forecast skill levels of an ocean-atmospheric coupled model (OAGCM) and an atmospheric model ECHAM4.5 (AGCM) in predicting seasonal rainfall totals, number of rainfall days exceeding pre-defined thresholds as well as the onset of the rainy seasons over South Africa. Although the aim of this research is to evaluate the models' ability in predicting intra-seasonal rainfall characteristics over South Africa, the models are first evaluated in predicting seasonal rainfall totals to determine whether the results of this study are comparable with previous studies of seasonal climate predictions. By evaluating seasonal predictability first it is subsequently shown that the model configurations have been set up properly and from these configurations additional properties of the season are predicted.

The model's forecast skill is assessed using ROC scores, reliability diagrams as well as Spearman's rank correlations. In addition to these measures of skill, CCA pattern analysis is also performed to determine the relationship between the dominant atmospheric circulation pattern and the observed variables. It was established that both the GCMs have skill (high ROC scores) in predicting the 3-month seasonal rainfall totals for OND, NDJ, DJF and JFM over South Africa. In fact the highest ROC scores are found during NDJ and DJF seasons. The reliability diagrams for NDJ seasons showed that both forecasting systems are over-confident (under-confident) in predicting dry (wet) conditions over South Africa. For DJF seasons the reliability diagrams indicate that both models are reliable in predicting wet conditions, however the forecast systems are always over-confident in predicting dry conditions. The Spearman's rank correlation coefficients for both systems also showed that simulated and observed seasonal rainfall totals are significantly (95%) correlated. High correlations are found when predicting DJF season totals as compared to NDJ seasons. The OAGCM seem to outperform the AGCM in predicting the seasonal rainfall totals during NDJ and DJF seasons. However, both models predict DJF totals better as compared to NDJ seasons. CCA pattern analysis is performed to determine the physical mechanism of atmospheric circulation patterns that are seen by the global models as responsible for rainfall during summer seasons. CCA maps for both prediction systems have shown that when there are strong high (low) pressure systems at the surface over South Africa, there are anomalously dry (wet) conditions for NDJ, DJF and JFM seasons over of South Africa.

When predicting the number of rainfall days exceeding 1mm, 5mm, 10mm, 15mm, 20mm, 30mm, 40mm and 50mm threshold values over South Africa both forecasting systems also have skill. The ROC scores have shown that both models have the attribute of discrimination in predicting the number of days exceeding threshold values less than or equal to 20mm. The highest ROC scores are found during NDJ and DJF for the OAGCM system and during DJF and JFM for the AGCM system. The reliability diagrams also indicate that both systems can reliably predict number of rainfall exceeding thresholds less or equal to 20mm, especially during DJF and JFM seasons. The Spearman's rank correlations for both systems also showed that simulated and observed number of rainfall days are significantly (95%) correlated, especially during DJF seasons. CCA analysis showed that when there are anomalously negative (positive) predicted 850hPa geopotential heights over South Africa, there are anomalously high (low) number of rainfall days exceeding the pre-defined threshold values for NDJ, DJF and JFM seasons over South Africa. Such configuration is also found for modelling seasonal rainfall totals as described earlier.

Both the forecasting systems also have skill (high ROC scores) in predicting rainfall totals for the onset months of the eight homogeneous rainfall regions of South Africa. The reliability diagrams also showed that both systems are reliable in predicting rainfall totals for the onset months, but both the prediction systems lack sharpness. The Spearman's correlations showed that both the OAGCM and the AGCM have skill (positive correlations) in predicting rainfall totals for onset months for the rainfall regions. CCA maps showed that in general a variety of atmospheric circulation systems are responsible for rainfall for the onset months of the eight rainfall regions of South Africa. In fact, the systems produced by the OAGCM are different from the ones produced by the AGCM.

The similarities of the CCA pattern analysis for the seasonal totals and the rainfall frequencies are a consequence of the fact that the same 3-month seasons were used for both predictands. Moreover, these patterns are similar to what has already been found with such statistical downscaling with an older version of the GCM (Landman and Goddard, 2001). When we applied equivalent downscaling for single month data, the months of onset are not the same throughout and consequently may lead to CCA patterns that are generally different for each month and from the 3-month seasons. Different atmospheric states may also be found for different months, for

example, December rainfall is often subject to both baroclinic and barotropic atmospheres, while January may be much more affected by barotropic atmospheres.

The following conclusions can be drawn out of this study:

1. The 850hPa geopotential heights of both the OAGCM and the AGCM can be used to predict the number of rainfall days exceeding 1mm, 5mm, 10mm and 20mm during NDJ, DJF and JFM seasons over South Africa. However, the OAGCM outperforms the AGCM.
2. The 850hPa geopotential heights of both the OAGCM and the AGCM can also be used to predict the rainfall totals of onset months for the homogeneous regions of South Africa.
3. Atmospheric circulation patterns that are responsible for seasonal rainfall totals are the same as the one responsible for number of rainfall days for summer seasons.
4. Different atmospheric circulation patterns are responsible for rainfall totals for the onset months of the homogeneous regions. Furthermore, atmospheric circulation systems produced by the OAGCM are different from that produced by the AGCM.

The format of seasonal forecasts issued by institutions such as SAWS has been for the most part focused on the likelihood of receiving predefined seasonal rainfall totals. That is, the forecasts have focused almost exclusively on predicting droughts or flood seasons as defined by accumulated rainfall totals over a season. Users of forecasts are interested to also find out what forecast for rainfall characteristics within a season might be like. For this reason, this study was conducted to test if our current forecast models can in fact skillfully predict such characteristics. Here the focus was on predicting the number of rainfall days exceeding predefined thresholds as well as the onset months of rainy seasons. The levels of skill in predicting these characteristics are similar to what has been known, and again demonstrated here, for South Africa. This work has paved the way for SAWS to issue forecasts for such rainfall characteristics, in addition to the traditional seasonal forecasts.

REFERENCES

- Ambrosino C., R.E. Chadler and M.C. Todd, 2011: Southern Africa monthly rainfall variability: An analysis based on generalized linear models, *Journal of Climate*, **24**, 4600-4617.
- Ashok K., S.K. Behera, S.A. Rao, H. Weng, and T. Yamagata, 2007: El Niño Modoki and its possible teleconnection, *Journal of Geophysical Research*, **112** (C11007), doi: 10.1029/2006JC003798.
- Ati O. F., C.J. Stigter and E.O. Oladipo, 2002: A comparison of methods to determine the onset of growing season in Northern Nigeria, *International Journal of Climatology*, **22**, 731-742.
- Bartman A.G., W.A. Landman and C.J. De W. Rautenbach, 2003: Recalibration of general circulation model output to austral summer rainfall over southern Africa, *International Journal of Climatology*, **23**, 1407-1419.
- Beraki A.F., D.G. DeWitt, W.A. Landman and C. Olivier. 2014, Dynamical climate prediction using an ocean-atmosphere coupled model developed in partnership between South Africa and the IRI, *Journal of Climate*, **27**, 1719-1741.
- Beraki A. F., W.A. Landman, D. DeWitt and C. Olivier. 2016, Global dynamical forecasting system conditioned to robust initial and boundary forcings: Seasonal Context, *International Journal of Climatology*, DOI: 10.1002/joc.4643.
- Bouagila B. and L. Sushama, 2013: On the current and future dry spell characteristics over Africa, *Atmosphere* 2013, **4**, 272-298, doi: 10.3390/atmos4030272.
- Brocker J. and L.A. Smith, 2007: Increasing the reliability of reliability diagrams, *Weather and Forecasting*, **22**, 651-661.
- Busuioc A., D. Chen, and C. Hellstrom, 2001: Performance of statistical downscaling models in GCM validation and regional climate change estimates: Application for Swedish precipitation, *International Journal of Climatology*, **21**, 557-578.

- Camberlin P. and D. Mbeye, 2003: Application of daily rainfall principle component analysis to the assessment of the rainy season characteristics in Senegal, *Climate Research*, **23**, 159-169.
- Chen J., F.P. Brissette and R. Leconte, 2012: Coupling statistical and dynamical methods for spatial downscaling of precipitation, *Climatic Change*, DOI: 10.1007/s10584-012-0452-2.
- Cook C., C.J.C. Reason and B.C. Hewitson, 2004: Wet and dry spells within particularly wet and dry summers in the South African summer rainfall region, *Climate Research*, **26**, 17-31.
- Cretat J., Y. Richard, B. Pohl, M. Roualt, C. Reason and N. Fauchereau, 2010: Recurrent daily rainfall pattern over South Africa and associated dynamics during the core of the austral summer, *International Journal of Climatology*, doi: 10.1002/joc.2266.
- de Coning E., 2013: Optimizing satellite-based precipitation estimation for nowcasting of rainfall and flash flood events over the South African domain, *Remote Sensing*, **5**, 5702-5724.
- Hewitson and Crane, 2002: Self-organizing maps: Applications to synoptic climatology, *Climate Research*, **22**, 13-26.
- Horel J.D. and J.M. Wallace, 1981: Planetary-Scale Atmospheric Phenomena Associated with the Southern Oscillation, *Monthly Weather Review*, **109**, 813-829.
- Hudson D., Alvies, H.H. Hendon and A.G. Marshall, 2011: Bridging the gap between weather and seasonal forecasting: Intraseasonal forecasting for Australia, *Q.J.R. Meteorol. Soc.* **137**, 673-689. DOI: 10.1002/qj.769.
- Izumo T., J. Vialard, M. Lengaigne, C.deB. Montegut, S.K Behera, J-J Luo, S. Cravatte, S. Masson, and T. Yamagata, 2010: Influence of the state of the Indian Ocean Dipole on the following year's El Niño, *Nature Geoscience*, DOI: 10.1038/NGEO760, www.nature.com/naturegeoscience.

Jones C., L.M.V. Carvalho, R.W. Higgins, D.E. Waliser and J.K.E. Schemm, 2004: A statistical forecast convective anomalies, *Journal of Climate*, **17**, 2078-2095.

Jolliffe I.T., N.T. Trendafilov and M. Uddin, 2003: A modified principal component technique based on the LASSO, *Journal of Computational and Graphical Statistics*, 12(3), pp. 531-547.

Kerandi N.M. and J.A. Omotosho, 2008: Seasonal rainfall prediction in Kenya using empirical methods, *Journal of Kenya meteorological Society*, **2(2)**, 114-124.

Kijazi A.L. and C.J.C. Reason, 2011: Intra-seasonal variability over the northeastern highlands of Tanzania, *International Journal of Climatology*, DOI: 10.1002/joc.2315.

Kniveton D.R., R. Layberry, C.J.R. Williams and M. Peck, 2008: Trends in the start of the wet season over Africa, *International Journal of Climatology*, DOI: 10.1002/joc.1792.

Kundzewicz Z.W., S. Kanae, S.I. Seneviratne, J. Handmer, N. Nicholls, P. Peduzzi, R. Mechler, L.M. Bouwer, N. Arnell, K. Mach, R. Muir-Wood, G.R. Brakenridge, W. Kron, G. Benito, Y. Honda, K. Takahashi and B. Sherstyukov, 2014: Flood risk and climate change: Global and regional perspectives, *Hydrological Sciences Journal*, **59**:1, 1-28, DOI: 10.1080/02626667.2013.857411.

Landman W.A. and A. Beraki, 2012: Multi-Model forecast skill for mid-summer rainfall over southern Africa, *International journal of Climatology*, **32**, 303-314.

Landman W.A. and W.J. Tennant, 2000: Statistical downscaling of monthly forecasts, *International journal of Climatology*, **20**, 1521-1532.

Landman W.A., S.J Mason, P.D Tyson, and W.J Tennant, 2001: Retro-active skill of multi-tiered forecasts of summer rainfall over southern Africa. *International Journal of Climatology*, **21**, 1-19.

Landman W.A. and L. Goddard, 2002: Statistical recalibration of GCM forecasts over Southern Africa using Model Output Statistics, *Journal of Climate*, **15**, 2038-2055.

- Landman W.A., D. DeWitts, D.E. Lee, A. Beraki and D. Lotter. 2012, Seasonal rainfall prediction skill over South Africa: One- versus two-tiered forecasting systems, *Weather and Forecasting*, **27**: 489-501.
- Landman W.A., M-J. Kgatuke, M. Mbedzi, A. Beraki, A. Bartman and A. du Piesanie, 2009: Performance comparison of some dynamical and empirical downscaling methods for South Africa from a seasonal perspective, *International Journal of Climatology*, **29**, 1535-1549.
- Liebmann B. and J.A. Marengo, 2001: Interannual variability of the rainy season and rainfall in the Brazilian Amazon Basin, *Journal of Climate*, **14**, 4308-4318.
- Liebmann B., S.J. Camargo, A. Seth, J.A. Marengo, L.M.V. Carvalho, D. Allured, R. Fu and C.S. Vera, 2007: Onset and end of the rainy season in South America in observations and the ECHAM4.5 Atmospheric General Circulation Model, *Journal of Climate*, **20**, 2037-2050.
- Liess S., D.E. Waliser and S.D. Schubert, 2005: Predictability studies of the intraseasonal oscillation with ECHAM5 GCM, *Journal of the Atmospheric Sciences*, **62**, 3320-3336.
- Lo F., M.C. Wheeler, H. Meinke and A. Donald, 2007: Probabilistic forecasts of onset of the North Australian wet season, *Monthly Weather Review*, **135**, 3506-3520.
- Luo L. and E.F. Wood, 2006: Assessing the idealized predictability of precipitation and temperature in the NCEP Climate forecast System, *Geophysical Research Letters*, **33**, L04708, doi: 10.1029/2005GL025292, 2006.
- Lyon B., 2009: Southern Africa summer drought and heat waves: Observations and Coupled Model behavior, *Journal of Climate*, **22**, 6033-6046.
- Lyon B. and S.J. Mason, 2007: The 1997-98 summer rainfall season in Southern Africa. Part I: Observations, *Journal of Climate*, **20**, 5134-5148.

- Majisola O.R., 2010: Trends in precipitation features as an index of climate change in the Guinea Savanna Ecological Zone of Nigeria: Its implications on crop production, *Global Journal of Science Frontier Research*, **10**, 13-23.
- Mandal V., K.D. Utpal and K.B. Biplab, 2007: Precipitation forecast verification of the Indian summer monsoon with intercomparison of three diverse regions, *Weather and Forecasting*, **22**, 428-443.
- Marengo J.A., B. Liebmann, V.E. Kousky, N.P. Filizola and I.C. Wainer, 2001: Onset and End of the rainy season in the Brazilian Amazon Basin, *Journal of Climate*, **14**, 833-852.
- Mason S.J., 1998: Seasonal forecasting of South African rainfall using a non-linear discriminant analysis model, *International Journal of Climatology*, **18**, 147-164.
- Matthews S., 2000 (Accessed April 2014): El Niño, *Coastal and Marine Environments: Phenomena*, Department of Environmental Affairs and Tourism (The Coastal Management Office), <http://sacoast.wcape.gov.za>.
- Mhita M.S. and I.R. Nassib, 1887: The onset and end of rains in Tanzania: *Proceedings of the First Technical Conference on meteorological Research in Eastern and Southern Africa*, Kenya Meteorology Department, Nairobi, 33-37.
- Murphy J., 1999: An evaluation of statistical and dynamical techniques for downscaling local climate, *Journal of Climate*, **12**, 2256-2284.
- Ndomba P.M., 2010: Development of rainfall curves for crops planting dates: A case study of Pangani River Basin in Tanzania, *Nile Basin Water Science and Engineering Journal*, Vol 3, Issuel, 2010.
- Nicholls N., 1984: A system for predicting the onset of the north Australian wet-season, *International Journal of Climatology*, **4**, 425-435.

- Ngaka M.J., 2012: Drought preparedness, impact and response: A case of the Eastern Cape and Free State provinces of South Africa, Jamba, *Journal of Disaster Risk Studies* 4 (1), Art No.47, 10 pages. <http://dx.doi.org/10.4102/jamba.v4i1.47>.
- Oldenborgh G.J., 2004: Evaluation of atmospheric fields from the ECMWF seasonal forecasts over a 15-year period. *Journal of Climate*, **18**, 3250-3269.
- Omotosho J.B., A.A. Balogun and K. Ogunjobi, 2000: Predicting monthly and seasonal rainfall, onset and cessation of the rainy season in West Africa using only surface data, *International Journal of Climatology*, **20**, 865-880.
- Otun J.A. and J.K. Adewumi, 2009: Drought quantifications in semi-arid regions using precipitation effectiveness variables, *18th World IMACS/MODSIM Congress*, Cairns, Australia 13-17 July 2009.
- Oyelade O.J., O.O. Oladipupo and I.C. Obagbuwa, 2010: Application of K-means clustering algorithm for prediction of students' academic performance, *International Journal of Computer Science and Information Security*, Vol 7. No 1, 2010.
- Pobon J.D. and J. Dorodo, 2008: Intraseasonal variability of rainfall over northern South America and Caribbean region, *Earth Sciences Research Journal*, **12**, 194-212.
- Philippon N, M. Rouault, Y. Richard and A. Favre, 2011: The influence of ENSO on winter rainfall in South Africa, *International Journal of Climatology*, DOI: 10.1002/joc.3403.
- Pohl B., Y. Richard and N. Fauchereau, 2007: Influence of the Madden-Julian Oscillation on Southern African summer rainfall, *Journal of Climate*, **20**, 4227-4242.
- Pohl B., N. Fauchereau, Y. Richard, C.J.C. Reason and M. Rouault, 2009: Interactions between synoptic intraseasonal and interannual convective variability over southern Africa, *Clim Dyn*, **33**, 1033-1050.

Rautenbach C.J. deW. and I.N. Smith, 2001: Tele-connections between global sea-surface temperatures and the inter-annual variability of observed and model simulated rainfall over southern Africa, *Journal of Hydrology*, **254**, 1-15.

Reason C.J.C., S. Hachigonta and R.F. Phaladi, 2005: Interannual variability in rainy season characteristics over the Limpopo region of Southern Africa, *International Journal of Climatology*, **25**, 1835-1853.

Reason C.J.C, W. Landman and W. Tennant, 2006: Seasonal to decadal prediction of Southern Africa climate and its links with variability of the Atlantic Ocean, *Bulletin of the American Meteorological Society*, vol. **87**, pp.941-955, doi: 10.1175/BAMS-87-7-941.

Roeckner E. and Coauthors, (1996), Simulation of present-day climate with the ECHAM4 model: Impact of model physics and resolution, Report No. 93, Max-Planck-Institut für Meteorologie, Hamburg, Germany, 171 pp.

Ropelewski C.F. and M.S. Halpert, 1987: Global and regional scale precipitation patterns are associated with the El Niño/Southern Oscillation, *Monthly Weather Review*, **115**, 1606-1626.

Schmidli J., C.M. Goodess, C. Frei, M.R. Haylock, Y. Hundecha, J. Ribalaygua and T. Schmith, 2007: Statistical and dynamical downscaling of precipitation: An evaluation and comparison of scenarios for the European Alps, *Journal of Geophysical Research*, Vol.**112**, D04105, doi: 10.1029/2005JD007026, 2007.

Schulze, R.E. 2005. Setting the Scene: The Current Hydroclimatic “Landscape” in Southern Africa. In: Schulze, R.E. (Ed) *Climate Change and Water Resources in Southern Africa: Studies on Scenarios, Impacts, Vulnerabilities and Adaptation*. Water Research Commission, Pretoria, RSA, WRC Report 1430/1/05. Chapter 6, 83 - 94.

Shongwe M.E., G.J. Van Oldenborgh, B.J.J.M. Van Den Hurk, B. De Boer, C.A.S. Coelho and M.K. Van Aalst, 2009: Projected changes in mean and extreme precipitation in Africa under global warming: Part I: Southern Africa, *Journal of Climate*, **22**, 3819-3837.

- Simmons A.J., D.M. Burridge, M. Jarraud, C. Girard and W. Wergen, 1989: The ECMWF medium-range prediction models: Development of the numerical formulations and the impact of increased resolution. *Meteorological Atmospheric Physics*, **40**, 28-60.
- Sivakumar M.V.K., 1988: Predicting rainy season potential from the onset of rains in Southern Sahelian and Sudanian climatic zones of West Africa, *Agricultural and Forest Meteorology*, **42**, 295-305.
- Sultan B., S. Janicot and C. Correia, 2009: Medium lead-time predictability of intraseasonal variability of rainfall in West Africa, *Weather and Forecasting*, **24**, 767-784.
- Tadross M.A., B.C. Hewitson and M.T. Usman, 2005: The international variability of the onset of the maize growing season over South Africa and Zimbabwe, *Journal of Climate*, **18**, 3356-3372.
- Tadross M., P. Suarez, A. Lotsch, S. Hachigonta, M. Mdoka, L. Unganai, F. Lucio, D. Kamdonyo and M. Muchinda, 2009: Growing-season rainfall and scenarios of future change in southeast Africa: Implications for cultivating maize, *Climate Research*, **40**, 147-161.
- Taljaard J.J., 1996: Atmospheric circulation systems, synoptic climatology and weather phenomena of South Africa. Part 6, Rainfall in South Africa. Technical Report, no 32. South Africa. Weather Bureau, Govt. Printer, Pretoria, 98p.
- Tam and Lau, 2004: The impact of ENSO on atmospheric intraseasonal variability as inferred from observations and GCM simulations, *Journal of Climate*, **18**, 1902-1924.
- Tanaka H.L., N. Ishizaki and A. Kitoh, 2004: Trend and interannual variability of Walker, monsoon and Hadley circulations defined by velocity potential in the upper troposphere, *Tellus* (2004), **56A**, 250-269.
- Thomas D.S.G., C. Twyman, H. Osbahr and B. Hewitson, 2007: Adaptation to climate change and variability: Farmer responses to intraseasonal precipitation trends in South Africa, *Climatic Change*, **83**, 301-322.

- Todd M.C., R. Washington and P.I. Palmer, 2004: Water vapour transport associated with tropical-temperate trough systems over southern Africa and the southwest Indian Ocean, *International Journal of Climate*, **24**, 555-568.
- Trenberth, 1997: The definition of El Niño, *Bulletin of the American Meteorological Society*, Vol. **78**, No. 12, December 1997.
- Usman M.T. and C.J.C. Reason, 2004: Dry spell frequencies and their variability over southern Africa, *Climate Research*, **26**, 199-211.
- Usman M.T., E. Archer, P. Johnston and M. Tadross, 2005: A conceptual framework for enhancing the utility of rainfall hazard forecasts for agriculture in marginal environments, *Natural Hazards*, **34**, 111-129.
- Van Heerden J. and J.J. Taljaard, 1998: Africa and Surrounding waters. Chapter 3D. *Meteorological Monographs*, **27**, 141-168.
- Vigaud N., Y. Richard and M. Rouault, 2007: Water vapour transport from the tropical Atlantic and summer rainfall in tropical southern Africa, *Climate Dynamics*, **28**, 113-123.
- Wang J., W. Wang, X. Fu and K.H. Seo, 2011: Tropical intraseasonal rainfall variability in the CFSR, *Climate Dynamics*, DOI: 10.1007/s00382-1087-0.
- Wang J. and V.R. Kotamarthi, 2013: Assessment of dynamical downscaling in near-surface fields with different spectral nudging approaches using the nested regional climate model (NCRM), *Journal of Applied Meteorology and Climatology*, **52**, 1576-1591.
- Washington R. and A. Preston, 2006: Extreme wet years over southern Africa: Role of Indian Ocean sea surface temperatures, *Journal of Geophysical Research*, vol. **111**, D15104, doi: 10.1029/2005JD006724.

- Williams C.J.R., D.R. Kniveton and R. Layberry, 2008: Influence of South Atlantic Sea Surface Temperatures on rainfall variability and extremes over southern Africa, *Journal of Climate*, **21**, 6498-6520.
- Winsemius H.C., E. Dutra, F.A. Engelbrecht, E. Archer van Garderen, F. Wetterhall, F. Pappenberger and M.G.F. Werner, 2014: The potential value of seasonal forecasts in a changing climate in southern Africa, *Hydrology and Earth System Sciences*, **18**, 1525-1538.
- Wong G., D. Maraun, M. Vrac, M. Widmann and J.M. Eden, 2014: Stochastic Model Output Statistics for bias correcting and downscaling precipitation including extremes, *Journal of Climate*, **27**, 6940-6959.
- Xu Z. and Z.L. Yang, 2012: An improved dynamical downscaling method with GCM bias corrections and its validation with 30 years of climate simulations, *Journal of Climate*, **25**, 6271-6286.
- Yuan M.J., E.F. Wood, N.W. Chaney, J. Sheffield, J. Kam, M. Liang and K. Guan, 2013: Probabilistic seasonal forecasting of African drought by dynamical models, *Journal of Hydrometeorology*, **14**, 1706-1720.
- Zhang H. and T. Casey, 2000: Verification of probability forecasts, *Weather and Forecasting*, **15**, 80-89.
- Zhang C. and Z. Fang, 2013: An improved K-means clustering algorithm, *Journal of Information and Computational Sciences*, 10:1 (2013) 193-199.